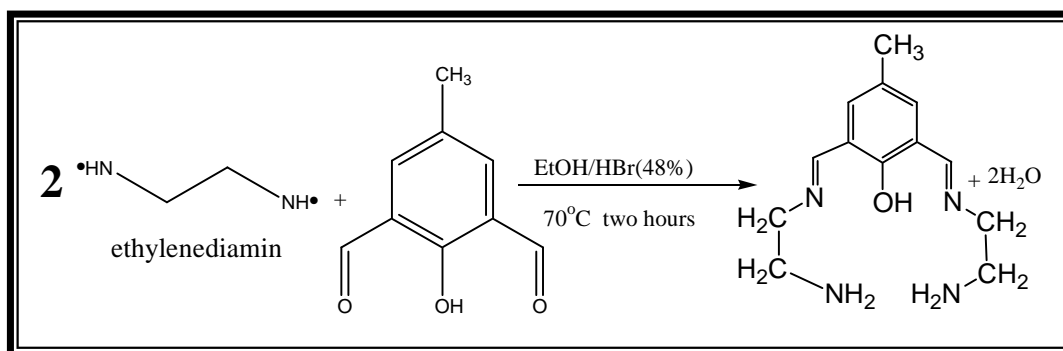


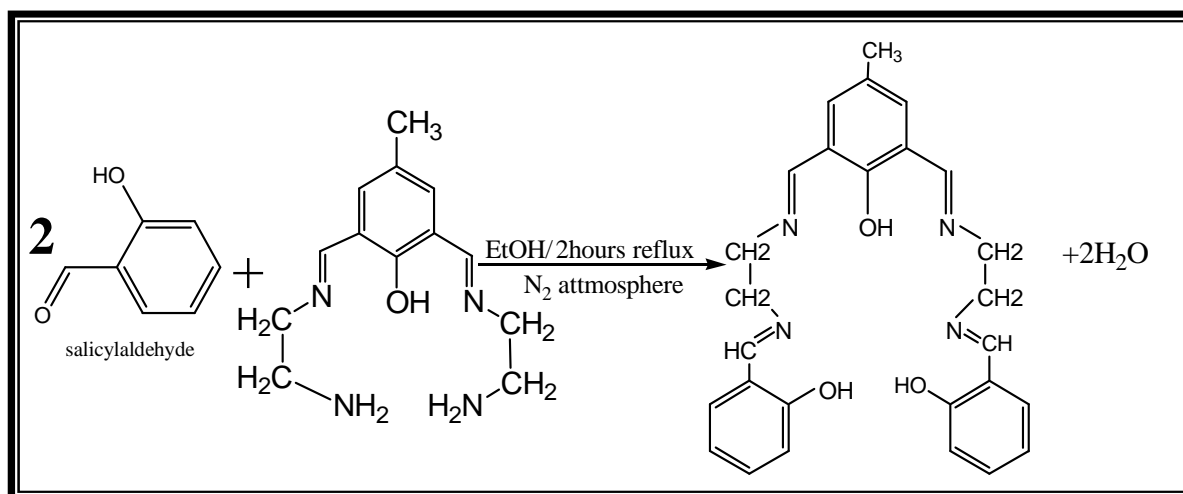
Summary

A new Schiff base polydentate ligand (tetra Aza) has been prepared: 2,6-bis-(Azomethine ethyl Azomethine ortho phenol) 4-methyl phenol.

Synthesis was carried out by two steps of condensation, first by the condensation of 2,6-diformyl-4-methyl phenol and ethylenediamine in the mole ratio (1:2) under nitrogen atmosphere.



The second step by condensation of the yield of the first step with salicylaldehyde in the mole ratio (1:2) under nitrogen atmosphere.

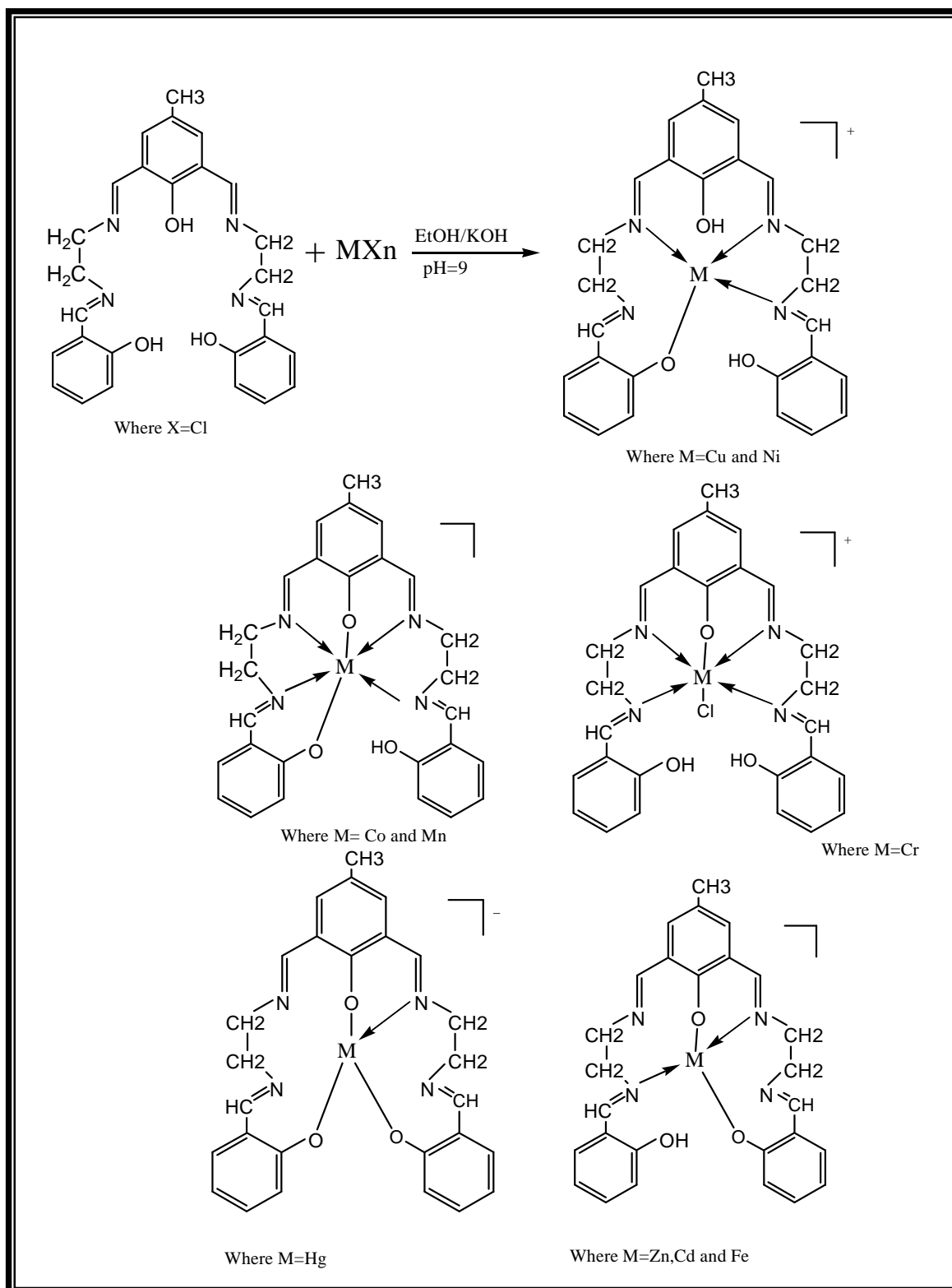


The ligand was characterized and its structure was elucidated depending upon nitrogen analysis by Kjeldahl modified method, spectral data (I.R, U.V-Vis, ^1H , $^{13}\text{CNMR}$ & atomic absorption). Series of metal complexes of the ligand with the metal ions Mn^{II} , Co^{II} , Ni^{II} , Cu^{II} , Zn^{II} , Cd^{II} , Fe^{II} , Cr^{III} and Hg^{II} were synthesized by adding the solution of ligand (L) with ethanol to a solution of each metal salt with ethanol and KOH (to keep pH ≈ 9) then refluxed it for two hours under nitrogen atmosphere. The complexes were characterized and their stereo chemical structures and geometries were suggested depending upon data of nitrogen analysis by Kjeldahl modified method, spectral studies (I.R, UV-Vis, ^1H and $^{13}\text{CNMR}$) as well as magnetic moments, (A.A), conductivity measurements, chloride contents & melting points. The following general formula were achieved: $[\text{M}(\text{L})]\text{Cl}$ where $\text{M} = \text{Cu}(\text{II})$, and $\text{Ni}(\text{II})$, $[\text{M}(\text{L})\text{Cl}]\text{Cl}$ where $\text{M} = \text{Cr}(\text{III})$, $[\text{M}(\text{L})]$ where $\text{M} = \text{Mn}(\text{II})$, $\text{Co}(\text{II})$, $\text{Fe}(\text{II})$, $\text{Cd}(\text{II})$, $\text{Zn}(\text{II})$ and $\text{K}[\text{M}(\text{L})]$ where $\text{M} = \text{Hg}(\text{II})$ ions.

The electronic spectra in DMF (10^{-3} M) supported by magnetic moments in solid state revealed octahedral geometries for $\text{Co}(\text{II})$, $\text{Mn}(\text{II})$ and $\text{Cr}(\text{III})$, tetrahedral geometries for $\text{Fe}(\text{II})$, $\text{Zn}(\text{II})$, $\text{Cd}(\text{II})$ and $\text{Hg}(\text{II})$, Square planner geometries for $\text{Cu}(\text{II})$ and $\text{Ni}(\text{II})$.

Conductivity measurements of the new synthesized complexes in DMF (10^{-3}) showed electrolytic nature of $\text{Cu}^{(\text{II})}$, $\text{Ni}^{(\text{II})}$, $\text{Cr}^{(\text{III})}$ and $\text{Hg}^{(\text{II})}$ complexes with chloride or potassium content and these complexes are ionic with the (1:1) of mole ratio, while $\text{Cd}^{(\text{II})}$, $\text{Zn}^{(\text{II})}$, $\text{Mn}^{(\text{II})}$, $\text{Co}^{(\text{II})}$ and $\text{Fe}^{(\text{II})}$ complexes are non electrolytic nature. Biological studies of the ligand and the complexes on two types of

micro organisms showed a wide range of activities compared with the biological activity of the ligand. Namely: Zinc, Cadmium and Mercury complexes exhibit greater inhibition than the ligand, while other complexes of Iron, cobalt, Nickel, Manganese, Copper and Chromium exhibit retarding effects, less than the ligand.



CERTIFICATION

We certify that, this thesis was prepared under my supervision at the Department of Chemistry, College of Science for women at Baghdad University in partial requirements for the **Degree of Master of Science in Chemistry**

Signature:

Supervisor:

Prof.Dr. Yahya Abdul Majid

Signature:

Supervisor:

Asst.Prof.Dr. Mohamad Jaber Al-Jeboori

In view of the available recommendations, I forward this thesis for debate by the examining committee

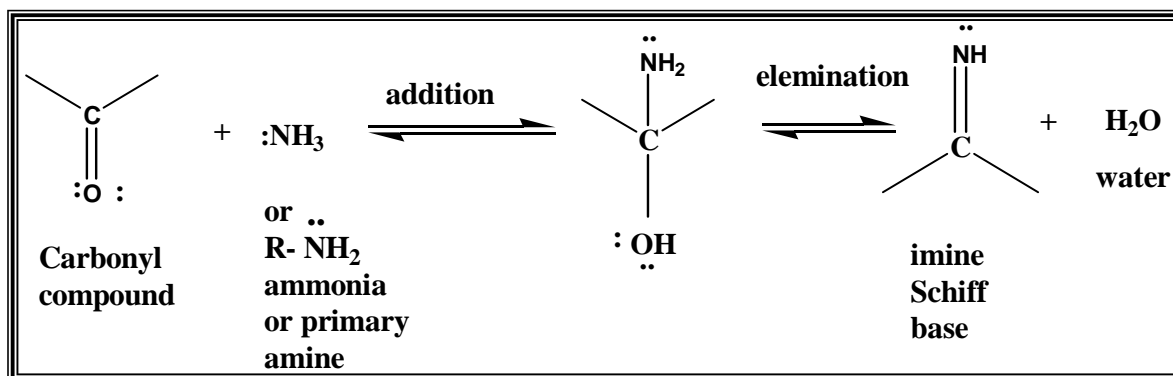
Signature:

Prof. Dr. Yahya Abudl Majid

Head of the Chemistry Department

(1.1) Schiff Bases

In (1864) Schiff reported⁽¹⁾ a new compound called Imine. It was a product by condensation of aldehydes or ketons with primary Amine. The Schiff bases have many various names⁽²⁾, such as Aniles, Benzanils, Azomethines and Ketimines or Aldimines according to the source of the compound; keton or aldehyde. The Schiff bases are recognized by the ability of forming coloured complexes with the transition metal ions⁽³⁾.



Scheme (1-1) The general equation of Schiff base

Imines, Schiff bases and other $\text{C}=\text{N}$ compound can be reduced with LiAlH_4 , NaBH_4 , Na-EtOH , hydrogen and a catalyst, as well as with other reducing agents⁽⁴⁾.

Schiff bases rapidly decompose in aqueous acidic media, but they are very stable in basic solutions⁽⁵⁾. These bases can also be prepared by refluxing of equimolar quantities of aldehydes or ketones with amine or by slow melting for 10 minutes and then isolating and purifying the product by recrystallization, or sublimation under reduced pressure^(6,7).

Staab prepared Schiff base by removing water which formed by condensation of aldehyde and amine by refluxing in benzene and then the residual solution is distilled under vacuum⁽⁸⁾.

Bidentate Schiff bases have been among ligands that are extensively used for preparing metal complexes. These ligands are described according to their donor set as N,N-donor Schiff bases and N,O-donor Schiff bases depending on their structure. Tridentate Schiff bases may be generally considered as derived from the bidentate analogues by adding another donor group, these have been utilized as an ionic ligands having (N,N,O), (N,N,S), (N,O,O) and (N,S,O) donor sets^(9, 10).

(1.2) Macrocycles

The field of the macrocyclic chemistry of transition metals was developed very rapidly because of its applications⁽¹¹⁾ and importance in the area of coordination chemistry⁽¹²⁾. Macrocyclic ligand systems often exhibit unusual properties and sometimes mimic related natural macrocyclic compounds. There is currently considerable interest in complexes of polydentate macrocyclic ligands because of the variety of geometrical forms available and the possible encapsulation of the metal ion⁽¹³⁾.

(1.2.1) Curtis Macrocycles

In 1961 Curtis and House proposed the structure of the first macrocyclic ligand, Fig. (1-1); this was the introduction of azamacrocycles. Since then Curtis had led the field of

mononucleating azamacrocycles. A Curtis macrocycle is an organic framework which holds a transition metal ion via nitrogen atoms, with varying substituents on the carbon atoms. These Curtis macrocycles were formed from the reaction of transition metal diamine complexes with acetone in a 2 + 2 condensation reaction, two acetone molecules are used to form the head-unit. These were condensed with metal ethylenediamine complexes, an example of this is $[\text{Ni}(\text{en})_3][(\text{ClO}_4)_2]$ which forms the side arms, to complete a cyclic Schiff-base structure⁽¹⁴⁾.

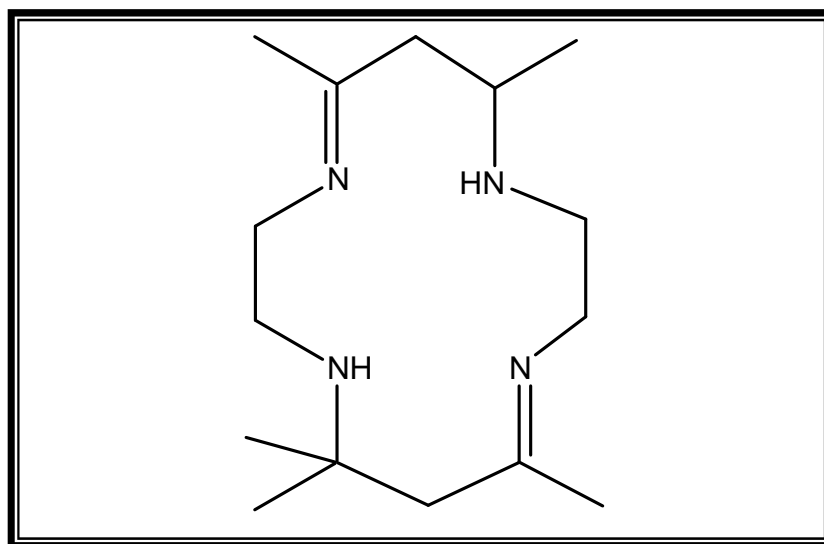


Fig.(1–1) Structure of the first macrocyclic ligand; 5,7,7,12,14,14-hexamethyl-1,4,8,11-tetraazacyclotetradeca-4,11-diene.

Macrocycles became of interest because of the effects they incur on the metals to which they are coordinated. This is due to the fact that macrocycles have fixed geometries because they form a framework to which the metal is coordinated. Therefore the macrocycle is able to impose its geometry on the metal, which can lead to altered properties of the metal. However, in most cases

cooperation to give geometries between those preferred by the metal and the macrocycle are encountered⁽¹⁵⁾.

In 1961 Curtis and House⁽¹⁶⁾ dissolved $[\text{Ni}(\text{en})_3][(\text{ClO}_4)_2]$ in acetone and yellow crystals were obtained, even though a purple solution was expected. This sufficiently bewildered Curtis that he attempted to determine the structure of the yellow crystals. They proposed structures (I) and (II), Fig. (1–2) because the product was diamagnetic and all NH_2 groups were eliminated⁽¹⁷⁾

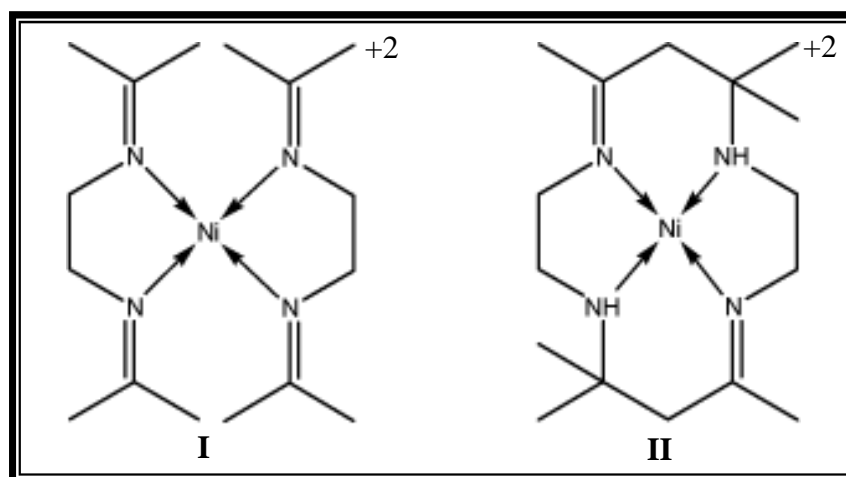


Fig.(1–2) Proposed structures of macrocycles; (I) and (II) respectively

However, IR spectra showed that there were still N–H bonds present so the compound was decomposed in cyanide. The only isolated compound from this was mesityl oxide, Fig. (1–3), from which, the structure was deduced to be that of (II), Fig. (1–2). The macrocycle consisted of four nitrogens, two amines and two imines, connected through two three-carbon bridges and two two-carbon bridges. The macrocycle formed when the two-carbon bridges are opposite each other and so are the three-carbon bridges. The trans

macrocycle, (where the imines are diagonally opposite) Fig. (1-2) (II)), was found to be the major product.

The *cis*, where the imine nitrogen atoms are directly opposite, was found to be the minor. These azamacrocycles formed from the template reactions of acetone with metal-amine compounds are now called “Curtis Macrocycles”⁽¹⁸⁾

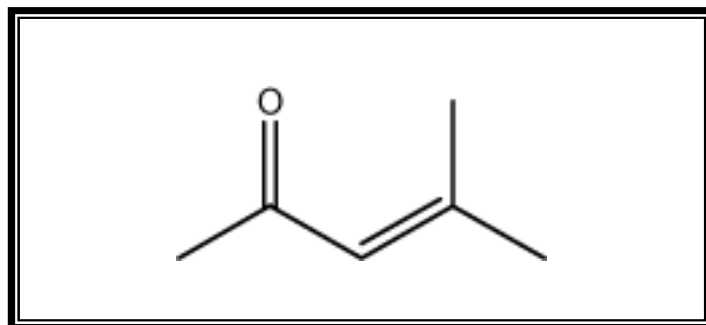


Fig. (1-3) Mesityl oxide

One of the most astonishing things in the creation of these macrocycles was the formation of bonds. not only when there C—N single and double bonds formed but also new C—C bonds. The macrocycles are formed by connecting the metal diamines with a three carbon bridge produced from two acetone molecules, Fig. (1-4)⁽¹⁹⁾.

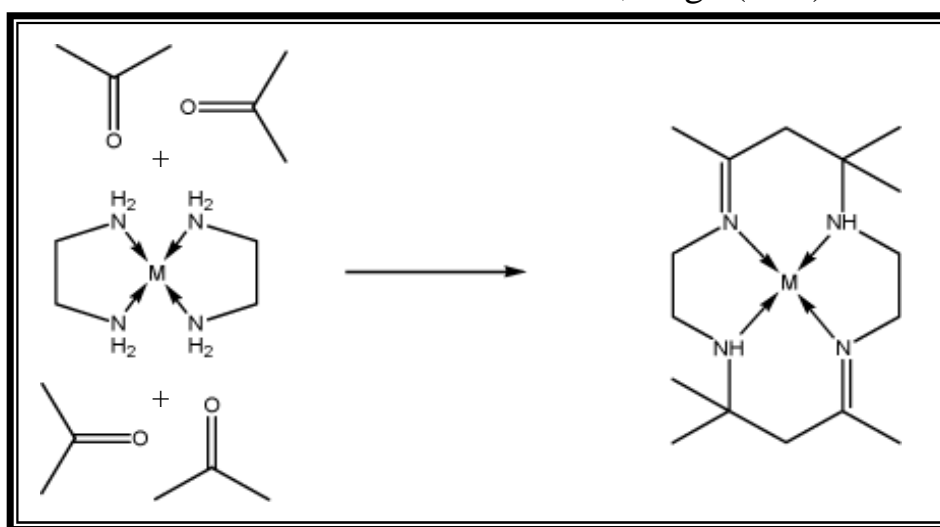


Fig. (1-4) Formation of a Curtis Macrocycle

(1.2.2) Robson Macrocycles

In 1970 Robson⁽²⁰⁾ prepared the first dinucleating Schiff-base macrocyclic ligand, Fig. (1–5) using 1,3–diaminopropane and 2,6–diformyl-4-methyl phenol (DFMP). so that phenol based ligands have played a large role in macrocyclic chemistry⁽²¹⁻²⁵⁾.

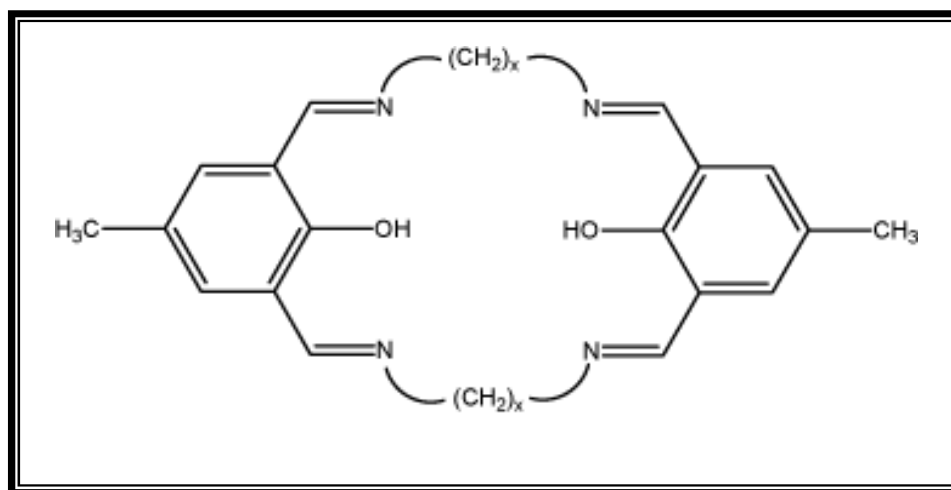


Fig. (1–5) Example of a simple Robson macrocycle

The fact that this Robson macrocyclic ligand was able to hold two metals in close proximity led to the possibility of developing these types of ligands as models for the active sites of metalloproteins^(26,27), many biological catalysts have two or more metals in the active site. Examples of these are hemocyanin, methane monooxygenase, urease Fig., (1–6) and the manganese cluster involved in the photosystem II (PSII) oxygen-evolving reaction in photosynthesis.⁽²⁸⁻³²⁾ The study of a small molecule analogues is important because the active sites of enzymes are surrounded by a protein polymer and difficult to access.

In terms of function, small molecule analogues are synthesized in an attempt to replicate and understand the mechanism of the enzyme.

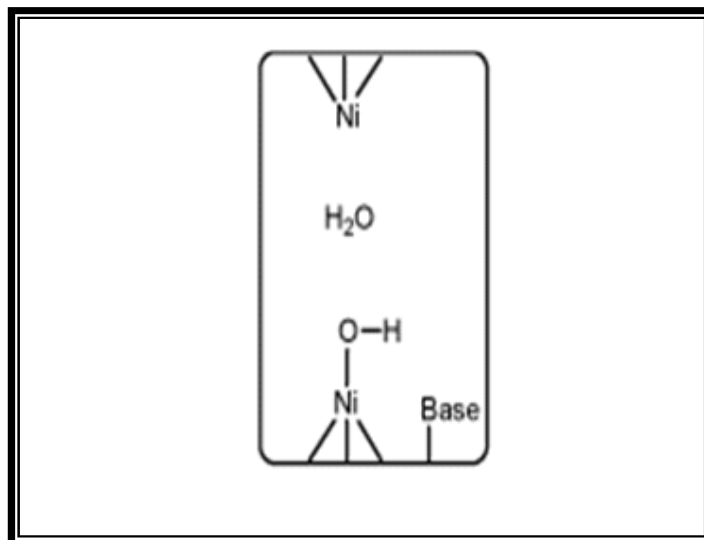


Fig. (1-6) Model for the active site of Urease, which illustrates an enzyme with more than metal present in the active site

(1.3) Compartmental Ligands

Fenton introduced the term “compartmental ligands” in 1977⁽³³⁾ Compartmental ligands are dinucleating ligands and can be divided into three groups⁽³⁴⁾, The first group is macrocyclic ligands, the other two remaining groups are acyclic and which be subdivided into “end-off” and “side-off” ligands, Fig. (1-7). These are also known as pendant-arm ligands. End-off ligands occur when a donor bridge is removed from the macrocycle resulting in one endogenous bridging site and one exogenous bridging site available between the two metals. Side-off ligands arise when a non-donor bridge is removed leaving two endogenous bridges accessible to the metal ions.

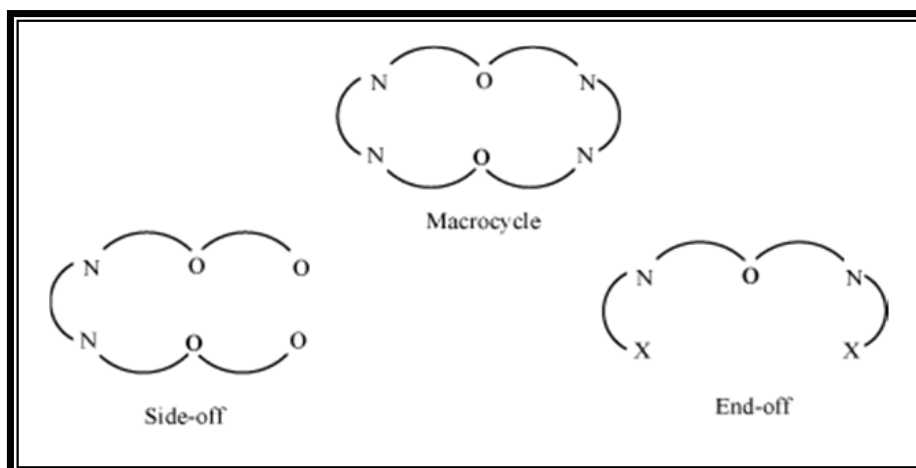
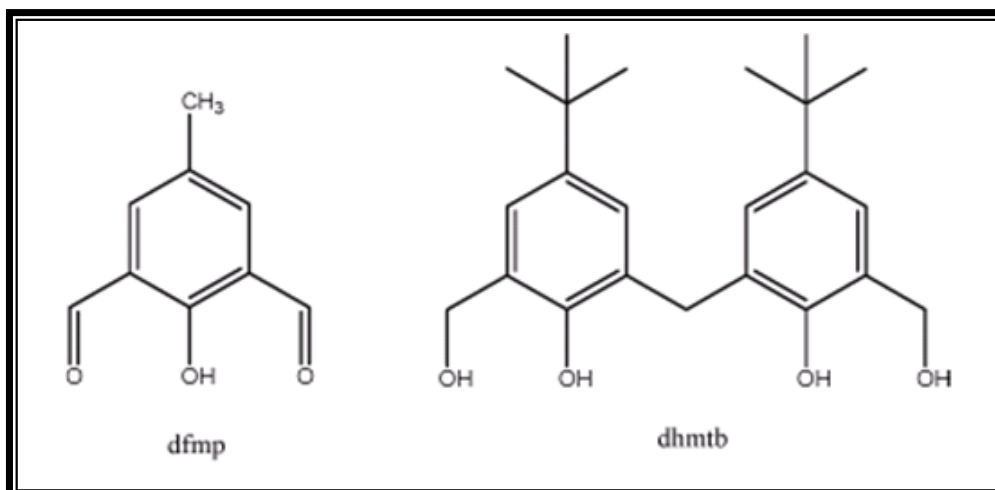


Fig. (1–7) Basic examples of different types of compartmental ligands

Acyclic compartmental ligands are good for mimicking enzymes because they are able to hold multiple metals in close proximity. However, end-off ligands have also enough flexibility to allow the metals to move away from each other if necessary. This is an advantage over traditional macrocycles, and their side-off counterparts, because these macrocycles have rigid and somewhat compact geometries.

(1.3.1) Head units

Pendant-arm ligands are divided into two parts; the head-unit and the pendant arms. Commonly used head-units are dicarbonyl compounds, more specifically 2,6-disubstituted phenols, an example of this is DFMP, which is a widely used head-unit in macrocycles and acyclic ligands^(35,36), 5,5'-Di-tert-butyl-2,2'-dihydroxy-3,3'-methanediyl-dibenzene methanol (DHTMBA) is an extension of this head unit. This has been used extensively by McKee in pseudocalixarene macrocycles and pendant arm ligands.

(1.3.1.1) DHTMBA**Fig.(1-8) DFMP and DHTMBA head units.**

It is an ideal head unit because it has flexibility which made it able to rotate around the carbon atom which joins the two rings, also there is a free rotation in the arms. There are two free phenol groups which creates uncertainty to where and how the metals will bind. The inclusion of the two phenol groups makes it possible for the ligand to bind with more than two metals.

(1.3.2) Pendant Arms

There are many types of pendant arms Fig. (1-9), both symmetric and unsymmetric have been used as ligand. However, if biomolecular modelling is the intention, arms with biological relevance have an obvious advantage.

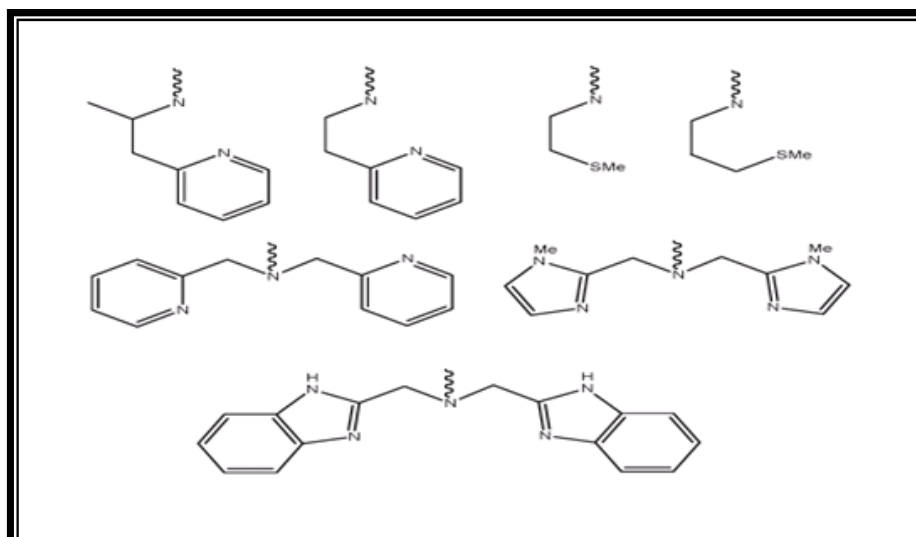


Fig. (1–9) Examples of pendant arms. The bottom structure is Bis(benzimidazole-2-ylmethyl)amine (BBIM)

(1.3.2.1) BBIM

The ligand, 2,2-(N,N'-bis(benzimidazole-2-ylmethyl)methylamine-5,5'-ditertiobutyl-3,3'methanediyl-dibenzyl alcohol Fig. (1–10) proposed in this study is an end-off compartmental ligand. It is a dinucleating ligand in which two separate donor areas are exist. The head-unit consists of DHTMBA. The arms are bis(benzimidazole-2-ylmethyl)amine (BBIM), which have been chosen because they contain imidazole groups which have biological relevance in two different manners, The first & the second is to do with inhibition of the yeast *Candida albicans*.

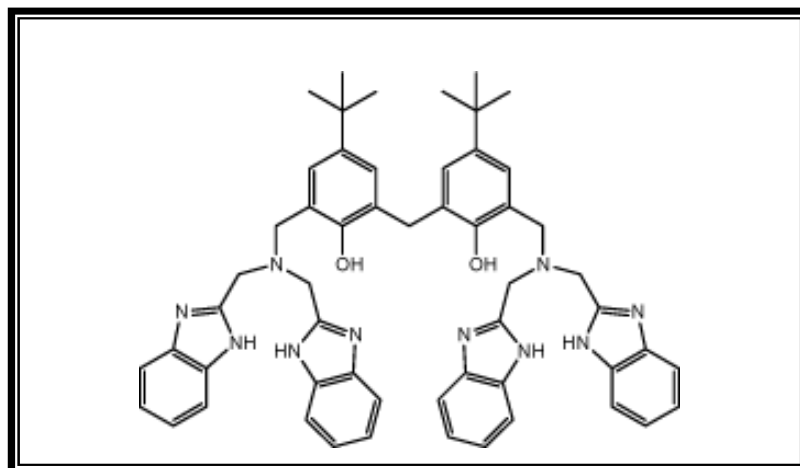


Fig. (1–10) 2,2-(N,N'-bis(benzimidazole-2-ylmethyl)methyl)amine-5,5'-ditertibutyl-3,3'-methanediyl-dibenzyl alcohol

Recent experiments have shown that metal complexes containing imidazole groups are effective in inhibiting the growth of the fungal yeast *Candida albicans*⁽³⁷⁾ Overuse of drugs in present times caused mutations in bacteria, fungi and viruses to take place more rapidly. When mutations take place the effectiveness of the drug designed to inhibit the disease can be compromised, this causes drug resistance. *Candida albicans* is a very common yeast which causes many diseases⁽³⁸⁾ This is why it is essential to create new drugs with new mechanisms of drug delivery. Metal complexes with imidazole groups have a potential here, the other more specific reason that the BBIM arms have a biological significance is that the benzimidazole segment is very similar to part of the histidine side chain Fig. (1–11) and many metal centers in enzymes are surrounded by histidines. A prime example of this is hemocyanin.

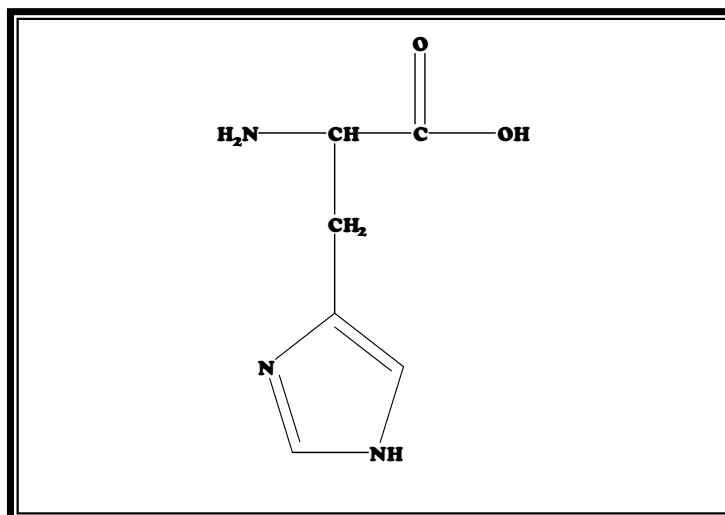


Fig. (1-11) part of the histidin side chain

(1.4) Macrocyclic compounds containing nitrogen as donor atoms.

Compounds containing nitrogen, oxygen, and sulfur as donor atoms play a vital role in preparation of complexes with different ions, as these complexes are most beneficial in medical diseases and cancers that catch the body. For example Tc and Re complexes have been prepared and used in radio pharmaceutical applications; furthermore complexes having sulfur, oxygen and nitrogen atoms have been used as mimics of some enzyme or coenzyme catalysts as nickel, copper and zinc complexes⁽³⁹⁻⁴³⁾.

(1.5) Reactivity of 2,6-diformylimin compounds toward metal ions

Metal complexes with open chain and macrocyclic tetrakis-Schiff base ligands are of great interest. Ligands derived from the

condensation of 2,6-diformyl-4-methyl phenol with diamine, have been studied extensively in view of their importance in basic and applied chemistry⁽⁴⁴⁾. The most usual ligand and complexes were obtained by Okawa and co-worker⁽⁴⁵⁾, they reported dinuclear complexes with Zn^{II} and Cu^{II} .

Infrared spectra showed that, the ligands coordinated to the metal ions through both nitrogen and oxygen atoms, Fig. (1–12)

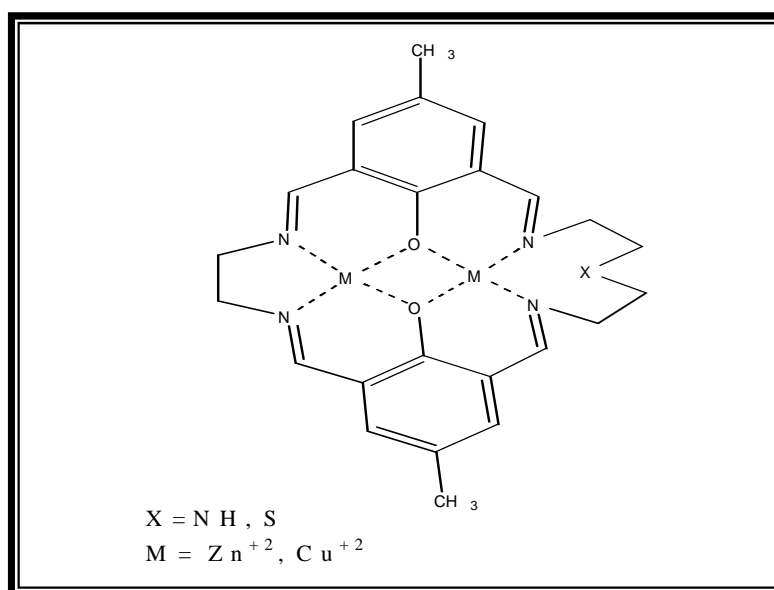


Fig. (1–12) the chemical structure of Zn^{II} and Cu^{II} complexes with macrocyclic ligands

Atkine and co-worker⁽⁴⁶⁾ have reported the synthesis of macrocycle ligand, which was prepared from the reaction of 2,6-diformyl-4-methyl phenol with 1,3-propylene diamine in presence of HBr (48%). Binuclear complex with $Pd^{(II)}$ was reported. Fig. (1-13).

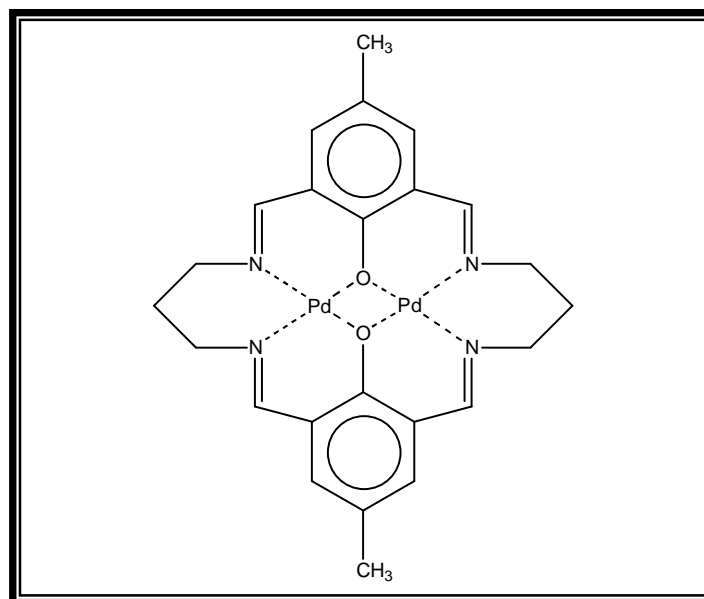


Fig. (1–13) The chemical structure of the binuclear complex of Pd^(II)

Santokh and co-worker⁽⁴⁷⁾ have studied the condensation of 2,6-diformyl-4-(R)-phenol(DFP) (R=Me, t-Bu) with 3,6-bis-(aminoethyl) thio-pyridazin (PTA). Fig. (1-14), they concluded the followings:

- 1- The reaction of Cu⁺² with these ligands resulted in a dinuclear complexes [Cu₂(L¹)] [BF₄]₂ and [Cu₂(L²)] [BF₄]₂.CH₃OH.
- 2- Complexes and ligands were characterized by spectroscopic (¹H NMR, Far-IR, FTIR and UV), magnetic and electrochemical properties.
- 3- X-ray crystal structure of the dinuclear copper II [Cu₂(L¹)] [BF₄]₂.H₂O [where L¹ = 34 memberd macrocyclic ligand], showed the geometry about Cu⁺² is distorted trigonal bipyramidal. The structure exhibits a significant distortion at the phenoxide-bridge dicopper centres and brings the pyridazine rings into a position for weak contact, Fig. (1–15)

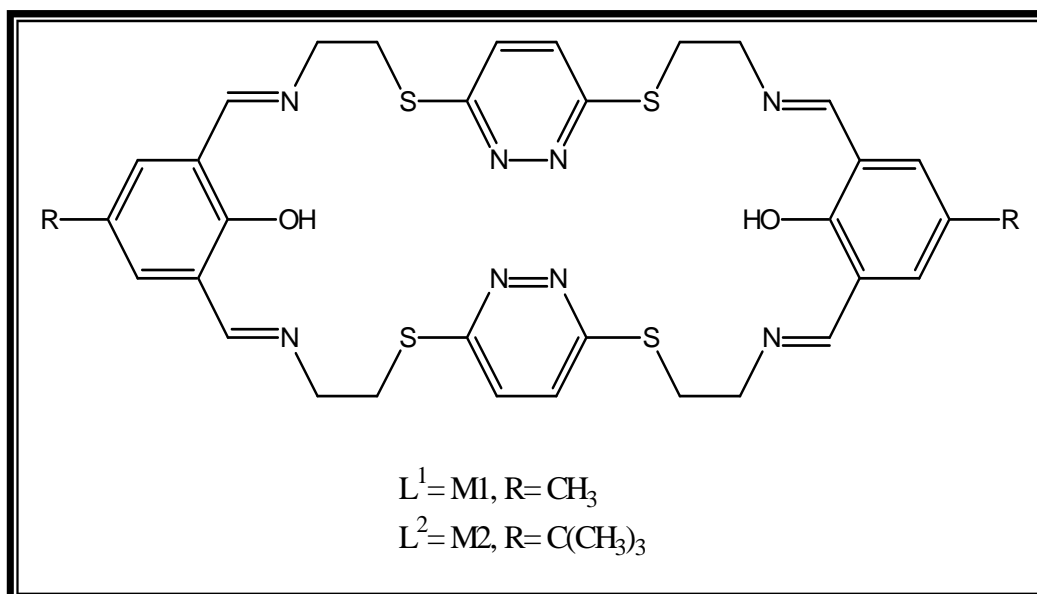


Fig.(1-14) The chemical structure of macrocyclic ligands

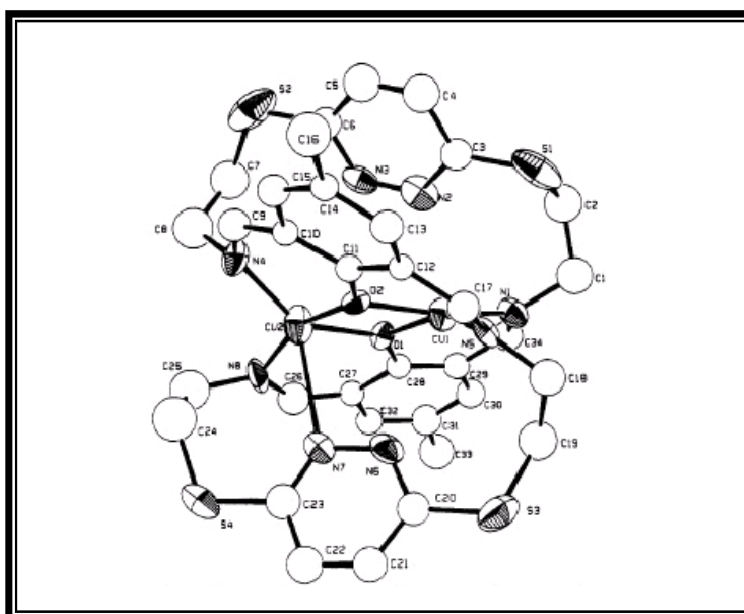
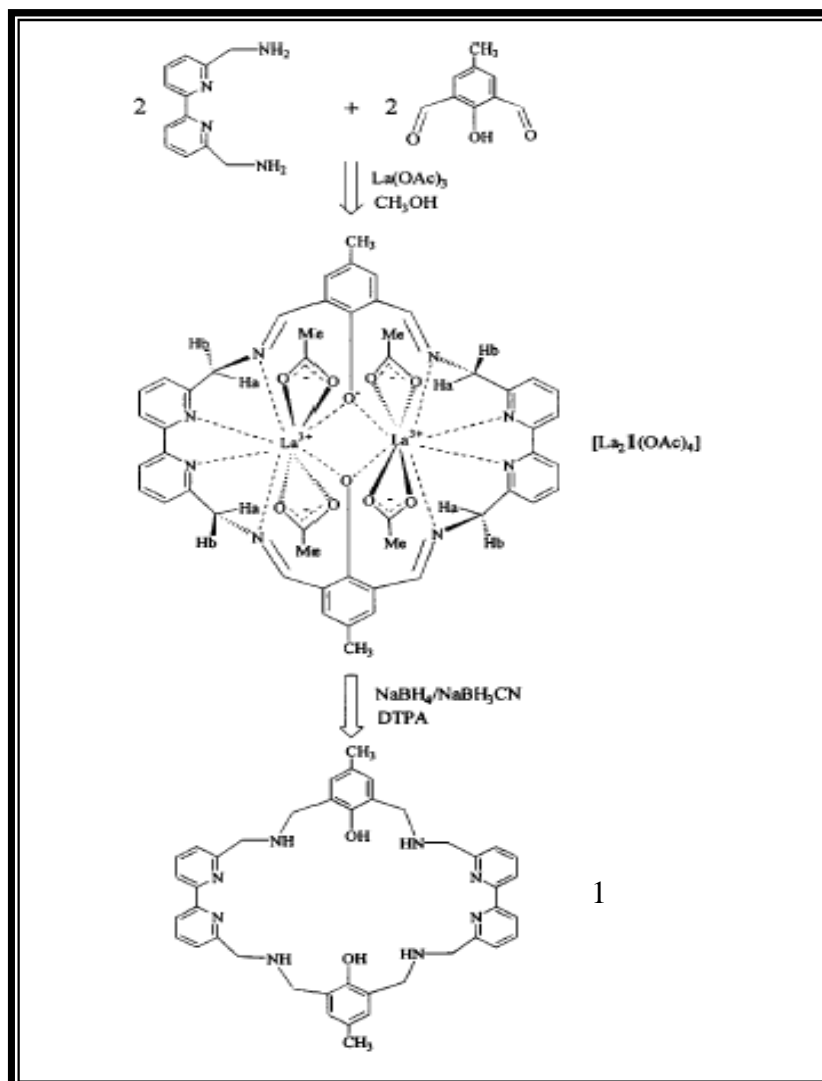


Fig. (1-15) X-ray Structure of $[Cu_2L^1][BF_4]_2 \cdot H_2O$

Wang and co-worker⁽⁴⁸⁾ have described the synthesis and characterisation of a series of four dinucleating polyaza macrocyclic ligands containing aromatic phenol, pyridine, or bipyridine units. The complexes were prepared by the [2+2] template condensation of 2,6-diformyl *p*-cresol with 6,6-bis-(aminomethyl)-2,2-bipyridyl in

the presence of lanthanum acetate. A homodinuclear complex of a Schiff base macrocycle $[\text{babp}]_2(\text{dfc})_2$ was reported [1].

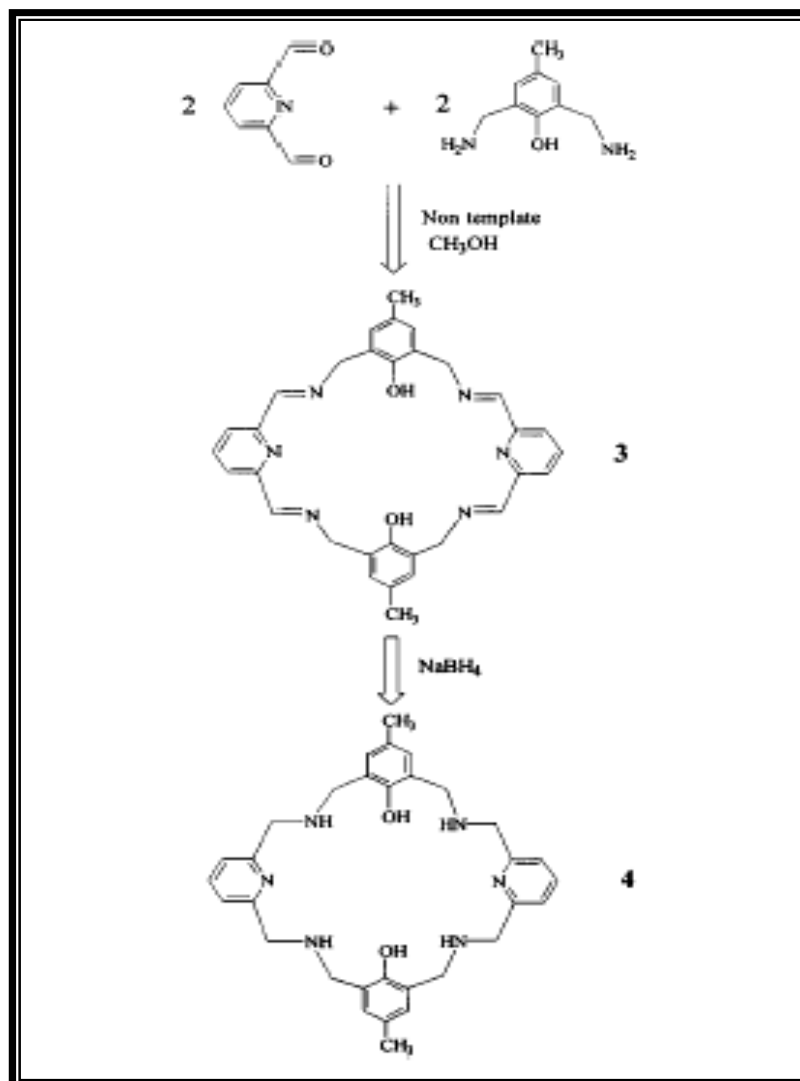
Hydrogenation of the solution of $[\text{La}_2(\text{L}^1)(\text{OAc})_4]$ with sodium cyanotrihydroborate in methanol gave the metal free macrocycle $[\text{babp}]_2(\text{dfc})_2$. [2]. The synthetic pathways illustrated in Scheme (1–2).



Scheme (1-2) The synthesis route of the template condensation of 6,6'-bis(aminomethyl)-2,2'-bipyridyl With 2,6-diformyl-*p*-cresol

Ligand (4) was prepared by two steps, the [2+2] metal-free condensation of 2,6-diformyl-pyridine with 2,6-bis(aminomethyl)-*p*-cresol gave the Schiff base macrocycle $(\text{bac})_2(\text{dfp})_2$ [3].

Reduction of $[(bac)_2 (dfp)_2]$ [3] with sodium borohydride resulted in the hydrogenated hexaaza– macrocycle $[R (bac)_2 (dfp)_2]$ [4] (where $R= Me, CH_3O$. The synthetic pathways illustrated in Scheme (1–3).



Scheme (1-3) The synthesis route of the non template condensation of 2,6–bis(aminomethyl)–*p*–cresol with 2,6–diformylpyridyl

Under strongly acidic condition (48% HBr), the free ligand [4] was crystallised as a hydrobromide salt $[L^4][H_2O \cdot 7HBr]$ in the monoclinic system.

The compounds $[La_2L^1(OAc)_4]$, [2], [3] and [4] were characterised by 1H , ^{13}C and $^1H-^1H$ 2D cosy NMR, UV-Vis and

FAB mass spectroscopy. Erxleben and Hermn⁽⁴⁹⁾ have reported the synthesis and characterisation of a series of Schiff base ligands derived from the reaction of 2,6-diformyl- methyl phenol with N,N'-dimethyl ethylene diamine in CHCl₃ Fig.(1-16).

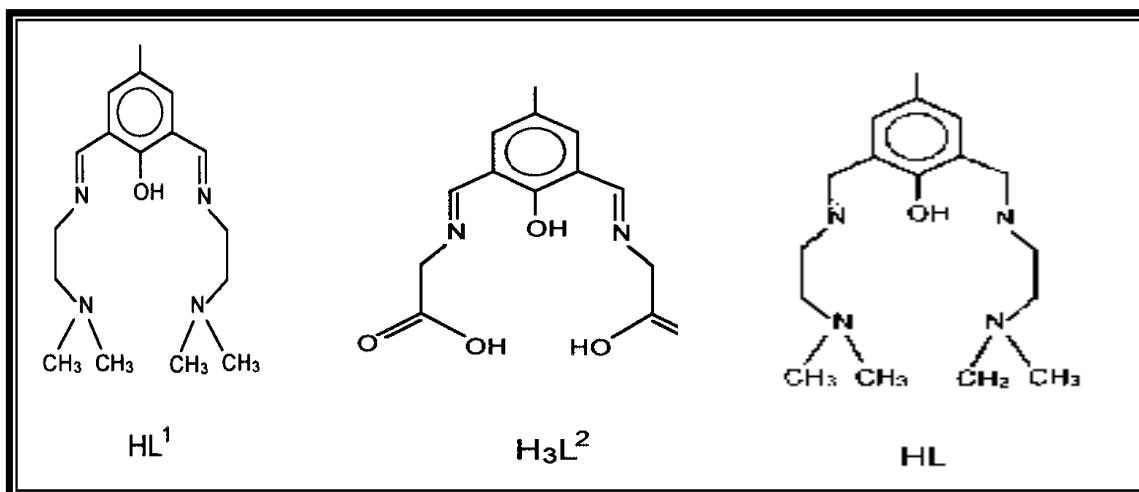
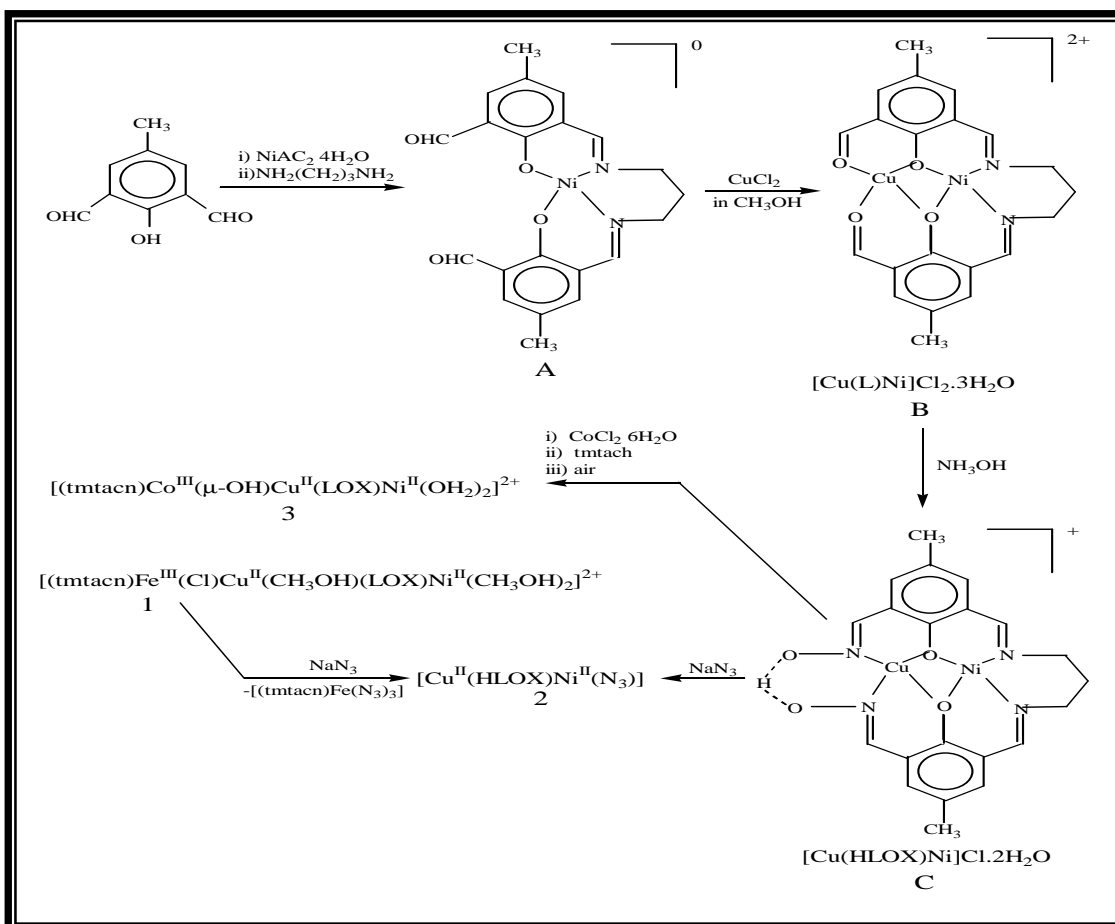


Fig. (1-16) The chemical structure of schiff base ligand

The reaction of Zn^{II} ion with these ligands gave complexes of the general formula [Zn₂(L¹)(CH₃CO₃)₂]X (where X=ClO₄ or PF₆), [(Zn₂(L²)(CH₃CO₃))₂,Zn(H₂O)₄].4.5H₂O and [Zn(L³)Cl₃] 1.5H₂O. The compounds have been characterised by elemental analysis, I.R, (UV-Vis), ¹H NMR and X-ray crystallography. The coordination geometry of Zn atom is best described as distorted trigonal bipyramidal.

Chaudhuri and co-worker⁽⁵⁰⁾ have reported the synthesis, characterisation and exchange coupling in bis-(heterodinuclear) and a linear heterotrinnuclear complexes of the general formula [(Cu^{II}(HLOX) Ni^{II}(N₃)₂)] and [(tmtacn) Co^{III}(μ-OH) Cu^{II}(LOX) Ni^{II}(HLOX) Ni^{II}(N₃)₂)] and [(tmtacn) Co^{III}(μ-OH) Cu^{II}(LOX) Ni^{II}(OH)₂]. The dinuclear complexes were prepared by a template reaction. The trinuclear complex [(tmtacn) Co^{III}(μ-OH)

$\text{CuII}(\text{LOX}) \text{NiII} (\text{OH})_2\}_2]^{+2}$ was prepared from the reaction of dinuclear complex with $\text{CoCl}_2 \cdot 6\text{H}_2\text{O}$ tmtacn using air as oxidant [Where (tmtacn) = 1,4,7-trimethyl – 1,4,7, triazacyclo norane; OX = oxime], Scheme (1–4).



Scheme (1–4) The preparation route of heteronuclear complexes

The complexes were characterised by IR, EPR spectroscopy, and X-ray single crystal. The X-ray single crystal for the trinuclear complex showed the geometry about (Ni, Co), (Cu) is octahedral and square pyramid respectively, Fig. (1–17).

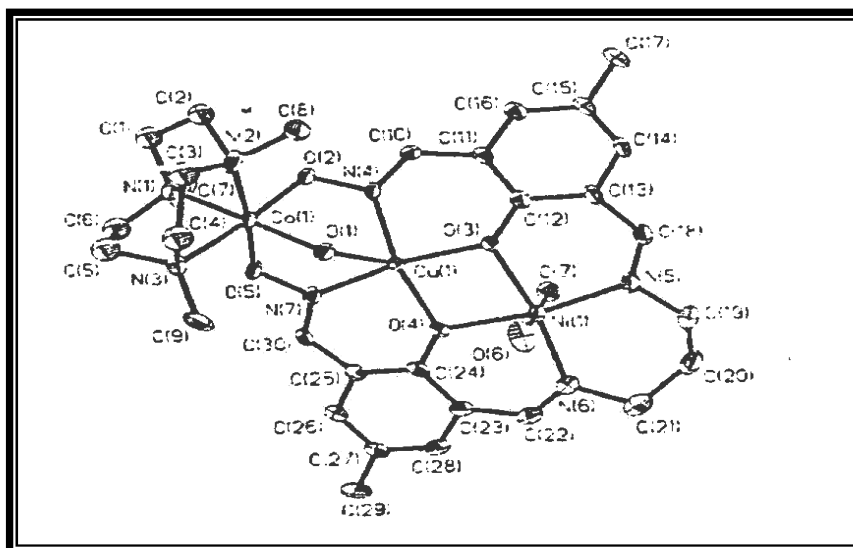


Fig. (1-17) X-ray Structure of Trinuclear Complex [(tmtacn) $\text{Co}^{\text{III}}(\mu\text{-OH})_2\text{Cu}^{\text{II}}(\text{LOX})\text{Ni}^{\text{II}}(\text{OH}_2)_2$] $^{+2}$

In (2002) a number of dinuclear complexes with macrocyclic ligands have been synthesised⁽⁵¹⁾, they were prepared from the reaction of (2,6-diformyl-4-methyl phenol) with 1,2-ethylenediamine and 1,2-phenylene diamine respectively. They were obtained as (Bph_4) salts, Fig.(1-18). The ligands were reacted with $(\text{Ni}^{\text{II}}, \text{Pd}^{\text{II}}, \text{and } \text{Pt}^{\text{IV}})$ Dinuclear complexes of the general formula were obtained.

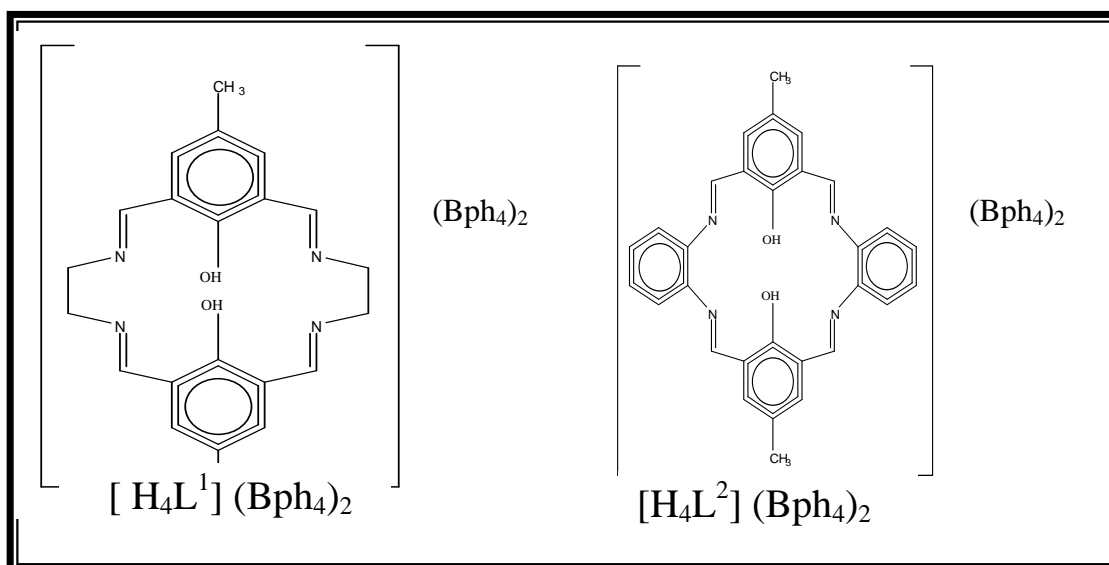


Fig. (1-18) The structure of macrocyclic ligand

$(\text{Et}_2\text{NH})_2 [\text{Pt}_2(\text{L}^1)]\text{Cl}_4$, $[\text{Ni}_2(\text{L}^1)](\text{Bph}_4)_2$ and $[\text{Pd}_2(\text{L}^1)](\text{Bph}_4)_2$, spectroscopic along with elemental analysis studies suggested square planar geometry about Ni^{II} and Pd^{II} while an octahedral structure is proposed about Pt^{IV} ion.

In (2002) Kong and co-workers⁽⁵²⁾ reported, the synthesis of homodinuclear ferrous complex with 2–6 membered macrocyclic ligand (BTBP) [Where BTBP=3,6,10,18,22,25-hexaaza–31, 32-dihydroxy-14,29-dimethyl–tricycle [25, 3, 1, 1, 11, 17] ol triaconta-1 (30), 12, 14, 16, (32), 27, 28-hexaene], Fig.(1–19). The complex was characterised by elemental analysis, NMR, FAB-ms electrochemistry and X-ray crystal structure.

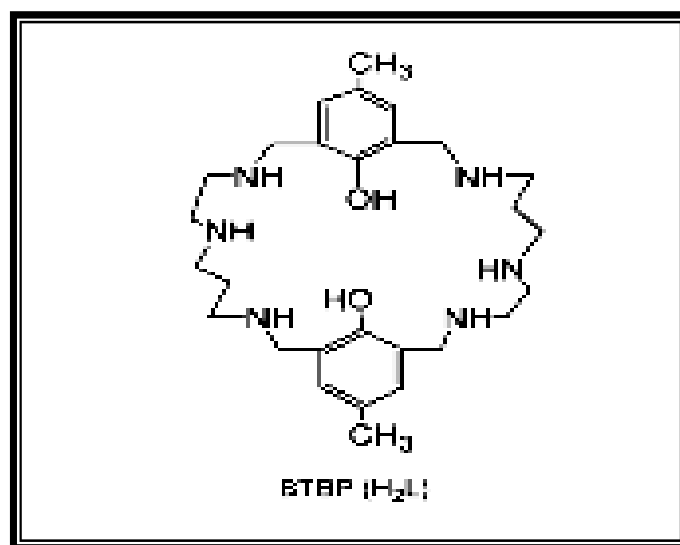
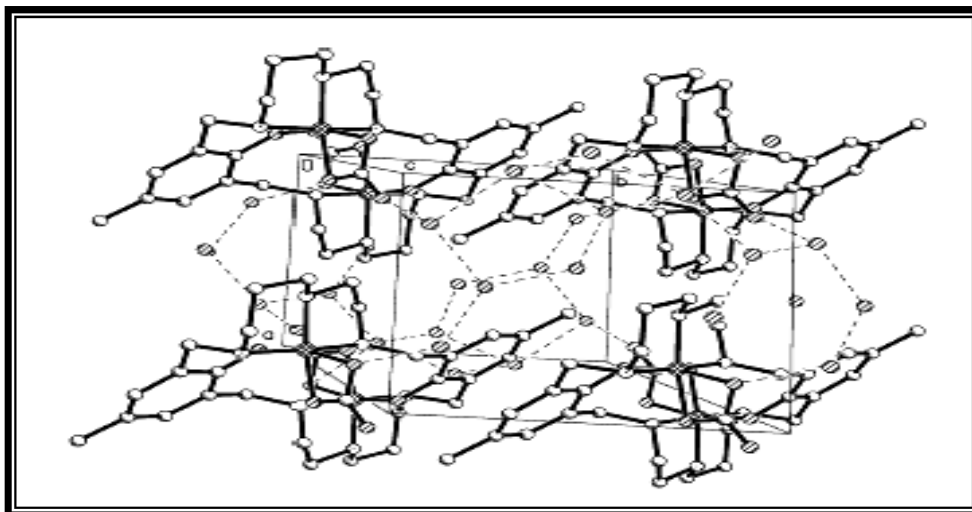


Fig. (1-19) The structure of [BTBP] ligand

Potentiometric equilibrium studies indicated that a variety of protonated, mononuclear and dinuclear complexes are formed with Fe^{II} and Fe^{III} from pH (2) through pH (12) in aqueous solution.

X-ray data showed two Fe^{II} ions are located in separate compartment and each of them is six-coordinated. The geometry

around the two iron atoms is the same, both being a pseudo-octahedral Fig. (1–20).



**Fig. (1–20) Cell packing diagram of homodinuclear
[Fe₂BTBP(CO₃)₂].(H₂O)₁₂ complex**

In (2002) Kong and co-worker⁽⁵³⁾ have reported the synthesis of nucleating hexaaza-diphenol macrocyclic ligand (BTBP) forming a number of protonated or hydroxomononuclear, [(M)(BTBP)], homodinuclear [(M₂)(BTBP)]⁺³ (M= Cu^{II}, Ni^{II}, Cd^{II}, Zn^{II} and Pb^{II}) and hetrodinuclear [Cu(M)BTBP] (M=Ni^{II}, Co^{II}, Fe^{II}, Zn^{II}, Cd^{II}) complexes. pH potentiometric studies showed that, the dinuclear complexes were formed via the mononuclear chelates in which two kinds of coordination patterns are observed, one is when metal ion binds half of the coordination sites of the macrocycle (N₃O⁻), Fig. (1–21) and the other is when metal ion occupied salen-like sites of the macrocycle (N₃O₂)⁻².

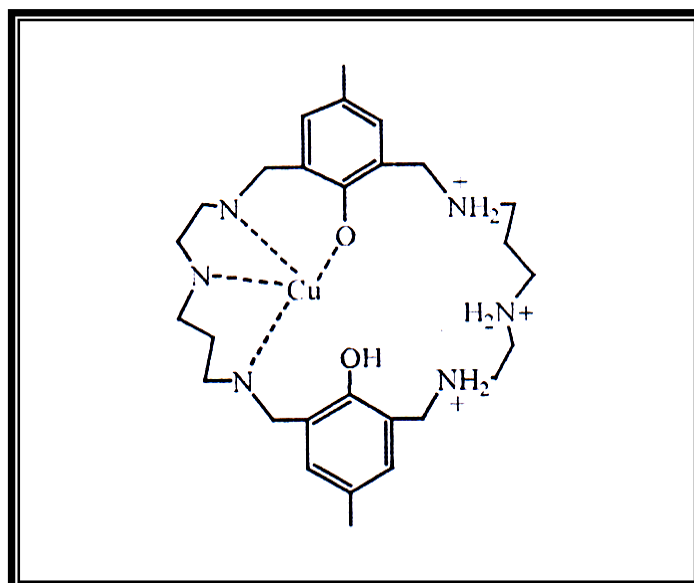


Fig. (1-21) Monochelate system of $[\text{Cu}(\text{BTBP})]^{+3}$ complex

Crystallographic result of a homodinuclear nickel complex, showed the geometry around Ni^{II} is an elongated octahedral, Fig. (1-22).

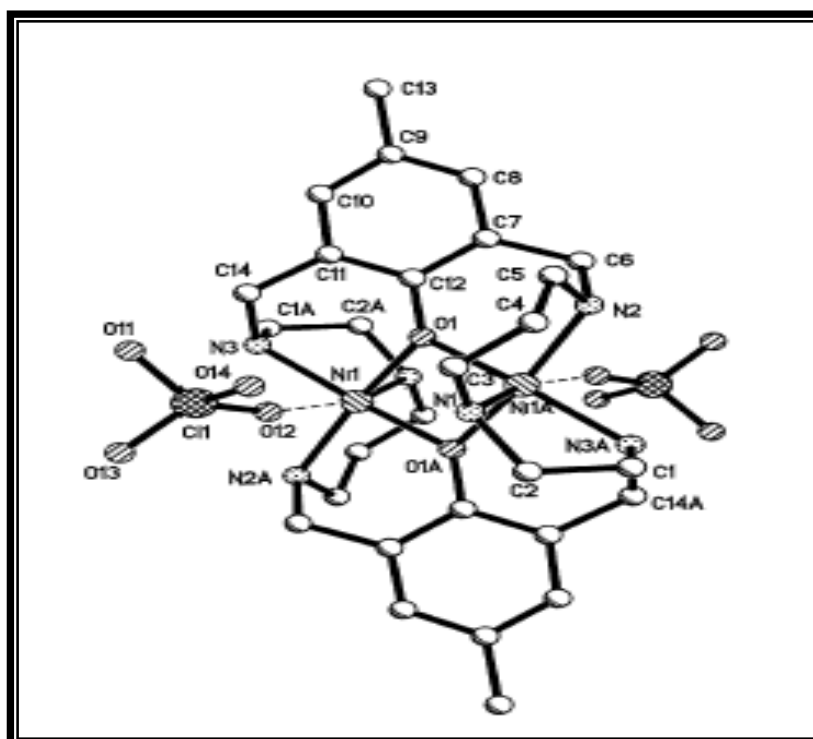


Fig. (1-22) ORTEP structure of homodinuclear $[\text{Ni}_2(\text{BTBP})].\text{ClO}_4$ complex

In (2003) Schröder and co-worker⁽⁵⁴⁾ have reported the synthesis of four binuclear Zn^{II} complexes of the Schiff base macrocycles, formed by the [2+2] template condensation of 2,6-diformyl-4-methyl phenol with 1,2-diaminoethane [H_2L^1], 1,3-diamino propane [H_2L^2], 1,4-diamino butene [H_2L^3] and 2,6-diacetyl-4-methyl phenol with diaminoethane [H_2L^4], Fig. (1-23).

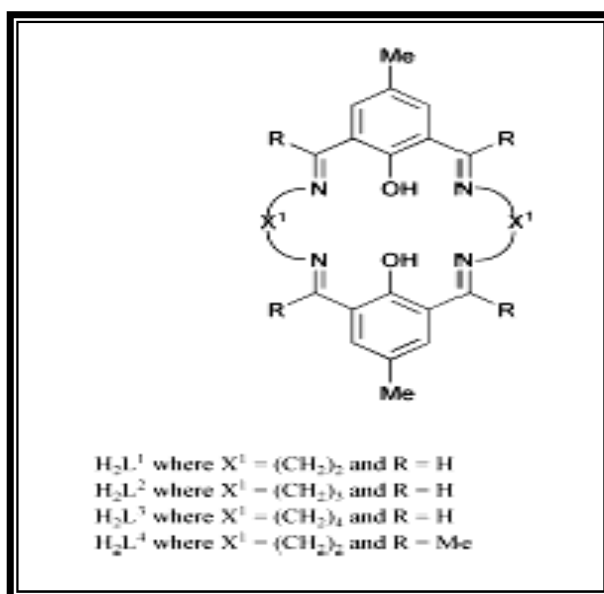
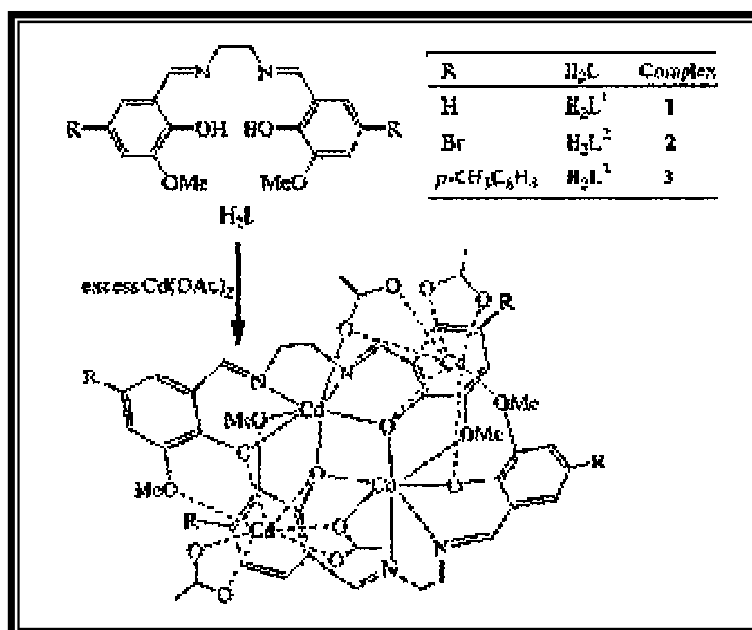


Fig. (1-23) The structure of four macrocyclic ligands

The complexes were characterised by IR, 1H NMR, FAB-mass spectroscopy, and microelemental analysis.

In (2005) Wing-Kit and co-workers⁽⁵⁵⁾, have described the synthesis and structural characterization of some tetranuclear Cd^{II} Schiff base complexes.

Reaction of the hexadentate Schiff base ligand (H_2L) with an excess of cadmium II acetate yield cadmium complexes of the general formula $[Cd_4(L^n)_2(OAc)_4]_2$ [Where; $L^1 = N,N$ bis(3-methoxysalicylidene) ethylene-1,2-diamine], Scheme (1-5).



Scheme (1-5) The synthesis route of $[\text{Cd}_4(\text{L}^n)_2(\text{OAc})_4]_2$ complexes

These new complexes were found to display rich photophysical properties, and they all exhibited low-temperature phosphorescence in the frozen state.

The complexes were fully characterised by spectroscopic (FT-IR, NMR and FAB-mass spectroscopy) methods. The X-ray crystal structure for $[\text{Cd}_4(\text{L}^1)_2(\text{OAc})_4]_2$ showed the geometry about Cd^{II} is pentagonal bipyramidal, Fig. (1-24).

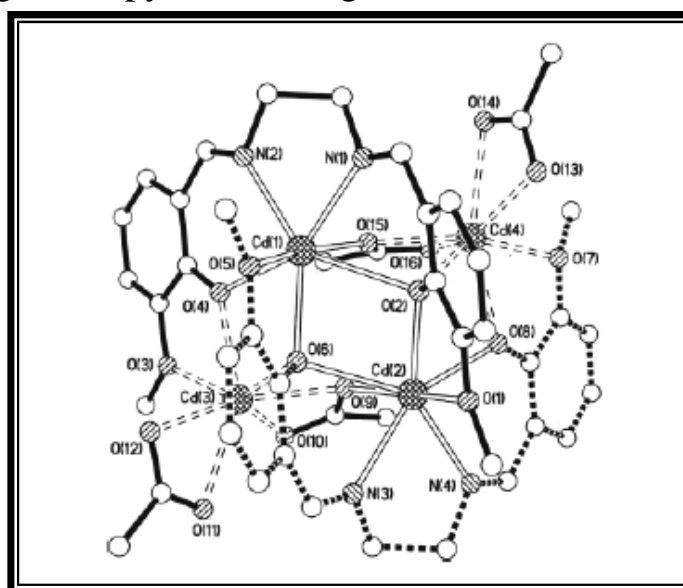


Fig.(1-24) Molecular Structure of $[\text{Cd}_4(\text{L})_2(\text{OAc})_4]_2$

In (2005) Aldulaimi has reported⁽⁵⁶⁾ the synthesis and characterisation of dinuclear complexes of the general formula $[M_2(HL)Cl_2(H_2O)_2]^n X$ [Where; HL=bis(2-hydroxy-3-formyloxime-5 methyl benzaidimine)N-ethylene], Fig.(1–25); $M=Cr^{III}$, $n=+1$, $X=Cl$; $M=Ni^{II}$, $n=0$, $X=0$ and $[M_2(HL)]^{+1}(Cl)(H_2O)$, [Where $M= Mn^{II}$, Fe^{II} , Co^{II} , Cu^{II} , Cd^{II}] and $[Zn_2(H_2L)Cl_2].H_2O$

These complexes were characterised by IR, UV–Vis, mass spectroscopy and elemental analysis [(C.H.N) and (A.A)].

The analysis showed the geometry about Cr^{III} , Ni^{II} as a distorted octahedral, while tetrahedral structure is reported for $[Mn^{II}$, Fe^{II} , Co^{II} , Cu^{II} and $Cd^{II}]$ complexes, Zinc complex showed a distorted trigonal bipyramidal structure about metal ion.

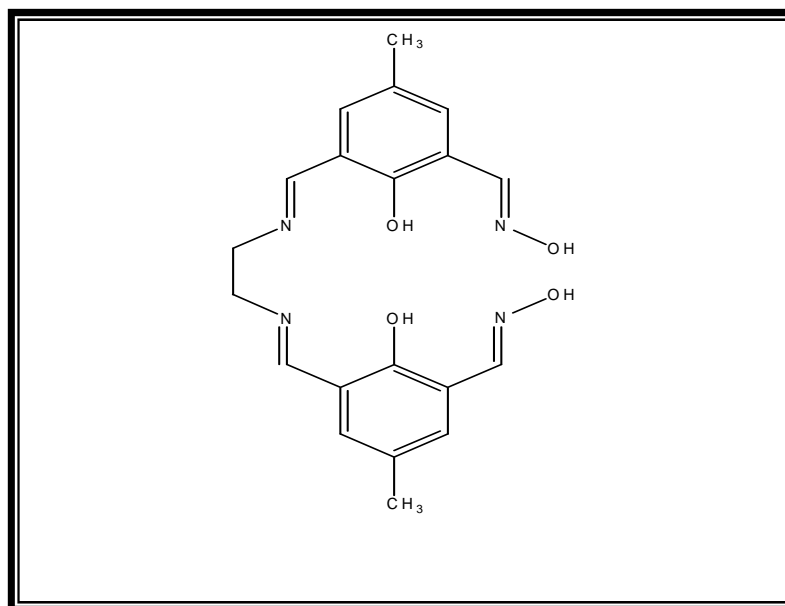


Fig. (1–25) The Structure of bis (2-hydroxy-3-formyloxime–5 methyl benzaidimine) N-ethylene] Ligand

In (2006) Tumer and co-workers⁽⁵⁷⁾ have reported the synthesis of a series of Schiff base ligands (HL^1 – HL^6) from the reaction of

2,6-diformyl-4-t-butyl phenol and 2,6-diformyl-4-methyl phenol with various aromatic amines in ethanolic solution Fig.(1-26).

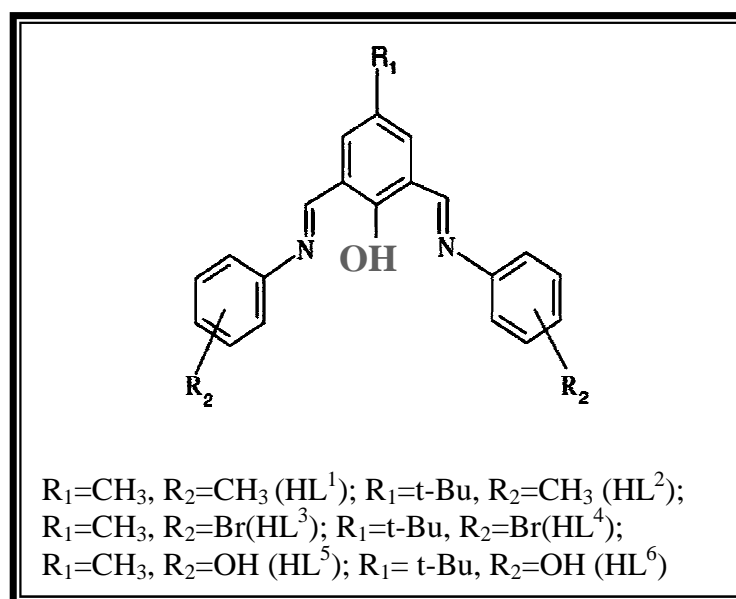


Fig. (1-26) General Structure of The Schiff Base Ligands .

The reaction of Cu^{II} with these ligands gave complexes of the general formula $[\text{Cu}_2(\text{L}^n)\text{Cl}_3]$ and $[\text{Cu}_2(\text{L}^n)(\text{dp})_2]\text{Cl}_3$, [Where $n = 1, 2, 3, 4, 5$ and 6 ; $\text{dp} = 2, 2$ -dipyridyl]⁽⁵⁸⁾.

The compounds have been characterised by elemental analyses, FT-IR, electronic spectra, ^1H and ^{13}C NM.R and mass spectroscopy. These studies revealed the geometry about Cu^{+2} is square planar, Fig. (1-27).

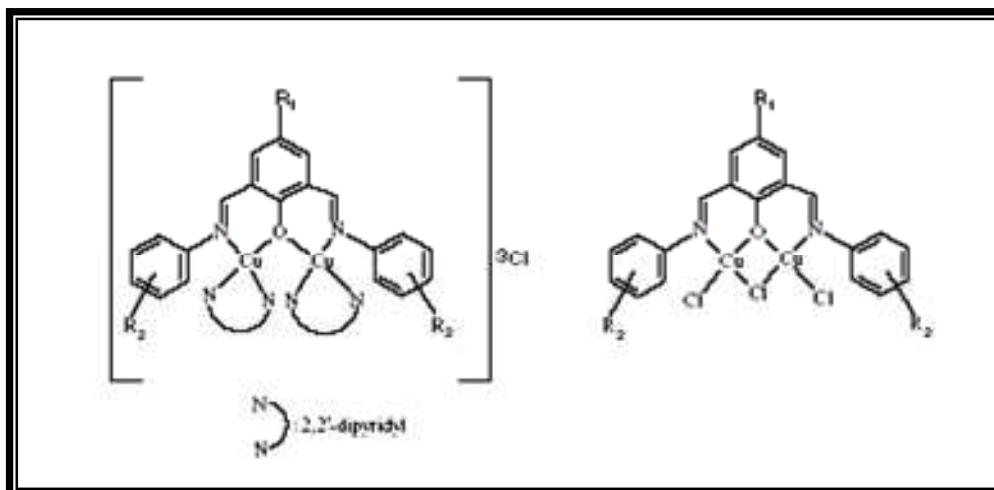


Fig. (1–27) The structure of $[\text{Cu}_2(\text{L}^n)\text{Cl}_3]$ and $[\text{Cu}_2(\text{L}^n)(\text{dp})_2]\text{Cl}_3$ complexes

(1.6) Uses and application of 2,6– Diformylimino and their complexes

2,6-Diformylimino compounds and their complexes with transition metals have played a great importance in industry, chemistry, medicine and biochemistry.

(1.6.1) Applications in industry

A binuclear homometallic macrocyclic (Cu) complex was prepared from the reaction of Cu^{+2} ion with the ligand resulting from the reaction of 2,6-diformyl-4-methyl phenol with 1,2-phenylene diamine. This complex was supported on zirconium pillared montmorillonite to obtain a heterogeneous catalyst^(59,60), this catalyst was used to carry out oxidation of cyclohexane using oxygen as oxidant in the absence of initiators and solvents⁽⁶¹⁾. Studies by Burrows and co-workers⁽⁶²⁾ and later by Kureshy⁽⁶³⁾ and co-worker proved that

manganese and nickel complexes with diformylimino ligands are also active catalysts in the epoxidation of alkenes.

(1.6.2) Applications In Biochemistry

Transition metals complexes of 2,6-diformyl-imino are of particular interest as biological model compounds. Numerous chemical studies have been made on the Zn^{II} complexes as a model in the active sites of number of biological systems including phospholipidase C and Teucine amino peptidase⁽⁶⁴⁾. Also ligands derived from the condensation of 2,6-diformyl-4-phenol with a diamine have been studied extensively in view of their significance as biomimetic catalyst in the process of oxygenation⁽⁶⁵⁾. Several chemical studies have been made on the diiron complexes derived from the condensation of 2,6-diformyl-4-phenol as a model for iron-oxoproteins⁽⁶⁶⁾.

(1.6.3) Applications in chemistry

Beside supramolecular and bioinorganic studies⁽⁶⁷⁾, cadmium–diformylimino–complexes also play an important role in luminescence. Numerous luminescent polynuclear transition metal complexes of d^{10} –transition metal such as Zn^{II} , Cd^{II} , Cu^I , Ag^I , Au^I have been reported⁽⁶⁸⁾. The use of Cd^{II} complexes as luminescence materials has added an advantage because the coordination environment of Cd^{II} is different from other d^{10} transition metal. Dinuclear lanthanide complexes have also been used to study the nature and application of lanthanide metal–metal interactions in

phosphor and they have been used as luminescence probes to determine the metal–ligand interactions and the local coordination symmetry⁽⁶⁹⁾.

(1.6.4) Applications in Medicine

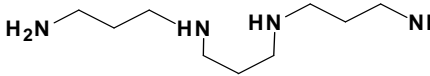
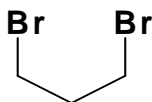
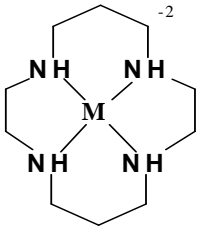

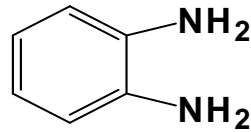
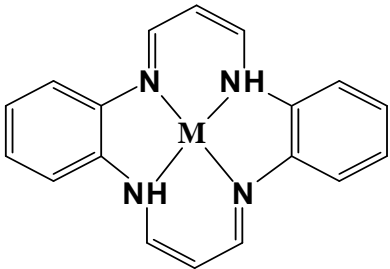
Macrocyclic complexes of lanthanides, derived from the condensation of 2,6-diformyl-4-phenol are currently attracting much attentions in medical applications as contrast enhancing agents in magnetic resonance imaging⁽⁷⁰⁾, one of these compounds is the dimmer compound $[La_2(L^1)(OAc)_4]$ which has been used as a brain imaging [where $L^1 = 6,6$ -bis(aminomethyl)-2,2-bipyridyn].

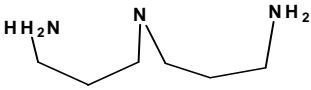
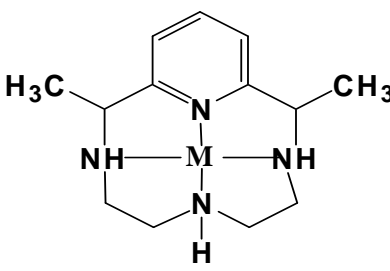
(1.6.5) Applications in Analytical chemistry

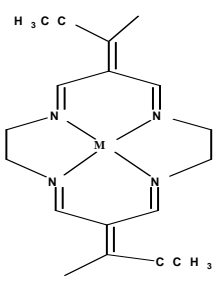
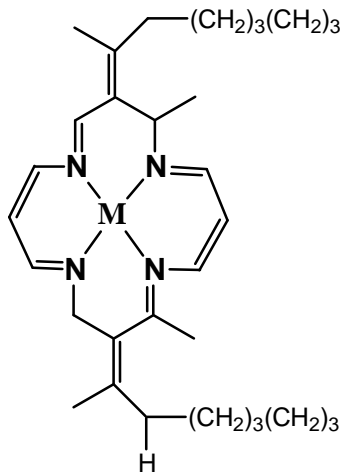
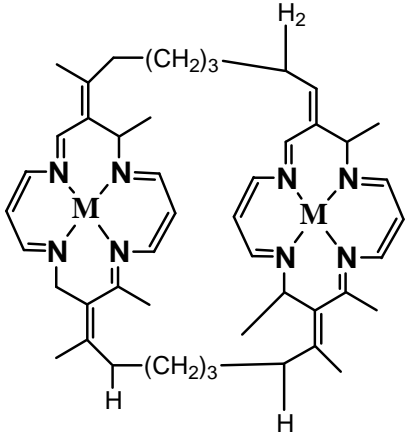
One of the analytical application of diformylimino compounds is their use as organic participating reagents for transition metal ions and of the analysis of Co^{II} in vitamin B_{12} ⁽⁷¹⁾.

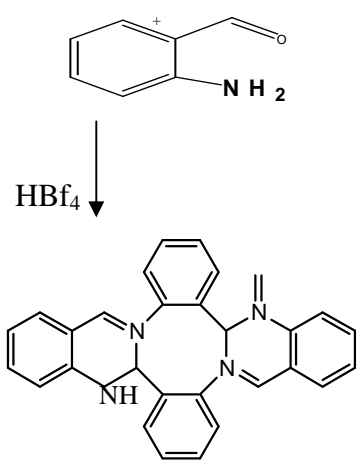
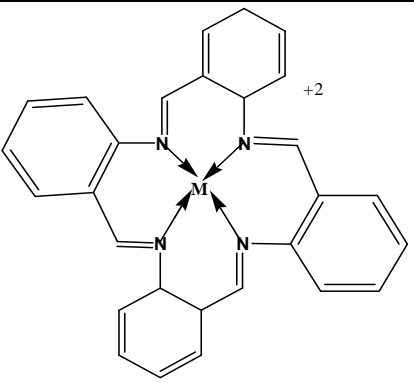
(1.7) Reactivity of tetraaza derivatives toward metal ions

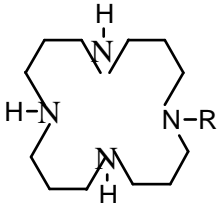
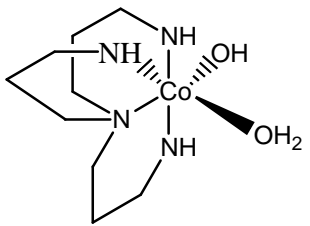
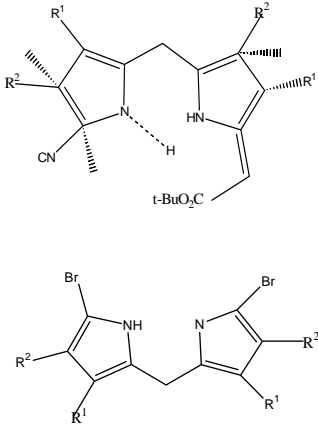
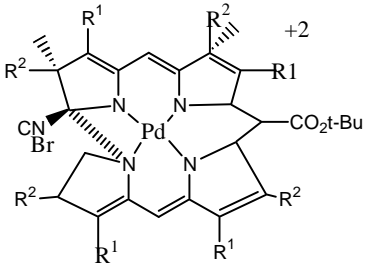
Table (1–1) Reactivity of tetraaza derivatives toward metal ions

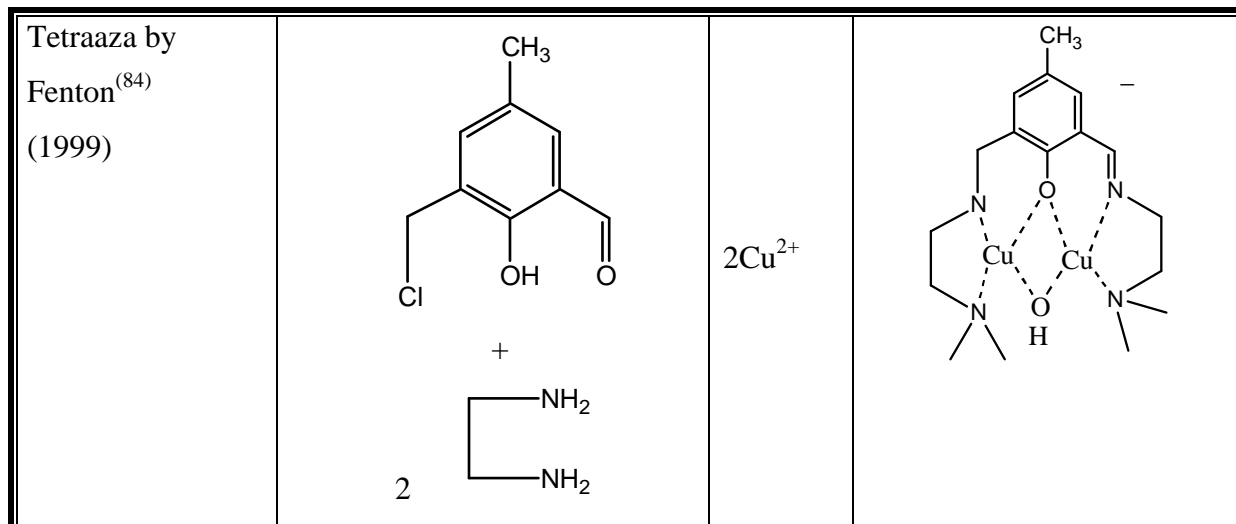
Type of the macrocyclic with workers name	Organic reactions	Metal Ion	Macrocyclic complexes
Tetraaza By Zolotov ⁽⁷²⁾ (1979) Bosnish ⁽⁷³⁾ (1965) Parker ⁽⁷⁴⁾ (1988)	 <p>Poly amine</p> <p>+</p>  <p>1,3-dibromo propane</p>	M^{+2}	 <p>$M = Cu^{(II)}, Ni^{(II)}$</p>
Tetraaza By Zolotov ⁽⁷²⁾ (1979) Floriani ⁽⁷⁵⁾ (1979)	 <p>Propynal</p> <p>+</p>  <p>O-phenylenediamin</p>	M^{+2} ↓ Fe^{+2} Co^{+2} Cu^{+2}	

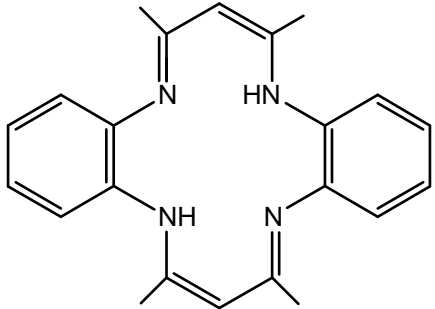
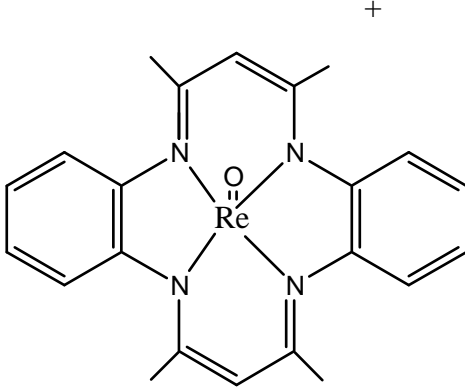
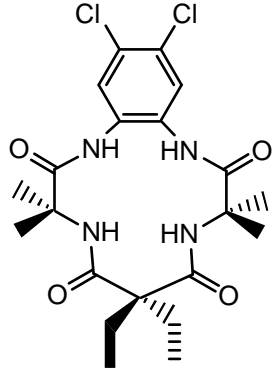
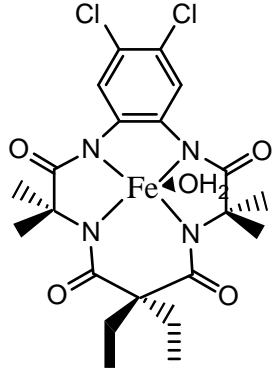
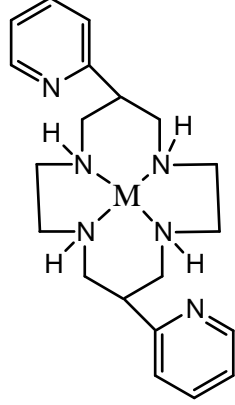
<p>Tetraaza By Rausch⁽⁷⁶⁾ (1969) Long⁽⁷⁷⁾ (1970)</p>	<p>2.6- di acetyl pyridine</p> <p>+</p>  <p>3.3-Di amino di propyl amine</p>	<p>M^{+2}</p> <p>↓</p> <p>Mn^{+2} Ni^{+2} Cu^{+2} Zn^{+2}</p>	
--	---	--	--

Type of the macrocyclic with workers name	Organic reactions	Metal Ion	Macrocyclic complexes
<p>Dimer tetraaza By Busch⁽⁷⁸⁾ (1981)</p>	 <p>+</p> 	<p>M^{+2}</p>	

<p>Tetraaza By Gugger⁽⁷⁹⁾ and co- workers (1989) Skuruto- wicz⁽⁸⁰⁾ (1977)</p>	 <p>HBF₄=Tetrafluoroboric acid</p>	<p>M^{+2}</p> <p>↓</p> <p>Ni^{+2} Cu^{+2} Cu</p>	
---	--	--	--

Type of the macrocyclic with workers name	Organic reactions	Metal Ion	Macrocyclic complexes
<p>(Tetraaza by Schneider and co-workers⁽⁸¹⁾ (1996)</p>	 <p>aquas</p>	<p>Co^{+2}</p>	
<p>Tetraaza by Mulzer⁽⁸²⁾ (1997) Morishima⁽⁸³⁾ (1995)</p>		<p>Pd^{+2}</p>	



Type of the macrocyclic with workers name	Organic reactions	Metal Ion	Macrocyclic complexes
Tetraaza by Burrell and co-workers ⁽⁸⁵⁾ (2000)	 <p>Tetra methel dibenzo tetraaza Annilene + $\text{ReOCl}_3(\text{PPh}_3)_2$/ Toluine</p>	$(\text{ReO})^{+3}$	
Tetraaz By Marlin and co-workers ⁽⁸⁶⁾ (2000)		Fe^{+2}	
Tetaaza By Comba and co-workers ⁽⁸⁷⁾ (2000)	<p>*1.2-diaminoethane *Ethyl2-pyridil acetate *formaldehyd</p>	M^{+2} Cu^{+2} Ni^{+2} Co^{+2} Zn^{+2}	

(1.8) Applications of tetraaza ligands and their complexes

(1.8.1) Medical uses of macrocyclic tetraaza compounds

Technetium complexes play a big role in radioactivity diagnoses because they have some nuclear properties as shown in table (1–2).

Producing the radioactive isotope for rhenium (^{186}Re , ^{188}Re) which can be used in nuclear medicine because it releases (Gamma and Beta \cdot rays which can be used in diagnoses and in therapy depending on their energies as show in Table (1–2)⁽⁸⁸⁻⁹⁰⁾.

Table: (1–2) Emission and half-life period of Technetium and Rhenium

Isotopic	Half-Life	Emission
$^{99\text{m}}\text{Tc}$	6 hours	γ , 143 Kev
^{186}Re	90 hours	γ , 137 Kev β , 1.07 Mev
^{188}Re	17 hours	γ , 155 Kev β , 2–12 Mev

The macrocyclic ligands have a big role in nuclear medicine through synthesis of complexes with the radioactive metals such as (^{188}Re , ^{186}Re , $^{99\text{m}}\text{Tc}$) which have high stability⁽⁹¹⁾, series from these complexes were prepared with the macrocyclic tetraaza which can be used in nuclear medicine, where they injected the patient with radio active complex solution and this will spread in the body through the blood circulation and this will collect in the infected

organ, the biotic distribution and the direction ability depend on the size of macrocyclic, the charge of complex, and the compensating groups in the cycle^(92,93).

(1.8.2) Macrocyclic and pharmacology

The metals, sodium, potassium, magnesium and calcium are considered the operation's axis in the biological activities which contain (%99) of all the metal ions in the organism body, the remaining are very little from iron, cobalt, copper, molybdenum and tin. The heavy metals are very important for the stability of any organ and controlling the cells activities by bonding with big proteins, as an example the metal enzymes and the blood proteins^(94,95). When the natural balance of the metal ions gets disturbed inside the body many of the major disease appeared, for example liver illness for patients who have Wilsons disease happened because of the disturbance in the natural mechanism which controls the concentration of (Cu^{II}), stopping the metabolism because the shortage of (Fe^{II}).

The shortage of vitamin (B_{12}) which contains cobalt ion causes anemia⁽⁹⁶⁾ ; also the great ability of the macrocyclic compounds to remove the poisonous effects of some metals inside the body play a big role in building the human body, The porphyrin unit Fig. (1-28) is an important macrocyclic molecule, it is found as Fe (II) complexes in red-blood corpuscles (hemoglobin)⁽⁹⁷⁾ plays a vital role in oxygen distribution, also it is found as myoglobin in muscles.

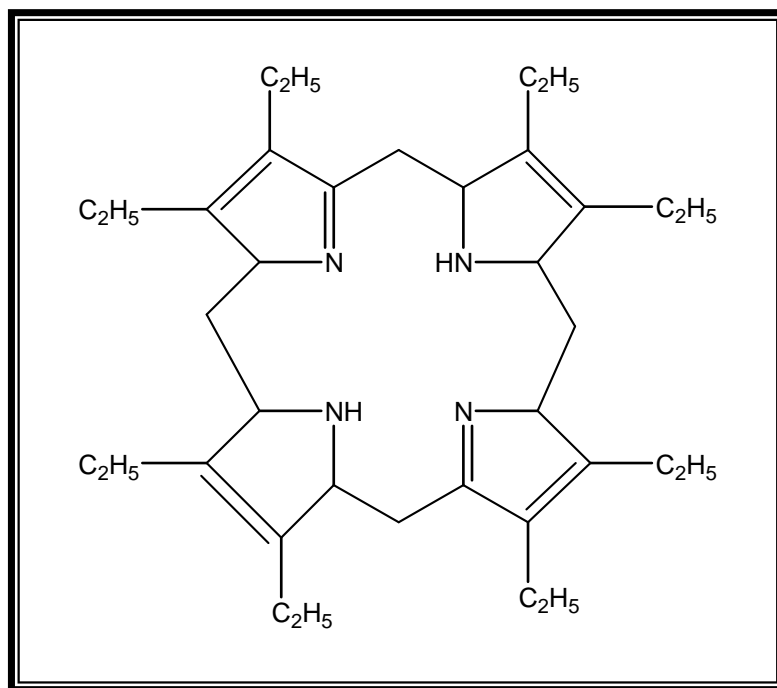


Fig. (1–28) Porphyrin structure

(1.8.3) Extraction and separation of metals using macrocyclic tetraaza molecules

Macrocyclic compounds have a high selectivity to extract some metal ions and separate them⁽⁷²⁾; this selectivity is controlled by many factors:

- 1- The size of the cavity inside the macrocyclic molecule compared to the radius of the metal ion substituted to be extracted.
- 2- The substituted groups on the cycle.
- 3- (pH) of the extraction solution.

Macrocyclic compounds are divided to two types: (saturated and unsaturated), saturated Fig.(1–29) can separate the transition metals.

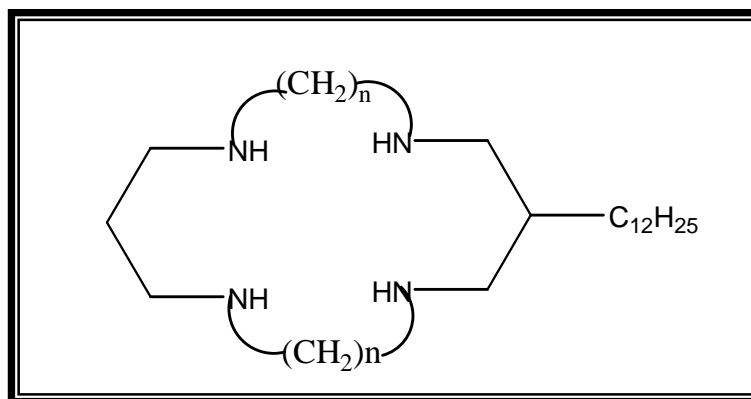


Fig. (1–29) Structure of saturated macrocyclic

Handel and co-workers⁽⁹⁸⁾ studied the extraction of (Co^{II} , Ni^{II} , Cu^{II} , Zn^{II} , Cd^{II} , Pb^{II} and Ag^{I}) with Lipophilic macrocyclic and became clear that the best extraction is when ($n=3$), for the metals (Co^{II} , Ni^{II} and Zn^{II}), when ($n=4$) for the metals (Cd^{II} , Pb^{II} and Ag^{I}). Where n = number of (CH_2) units.

The unsaturated macrocyclic compounds like (the macrocyclic Amide)⁽⁹⁹⁾ Fig. (1–30) they are used in the extraction using basic medias in case of Cu^{II} at $\text{pH}=9$.

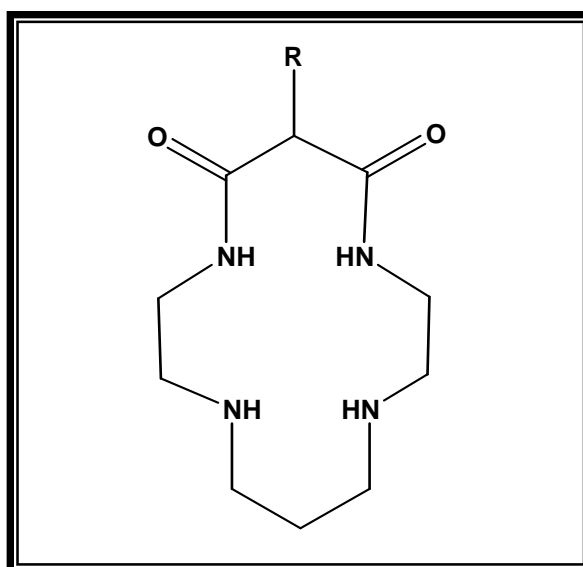


Fig. (1–30) The structure for unsaturated macrocyclic amide

The macrocyclic Fig.(1-31)^(100,101) have a high ability to extract metal ions: Mn^{II} , Fe^{II} , Co^{II} , Ni^{II} , Cu^{II} , Ag^I , Zn^{II} , Cd^{II} , Hg^{II} , Ti^I , Pb^{II} , Eu^{III} , Gd^{II} and U^{III} , while Cu ion can be extracted when pH = 5–9 depending on (n), and Co ion in media pH = 9–10.

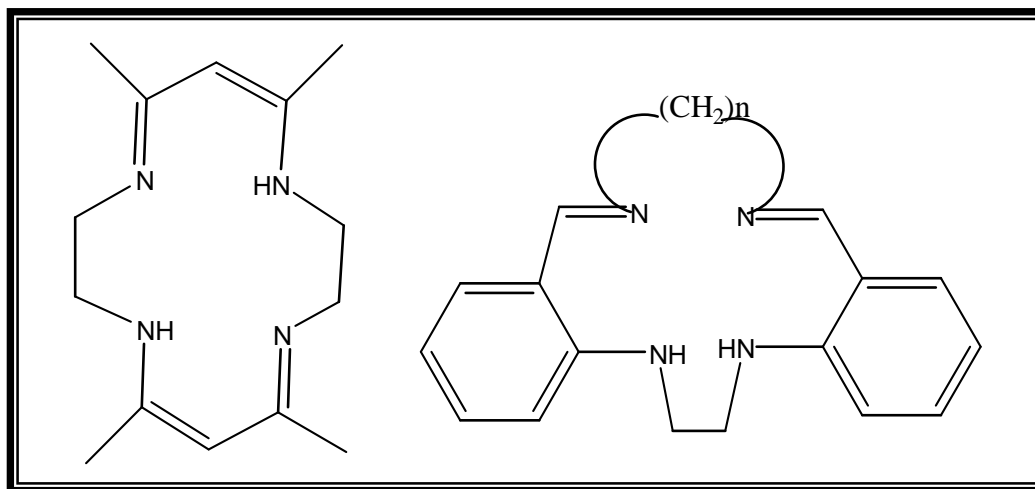


Fig. (1-31) The structure of the unsaturated compounds

The porphyrin compounds, Fig. (1-28) and phthalosyanin⁽¹⁰²⁾ Fig (1-32) are used to extract the low concentration metal ions like: Pd^{II} , Mn^{II} , Co^{II} , Pb^{II} , Zn^{II} and Cu^{II} .

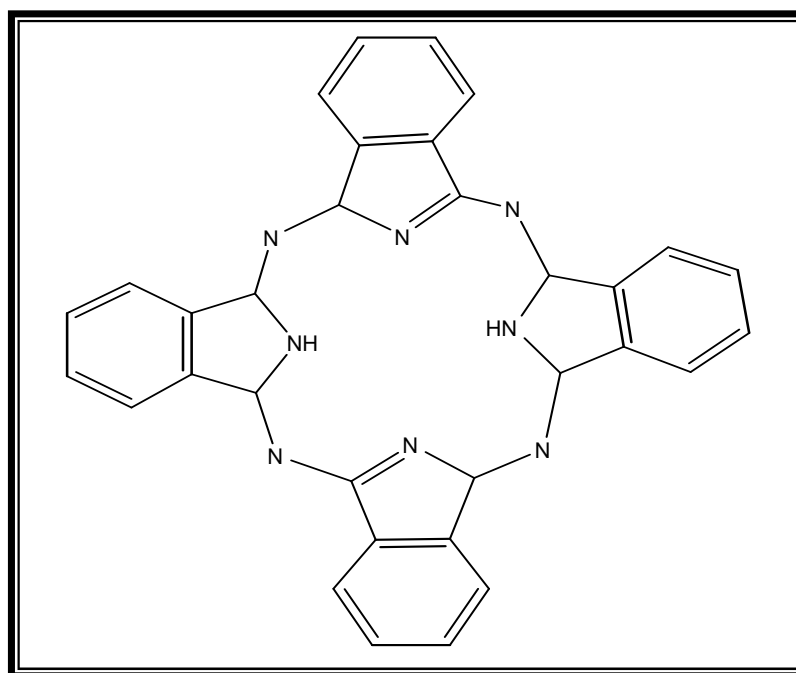


Fig. (1-32) Phthalosynin structure

(1.9) The Aim of the Work

1. Synthesis of new macrocyclic ligand, and its complexes of some metal ions.
2. Physical and spectroscopy studies of the ligand and complexes.
3. Carry out of bioactivity of the ligand and complexes.
4. Preparation of radio active Re and Tc, complexes and application in medicine as tracers and radiotherapeutical agents.
5. Extraction of metal ions through metal complex formation of the prepared ligand.
6. Use of the prepared ligand as a monitor for the environmental pollution by metals.

(2.1) Chemicals

All chemicals and solvents used in this work and their suppliers are listed in Table (2–1). These materials were used as received without further purification.

Table (2–1) Chemicals used in this work and their suppliers

No.	Material	Company source of supply	Purity %
1.	Zinc (II) chloride	Aldrich	99
2.	Hexamethylenetetramine	B.D.H	99
3.	Ethanol	B.D.H	99
4.	Methanol	B.D.H	99.5
5.	Cadmium (II) chloride hexahydrate	B.D.H	99
6.	Carbon tetrachloride	B.D.H	99
7.	Chloroform	B.D.H	99
8.	Diethylether	B.D.H	99
9.	Hydrogen bromide 48%	B.D.H	98
10.	Mercury (II) chloride	B.D.H	99
11.	Paraformaldehyde	B.D.H	99.9
12.	Acetic acid	Evans	99
13.	Nickel (II) chloride	Fluka	99
14.	Iron (II) chloride hexahydrate	Fluka	99
15.	Acetone	Fluka	99
16.	Diethylformamide	Fluka	99
17.	Potassium hydroxide	Fluka	98
18.	Salicylaldehyde	Fluka	98

19.	Chromium (III) chloride hexahydrate	Merck	99
20.	Copper (II) chloride hexahydrate	Merck	99
21.	Sulfuric acid (98%)	Merck	
22.	Manganese (II) chloride hexahydrate	Merck	99
23.	1,2-Ethylenediamine	Merck	99
24.	Benzol	Riedel-Dehaen	99.6
25.	Cobalt (II) chloride hexahydrate	Riedel-Dehaen	99
26.	ρ -Cresol	Riedel-Dehaen	99.9

(2.2) Instruments

The following measurements were used to characterize the ligand and its complexes.

(2.2.1) Melting point measurements

Melting point of the precursor, ligand and complexes were measured with an Electrothermal stuart melting point apparatus.

(2.2.2) Infrared spectra

Infrared spectra were recorded as (KBr) discs using (8300) (FT-IR) Shimadzu spectrophotometer in range (4000–400) cm^{-1} .

(2.2.3) Electronic spectra

(UV-Vis) spectra for the compounds were measured in the region (200–1100) nm for 10^{-3} M solution in DMF at 25°C with (UV-Vis) Spectrophotometer type Shimadzu, 160, using a quartz cell of (1.0) cm length.

(2.2.4) Metal analysis

The metal contents of complexes were determined by atomic absorption (A.A) techniques, using a Shimadzu (A.A) 680 Flame atomic absorption spectrophotometer.

(2.2.5) Chloride contents

The chloride contents for complexes were determined by potentiometer titration method on 686-titro processor-665, Dosinatmetrom Swiss.

(2.2.6) Conductivity measurements

Electrical conductivity measurements of the complexes were recorded at (25°C) for 10^{-3} M solutions of the sample in DMF, using a Jenway Ltd. digital conductivity meter.

(2.2.7) Proton Nuclear Magnetic resonance spectra ($^1\text{H-NMR}$) and Carbon Nuclear Magnetic resonance spectra ($^{13}\text{H-NMR}$)

^1H NMR spectra for the ligand and complexes were recorded in CDCl_3 and DMSO-d_6 using a Bruker 400 MHz , Jeol EX 400 MHz and a Jeol 270 MHz and 60 MHz instruments with a tetramethylsilane (TMS) as an internal standard. The samples were recorded at Queen Mary/ University of London/ United Kingdom and Al-Baath University/ Homs-Syria.

(2.2.8) Magnetic Measurements

Magnetic Measurements were recorded on a Bruker BM6 instrument at 25°C following the Farady's method.

(2.2.9) Determination of Nitrogen by modified Kjeldahl method

In this method sulfuric acid was employed as an oxidizing agent for more resistant organic Materials; in this oxidation, carbon and hydrogen are oxidized to carbon dioxide and water, while the sulfate ion is reduced to sulfur dioxide, the amino group is converted to ammonia and held as an ammonium salt.

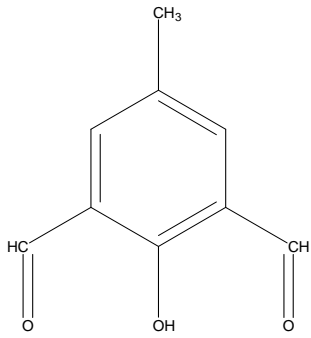
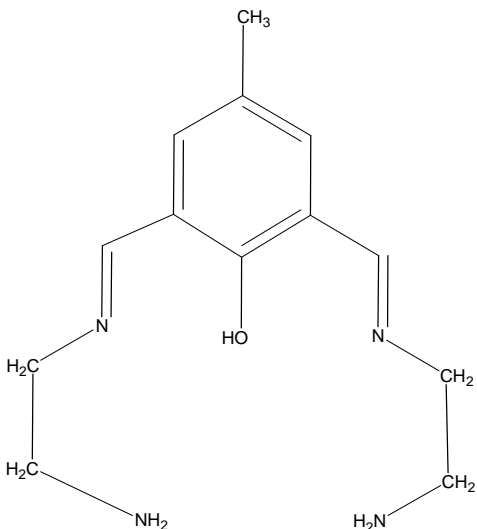
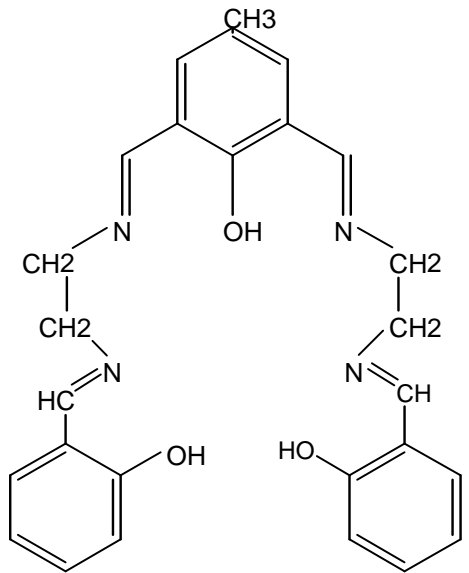
(2.2.10) The proposed molecular structure

The molecular structures of the complexes were determined using Chem. Office 2003, 3DX program.

(2.3) Abbreviation of the precursors and ligand

Table (2-2) describes the suggested abbreviation structure and nomenclature of the synthesized precursor and ligand.

Table (2–2) Abbreviation of structure and nomenclature of the ligand and precursor

Symbol	Structure	Nomenclature
Precursor I		2,6-dimethylol 4-methyl phenol
Precursor II		2,6-bis-(Azomethine-ethylamine)-4-methyl phenol
Ligand		2,6-bis-(Azomethine ethyl Azomethine ortho phenol)-4-methyl phenol

(2.4) Synthesis of precursor (I) 2,6-diformyl-4-methyl phenol

The compound [2,6-diformyl 4-methyl phenol] was synthesized by two different methods. The first one takes a long time with many steps and needs large quantities of starting materials, while the second method is considerably more straightforward and requires short time.

(2.4.1) Synthesis of [2,6-diformyl-4-methyl phenol] the first method⁽¹⁰³⁾

In a one liter beaker 10g., (33mmole) from 2,6-diformyl-4-methyl benzene sulfonyl phenol, was added slowly to 30 g. of 98% H₂SO₄ with stirring to give a very dark solution which was stirred with cooling in an ice bath for 30 minutes. Ice was slowly added to the solution, causing the dialdehyde to crystallise out as irregular brown plates. The brown precipitate was filtered off, recrystallised from acetone-water, washed with cold water, dried in vacuum. Yielded 5 g., (92%), m.p. 134°C from 2,6-diformyl-4-methyl phenol.

(2.4.2) Synthesis [2,6 diformyl-4-methyl phenol] the Second method⁽¹⁰⁴⁾

The dialdehyde was prepared by a completely different method as follows: to a solution 10.8 g., (10 mmole) of *p*-cresol in 50 mL, 28.2 g., (20 mmole) acetic acid, hexamethylenetetramine and 30g., (100 mmole) of paraformaldehyde were added. The mixture was allowed to stirred continuously until the light brown viscous

solution was obtained then heated to 70-90°C for two hours. The solution was cooled to room temperature and 10 mL of concentrated H₂SO₄ was carefully added. The resulting solution was refluxed for half-an hour, and then on treatment with distilled water (400 mL), a light yellow precipitate was formed, which was left overnight at 4°C. The yellow product was isolated by filtration and washed with small amount of cold methanol.

A more pure product was obtained by means of recrystallisation from toluene, yielding 5.7 g. (35%), m.p. 132–134°C.

(2.5) Synthesis of the precursors(II) 2,6-bis(Azomethine-ethylamine)-4-methyl phenol

A solution of ethylenediamine 3.62 g., (4.03 mL, 0.06 mole) was added to 10 mL of ethanol; this mixture was added gradually with stirring under nitrogen atmosphere to a mixture of precursor(I) 4.9 g., (0.03 mole) dissolved in 50 mL of ethanol, and with continuous stirring under the same atmosphere 0.3 mL of HBr (48%) added to this mixture then left for 4 hours under reflux, The mixture was filtered, the resulted solution was separated and 5 mL diethyl ether was added to it and left to evaporate at room temperature for few days or evaporated it under vacuum then filtered off, the precipitate was left to stand overnight at room temperature to dry, yielding 5.3 g., (72%) m.p. 148 °C.

(2.6) Synthesis of ligand [2,6-bis(Azomethine ethyl Azomethine ortho phenol) 4-methyl phenol]

A solution of salicylaldehyde 5.3 g., (4.6 mL, 0.04 mole) was diluted with 20 mL of ethanol was added gradually to a solution of precursor(II), 5.3 g, (0,02 mole) dissolved in 120 mL of ethanol. The mixture was refluxed for 2 hours at 70°C under nitrogen atmosphere then cooled and left to dry at room temperature. The product was 8.7 g., (89%), m.p. 154°C.

(2.7) Synthesis of the [L] complexes.

(2.6.1) Synthesis of the $[\text{Cr}^{\text{III}}(\text{L})\text{Cl}]\text{Cl}$

A solution of 0.1 g., (0.2 mmol) from [L] in 10 mL ethanol was added to a solution of 0.0589 g., (0.2 mmol) of $(\text{CrCl}_3 \cdot 6\text{H}_2\text{O})$ in 10 mL ethanol, the pH was adjusted to ≈ 9 by ethanolic solution of potassium hydroxide, the resulting mixture was refluxed under nitrogen atmosphere for two hours during which the color of the solution became green. The solution was cooled at room temperature and a green solid was collected, washed with 5 mL diethyl ether and dried under vacuum to give 0.19g. (78%) yield of the title compound, m.p. 200°C.

(2.6.2) Synthesis of $[\text{Mn}^{\text{II}}(\text{L})]$, $[\text{Fe}^{\text{II}}(\text{L})]$, $[\text{Co}^{\text{II}}(\text{L})]$, $[\text{Ni}^{\text{II}}(\text{L})]\text{Cl}$, $[\text{Cu}^{\text{II}}(\text{L})]\text{Cl}$, $[\text{Zn}^{\text{II}}(\text{L})]$, $[\text{Cd}^{\text{II}}(\text{L})]$ and $\text{K}[\text{Hg}^{\text{II}}(\text{L})]$

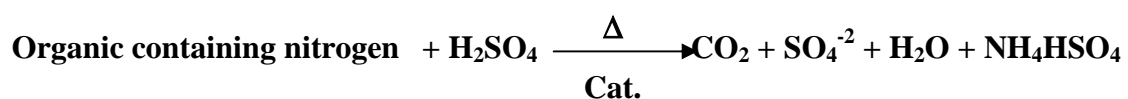
A similar method to that mentioned in preparation of Cr^{III} complex was used to prepare the complexes of $[\text{Mn}^{\text{II}}$, Fe^{II} , Co^{II} , Ni^{II} , Cu^{II} , Zn^{II} , Cd^{II} and Hg^{II}] with [L]. Table (2-3) shows some physical properties and reactant amount of the prepared complexes.

Table (2-3) some physical properties of the prepared [L] complexes and their reactant quantity & yield

Complex	Weight of metal salt	Complex yield %	Complex color	Melting point ($^{\circ}\text{C}$)
$[\text{Mn}^{\text{II}}(\text{L})]$	0.043 g.	66	Dark brown	215
$[\text{Fe}^{\text{II}}(\text{L})]$	0.0355 g.	70	Dark red	230
$[\text{Co}^{\text{II}}(\text{L})]$	0.052 g.	77	Black	246
$[\text{Ni}^{\text{II}}(\text{L})]\text{Cl}$	0.052 g.	71	Dark red	Dec over 280
$[\text{Cu}^{\text{II}}(\text{L})]\text{Cl}$	0.0374 g.	68	Dark red	230
$[\text{Zn}^{\text{II}}(\text{L})]$	0.0295 g.	81	Orange	240
$[\text{Cd}^{\text{II}}(\text{L})]$	0.05 g.	83	Yellow	238
$\text{K}[\text{Hg}^{\text{II}}(\text{L})]$	0.0595 g.	71	Dark yellow	230

(2.8) Determination of Nitrogen by modified Kjeldahl method⁽¹⁰⁵⁾

In this method sulfuric acid was employed as an oxidizing agent for more resistant organic material, in this oxidation carbon and hydrogen are oxidized to carbon dioxide and water, while the sulfate ion is reduced to sulfurs dioxide, the amino group is converted to ammonia and held as an ammonium salt.



The oxidation proceeds rapidly at a temperature slightly above the boiling point of sulfuric acid (340°C). The boiling point of the acid is increased by addition of sodium or potassium sulfate. Catalysts are used to accelerate oxidation, an effective catalyst is made of [32 g. potassium sulfate + 5 g. mercuric sulfate + 1 g. of selenium powder]. Only 2 g. of the catalyst was used in each determination.

The following procedure was adopted:

A. Digestion of samples

1. A weighed sample between 0.02–0.03 g. was transferred into Kjeldahl flask with a long neck.
2. Two grams of catalyst was added.
3. Three milliliters of concentrated sulfuric acid was added.
4. A reflux condenser was connected, and then the temperature was raised gradually to the boiling temperature.
5. The mixture was left for 45 minutes at this temperature.
6. The mixture was left to cool to room temperature.

B. Distillation and titration of the digested mixtures.

1. Add 25 mL of distilled water to each of the above mixtures.
2. The clear liquid into a round bottom flask was transferred.
3. Add to each mixture (4.5 g) of NaOH dissolved into (10 mL) of distilled water gradually.
4. Add 3–4 small boiling stones
5. The round bottom flask with water condenser open end dipped into conical flask containing exactly 50 mL of 0.05 N HCl or H₂SO₄.
6. The mixture was gently heated for 30 minutes.
7. Prepare 250 mL of 0.05N NaOH solution.
8. Titrate the remaining acid in the conical flask with the prepared NaOH solution using methyl orange indicator.

C. A blank experiment was made using glucose (0.03 g).**D. Calculations.**

V_{HCl} = volume of HCl used by liberated ammonia = $(50 - V_{\text{NaOH}} \text{ 0.05 N})$

$V_{2\text{HCl}}$ (blank expt.) = $(50 - V_{\text{NaOH}} \text{ 0.05N used in the blank expt.})$.

$$\% \text{Nitrogen} = \frac{(V_{\text{HCl}} - V_{2\text{HCl}}) \times 0.05 \times 1.401}{\text{Weight of sample}}$$

**Table (2-4) Determination of Nitrogen content by modified
Kjeldahl method**

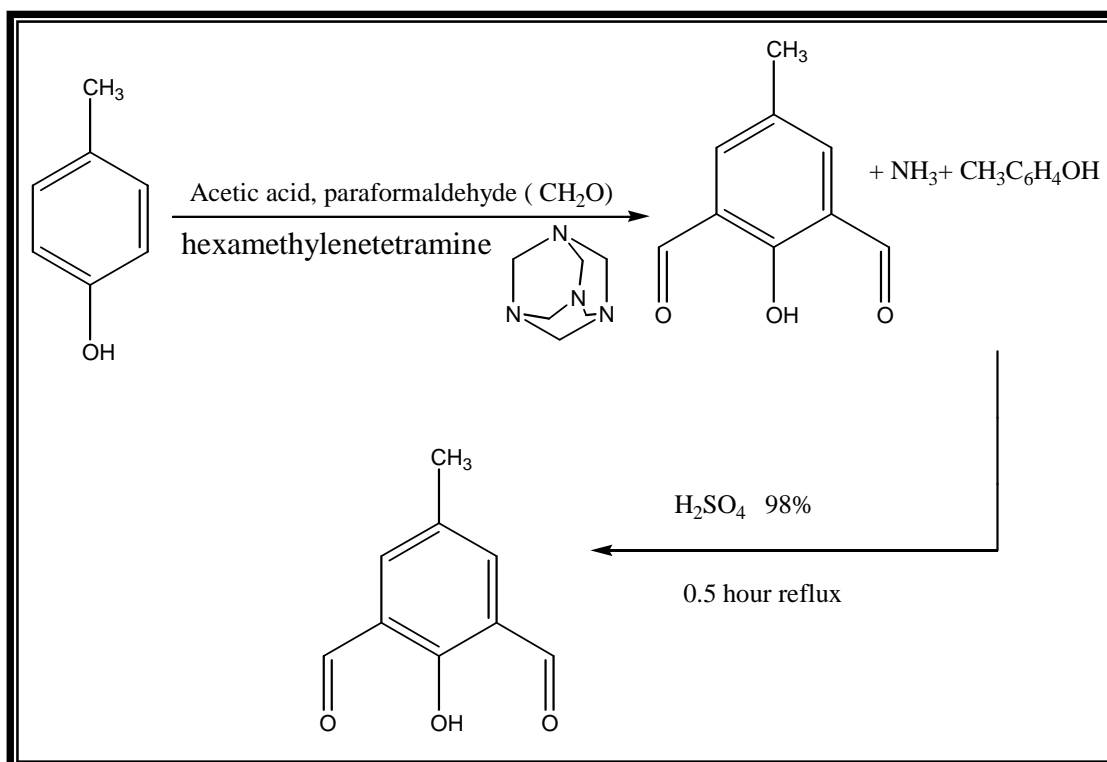
No.	Compound	N% theoretical	N% found
1	[L]	12.27	12.05
2	[CuL]Cl	10.10	10.0
3	[FeL]	10.97	10.5
4	[NiL]Cl	10.19	10.2
5	[CrLCl]Cl	9.68	11.6
6	[CoL]	10.91	10.5
7	[ZnL]	10.77	10.6
8	[CdL]	9.88	9.82
9	K[HgL]	8.08	8.00
10	[MnL]	11.0	10.80

(3.1) Synthesis and characterization of the precursors and ligand

New polydentate ligand with (N₄) donor atoms has been synthesized. Macrocycles with pendant functional groups include polyaza macrocycles that have coordinating side arms attached to the nitrogen. Chelation will be more efficient because the donor atoms are held near the central metal ion⁽¹⁰⁶⁾

(3.1.1) Synthesis and characterization of [2,6-diformyl-4-methyl phenol]

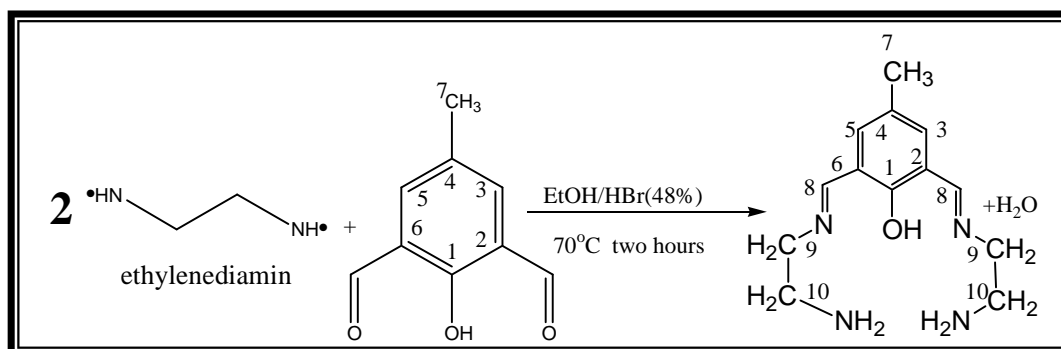
The procedure used to prepare [2,6-diformyl-4-methyl phenol] is one pot reaction *p*-cresol, paraformaldehyde, acetic acid and hexamethylenetetramine were mixed and reflux to obtain the compound. Sulfuric acid (98%) was used to neutralize the ammonia and to dissolve the unreacted phenol, Scheme (3–1). This procedure is easy formed and requires a short time to obtain the compound⁽¹⁰⁷⁾.



Scheme (3-1) One pot synthesis route of 2,6-diformyl-4-methyl phenol

(3.1.2) Synthesis and characterization of [2,6-bis-(Azo methine-ethylamine)-4-methyl phenol]

Precursor II was prepared from the reaction of two equivalents of ethylenediamine with one equivalent of 2,6-diformyl-4-methylphenol using ethanol as a solvent, HBr 48% were added to the mixture according to the following route, Scheme (3–2).

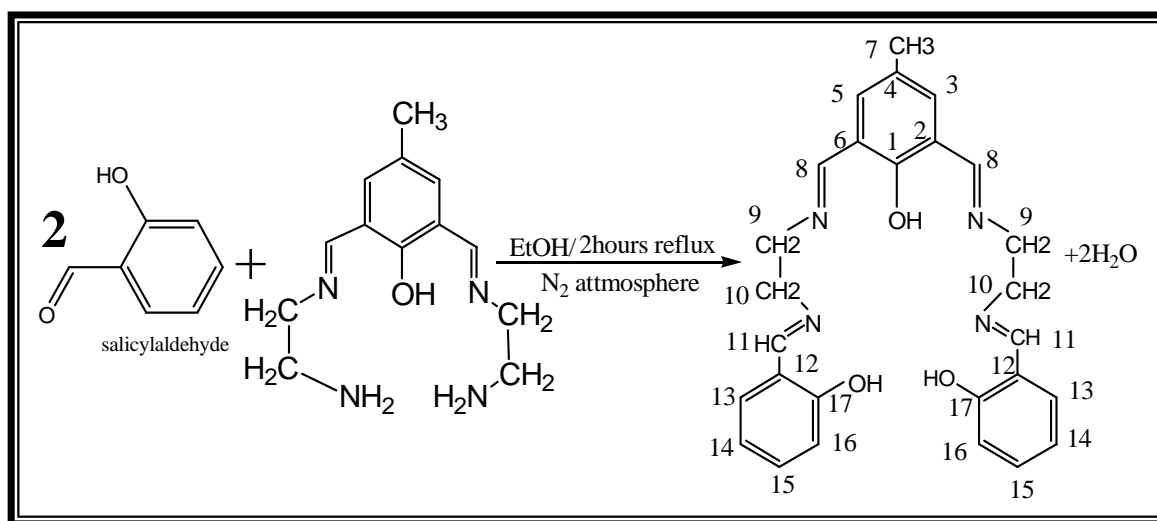


Scheme (3–2) Synthesis route of precursor II

The prepared precursor was characterized by IR and elemental macroanalysis, Table (3–1).

(3.1.3) Synthesis and characterization of ligand [2,6-bis-(2-Azomethine ethyl Azomethine ortho phenol) 4-methyl phenol]

The ligand was synthesized by adding a solution of two equivalents salicylaldehyde to one equivalent of the precursorII [2,6-bis(Azomethine -ethylamine)-4-methyl phenol] to give the ligand, using ethanol as a solvent with a reflux for two hours under nitrogen atmosphere, according to the following route, Scheme (3–3).



Scheme (3-3) Synthesis route of ligand

The ligand was obtained in a good yield 8.7g., (89 %) as a orange crystalline solids, m.p 154°C, soluble in hot ethanol, hot methanol, DMSO and DMF.

The polydentate ligand with N₄ donor atoms was characterized by ¹H NMR, ¹³C NMR, I.R, UV–Vis and elemental microanalysis,

Table (3–1) represent the solubility of the ligand and precursor in different solvents.

Table (3–1) The elemental analysis and some physical properties of precursors and ligand

Compound	Empirical Formula	M.W	Yield %	M.P °C	Color	Micro analysis (calc) %		
						C	H	N
Precursor (I)	C ₉ H ₈ O ₃	164.16	35	134	yellow	65.85	4.91	
Precursor (II)	C ₁₃ H ₂₀ N ₄ O	248.32	72	148	orange	62.88	8.12	22.56
Ligand	C ₂₇ H ₂₈ N ₄ O ₃	456.54	89	154	orange	71.03	6.18	12.27

Table (3-2) The solubility of the prepared precursors and Ligand in different solvents

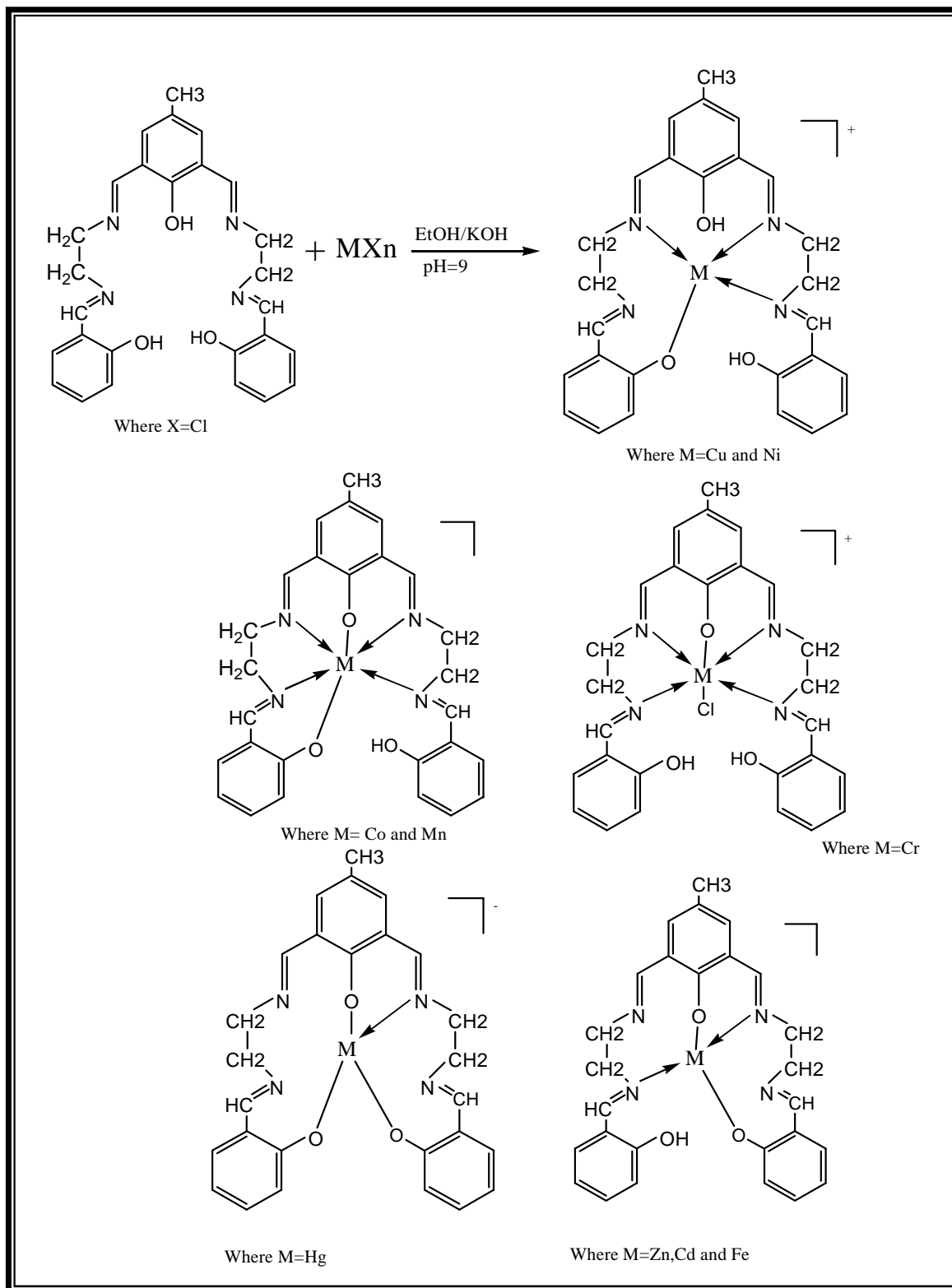
Compound	H ₂ O	Hot MeOH	Hot EtOH	CHCl ₃	C ₆ H ₆	DMF	DMSO
Precursor (I)	÷	+	+	+	-	+	+
Precursor (II)	÷	+	+	+	-	+	+
Ligand	+	+	+	+	-	+	+

(+) soluble, (-) insoluble, (÷) sparingly

(3.2) Synthesis and characterization of the complexes

All complexes were prepared by a similar method, as in scheme (3–4).

The complexes were prepared from the reaction of the ligand with metal chloride salt, refluxed in methanol, potassium hydroxide was used as a base. Pure complexes formed only at pH \approx 9.



Scheme (3-4) Synthesis route of complexes

The complexes were prepared by a similar method, Table (3-3) display the solubility of the complexes in different solvents.

Microanalyses of the complexes along with metal and chloride analysis are in a good agreement with the calculated values, Table (3-4). Spectroscopic methods (FT-IR), (UV-Vis) along with molar conductivity and melting point were used to characterize the complexes.

Table (3-3) The solubility of [L] complexes in different solvents

Complexes	H ₂ O	Hot MeOH	Hot EtOH	CHCl ₃	C ₆ H ₆	DMF	DMSO
[Cu ^{II} (L)]Cl	-	+	+	-	-	+	+
[Fe ^{II} (L)]	-	+	+	+	÷	+	+
[Ni ^{II} (L)]Cl	-	+	+	+	÷	+	+
[Cr ^{III} (L)Cl]Cl	-	+	+	÷	÷	+	+
[Co ^{II} (L)]	-	+	+	-	-	+	+
[Zn ^{II} (L)]	-	+	+	-	-	+	+
[Cd ^{II} (L)]	-	+	+	÷	÷	+	+
K[Hg ^{II} (L)]	-	+	+	÷	-	+	+
[Mn ^{II} (L)]	-	+	+	÷	-	+	+

(+) soluble, (-) insoluble, (÷) sparingly

Table (3-4) Results of Analysis of metal ions, chloride ions and Nitrogen percentage of metal complexes

No.	Complexes	N% Found	Metal ions		Chloride ion		Ratio[Cl/M] mole
			gram %	Mole %	Gram %	Mole %	
1	[Cu(L)]Cl	10.0	11.46	18.0	6.41	18.05	1.01
2	[Fe(L)]	10.50	10.95	19.59	–	–	–
3	[Ni(L)]Cl	10.2	10.68	18.19	6.46	18.2	1.01
4	[Cr(L)Cl]Cl	11.6	8.99	17.29	12.28	34.6	2.00
5	[Co(L)]	10.5	11.499	19.49	–	–	–
6	[Zn(L)]	10.6	12.58	19.24	–	–	–
7	[Cd(L)]	9.82	19.83	17.67	–	–	–
8	K[Hg(L)]	8.00	28.96	14.43	–	–	–
9	[Mn(L)]	10.80	10.78	19.64	–	–	–

(3.3) I.R Spectra of compounds

(3.3.1) I.R Spectrum of the precursor (I)

The IR spectrum of 2,6-diformyl-4-methyl phenol, Fig. (3–1) exhibits band at 2870 cm^{-1} which may be attributed to $\nu(\text{C–H})$ aldehydic stretching. The shifting of this band to lower wave number is related to intramolecular hydrogen bonding between the hydroxyl group and aldehydic carbonyl group⁽¹⁰⁹⁾. The bands at 1682 and 1667 cm^{-1} assigned to $\nu(\text{C=O})$ stretching, the two carbonyl groups are no equivalent due to the intramolecular hydrogen bonding. The bands at 1603 and 1458 cm^{-1} assigned to $\nu(\text{C=C})$ stretching, the bands at 1404 and 1216 cm^{-1} can be attributed to $\delta(\text{O–H})$ bending

phenolic $\nu(\text{C}-\text{O})$ stretching respectively, while the bands at 962, 748 cm^{-1} are assigned to $\delta(\text{C}-\text{H})$ bending in plane and out of plane respectively. The assignment of the characteristic bands is summarized in Table (3-5).

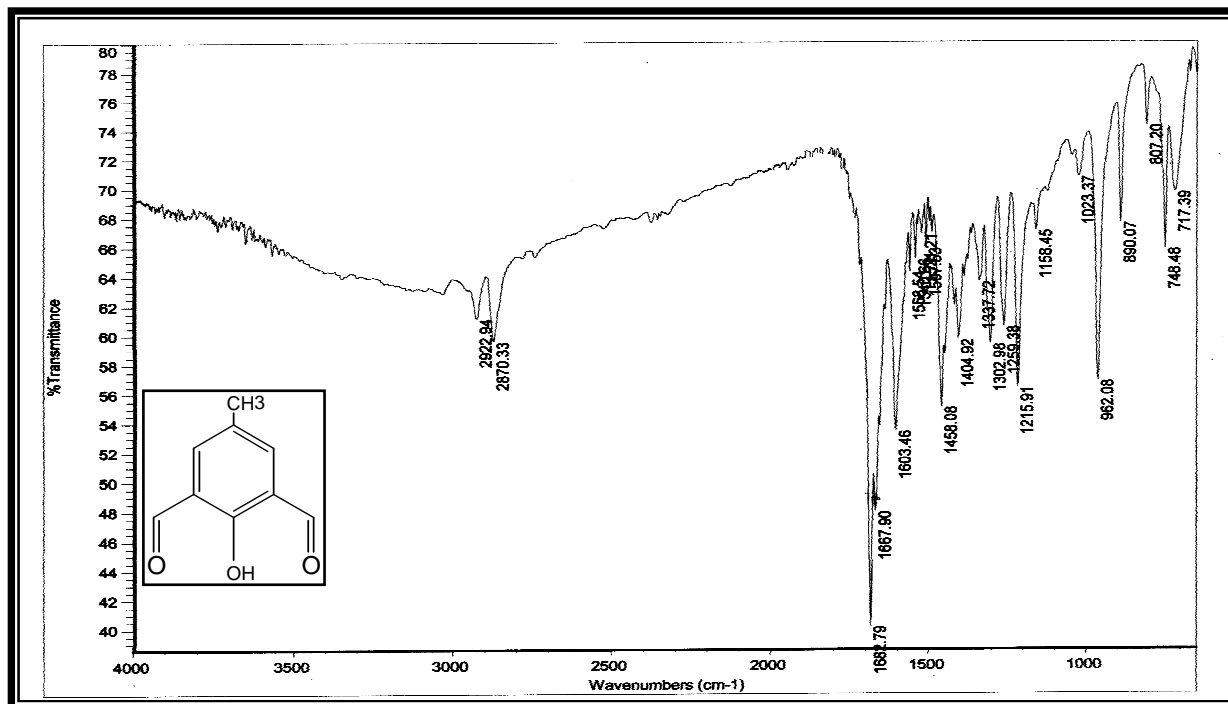


Fig. (3-1) I.R spectrum for precursor (I)

(3.3.2) I.R Spectrum for the precursor (II) 2,6-bis-(Azo-methine- ethyl amine)-4-methyl phenol

The I.R spectrum for precursor(II), Fig. (3-2) exhibits bands at 2850 cm^{-1} attributed to $\nu(\text{C}-\text{H})$ stretching, the band at (1114 cm^{-1}) is assigned to $\nu(\text{C}-\text{N})$ stretching, the broad band at 2900 cm^{-1} is assigned to $\nu(\text{N}-\text{H})$, this band is confirmed by a weak bands observed at 1696 cm^{-1} for in plane bending and 962 cm^{-1} for out of plane bending. On the other hand the bands at 2850 cm^{-1} and at 2950 cm^{-1} are assigned to the $\nu(\text{C}-\text{H})$ stretching for aromatic and aliphatic (C-H) bands.

The bands at 1675 cm^{-1} and 1620 cm^{-1} are attributed to asymmetric and symmetric stretching of the (C=N) imine group⁽¹¹⁰⁾. The assignment of the characteristic bands are summarized in Table (3-5).

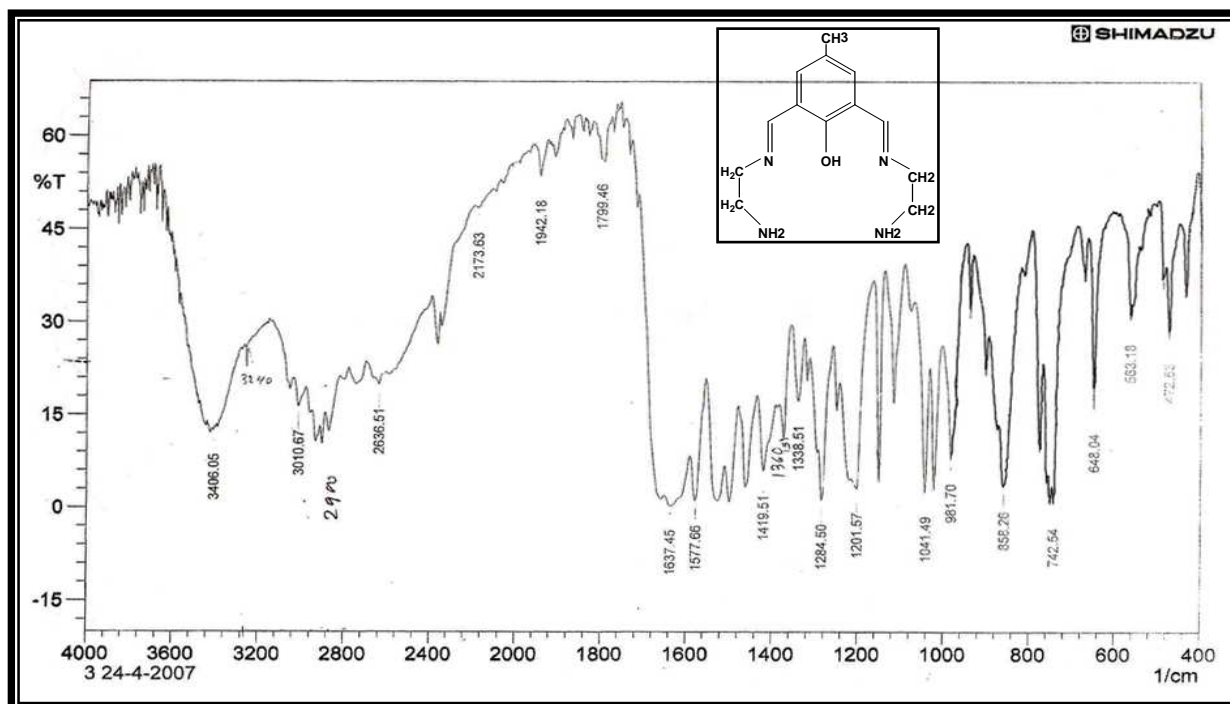


Fig. (3-2) I.R spectrum for precursor (II)

(3.3.3) (I.R) Spectrum for the ligand 2,6-bis-(2-Azomethine phenol-ethyl-Azomethine)-4-methyl phenol

The (I.R) spectra for precursor (I) and precursor (II) are shown in Figs. (3-1 and 3-2) and discussed in section (3.3.1) and (3.3.2) respectively, the (I.R) spectrum of the ligand, Fig. (3-3) showed characteristic bands at 1640 cm^{-1} and 856 cm^{-1} attributed to $\nu(\text{C}=\text{N})$ and $\nu(\text{C}-\text{N})$ stretching respectively.

The medium band at 1496 cm^{-1} is assigned to the broad bands observed at 1200 and 3394 cm^{-1} assigned to $\nu(\text{C}-\text{O})$ and $\nu(\text{O}-\text{H})$ respectively. The assignment of the characteristic band are

summarized in table (3–5). An important observation found with some exceptions are the reduction of all values of vibrations with increasing molecular weight of the compounds.

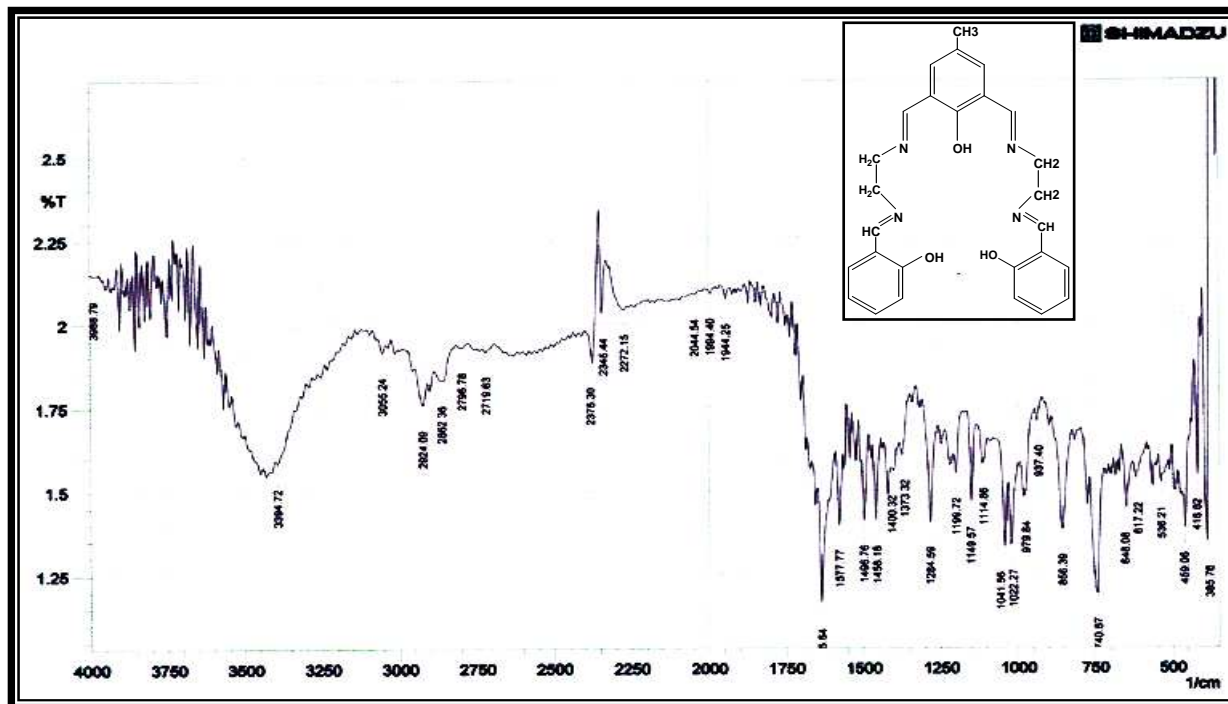


Fig. (3–3) I.R spectrum for ligand

Table (3-5)

(3.4) (I.R) Spectral Data for the [L] complexes

The (I.R) spectral for all nine complexes are shown in Figures (3–4), (3–5), (3–6), (3–7), (3–8), (3–9), (3–10), (3–11) and (3–12) respectively.

The double bands at 1660 and 1650 cm^{-1} which are corresponding to asymmetric and symmetric stretching $\nu(\text{C}=\text{N})$ in the free ligand (L), are shifted to lower frequencies as can be seen in Table (3–6). The shift of (C=N) to lower wave number can be attributed to delocalization of metal electron density into the π -system⁽¹¹¹⁾ (Homo \rightarrow Lumo). [Where: Homo = Highest Occupied Molecular Orbital, Lomo= lowest Unoccupied Molecular Orbital]. This shifting increases the electro positivity on the nitrogen atoms and depresses the electron density of the π -bonding, namely (C=C) of the free ligand at 1496 cm^{-1} and lowering the wave number about 54–16 cm^{-1} , these observations are in a good agreement with that reported in literature⁽¹¹²⁾.

The medium band at 1200 cm^{-1} assigned to the $\nu(\text{C}-\text{O})$ stretching for free ligand is shifted to higher frequency, confirming the coordination of the ligand through oxygen atom to the metal ion⁽¹¹³⁾. This is presumably due to the increase in the bond order character of (C–O), upon complexation with metal ion.

The I.R spectra for complexes exhibited weak absorption bands in the ranges (675–570) and (447–390) cm^{-1} which are attributed to $\nu(\text{M}-\text{N})$ and $\nu(\text{M}-\text{O})$ respectively⁽¹¹⁴⁾ [M=metal ion], Table (3–6). These bands support the coordination of the ligand to metal centre through nitrogen and oxygen atoms⁽¹¹⁵⁾.

The (I.R) spectrum for chromium complex exhibits sharp absorption band at $(430)\text{cm}^{-1}$ due to $\nu(\text{M}-\text{Cl})$ stretching vibration.

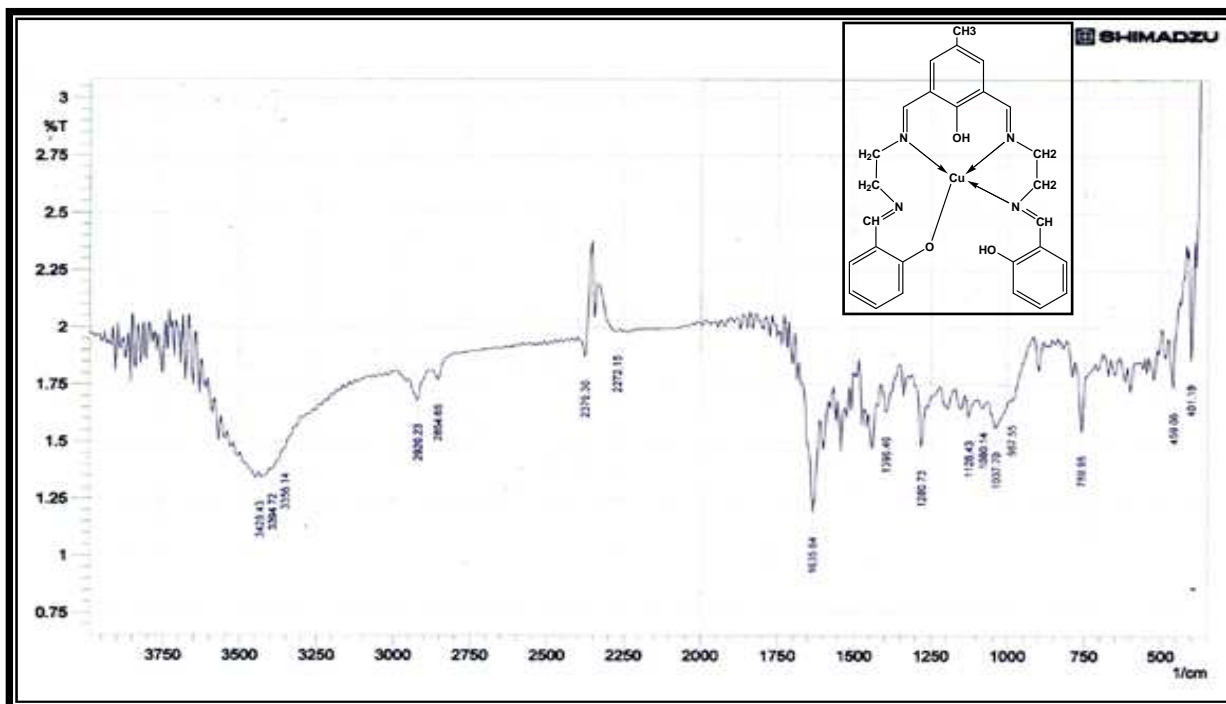


Fig. (3-4) I.R spectrum for [Cu(L)]Cl complex

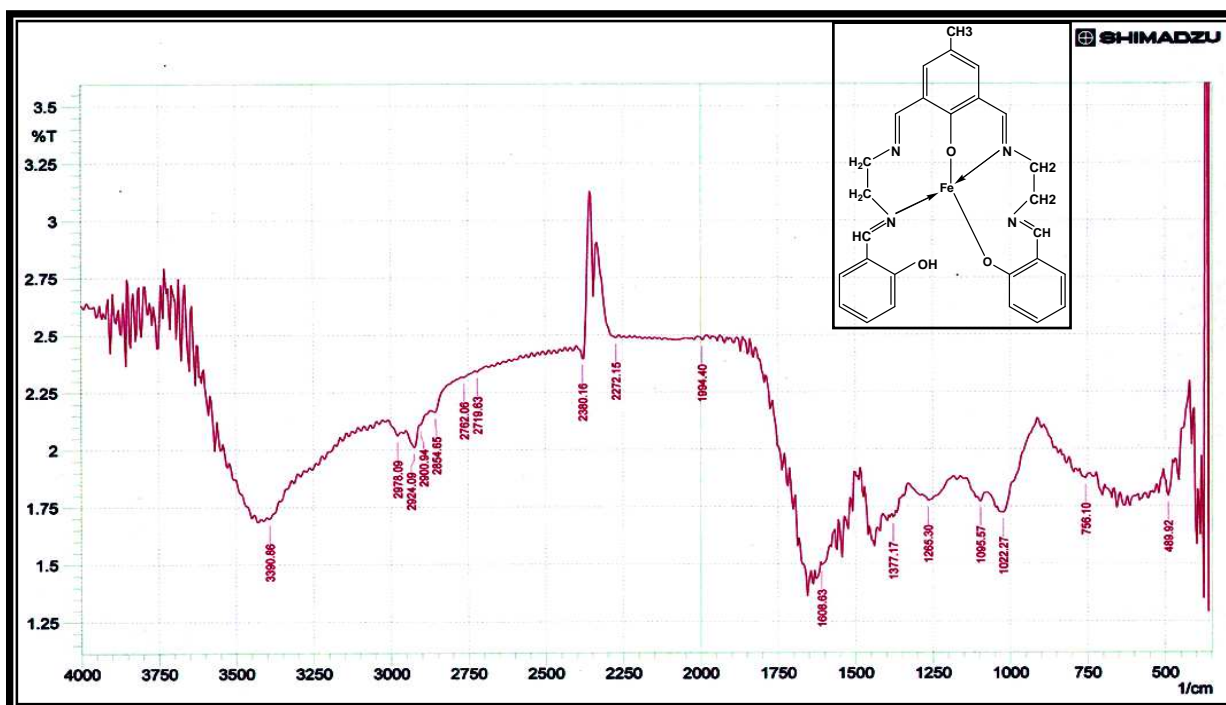


Fig. (3-5) I.R spectrum for [Fe(L)] complex

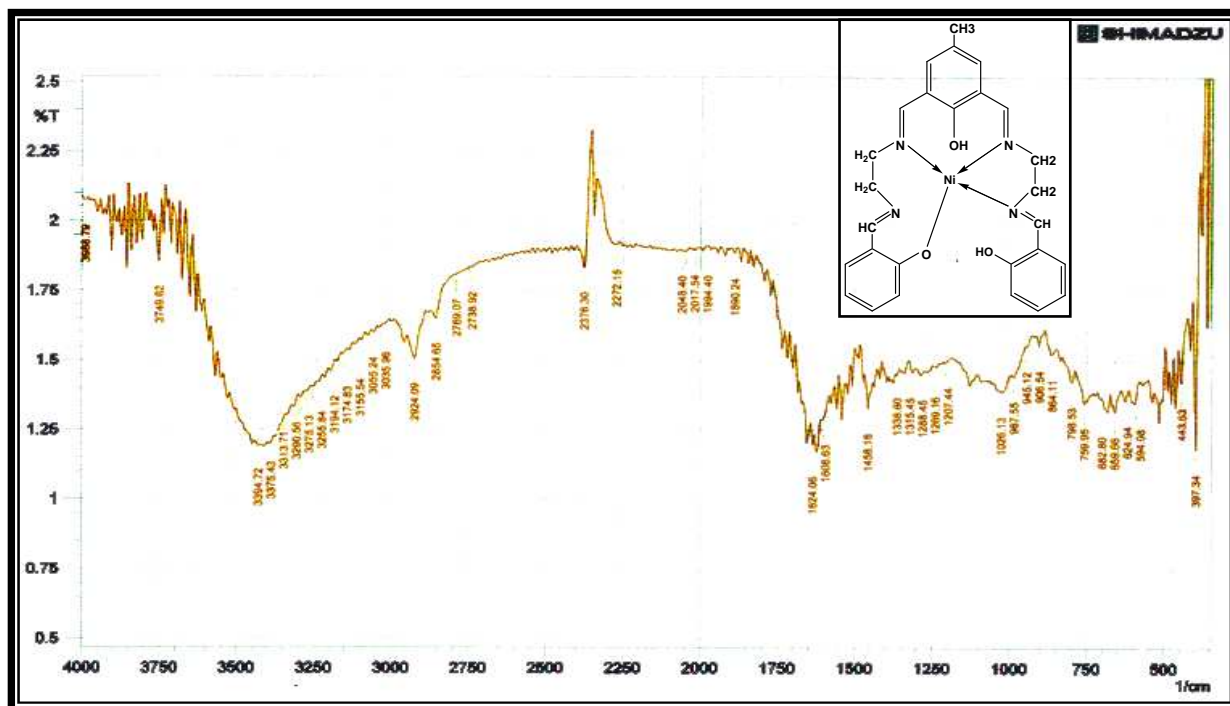


Fig. (3-6) I.R spectrum for [Ni(L)]Cl complex

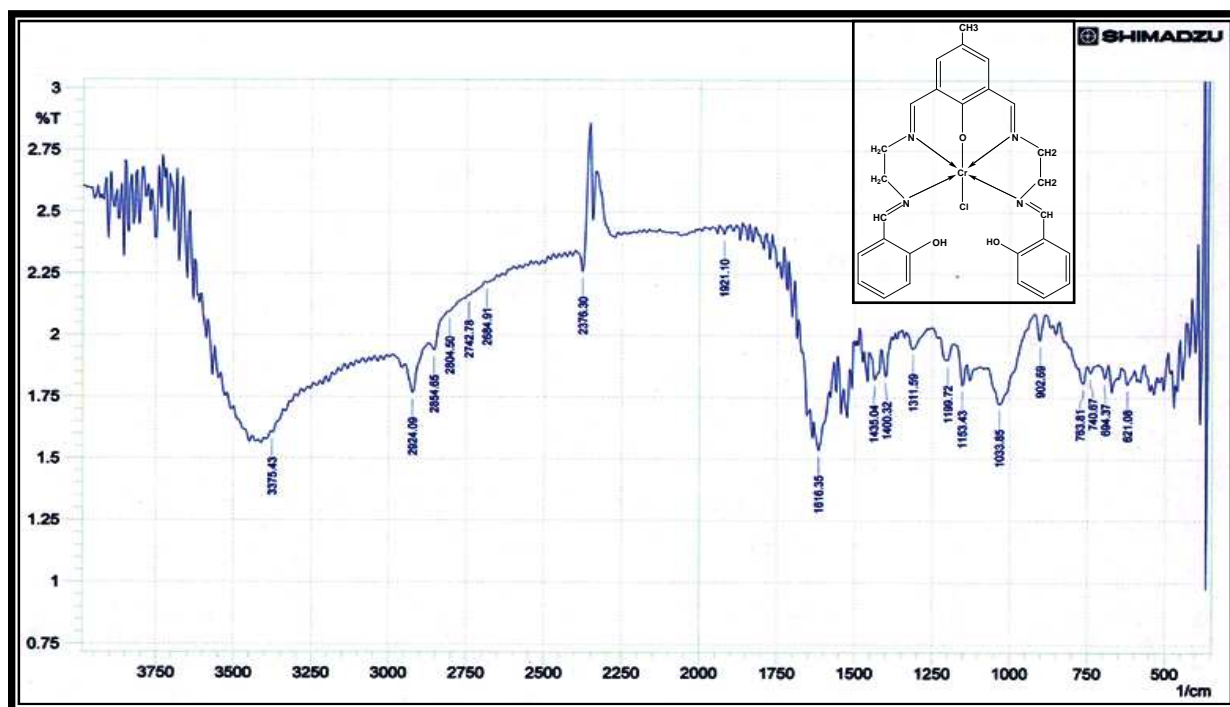


Fig. (3-7) I.R spectrum for [Cr(L)Cl]Cl complex

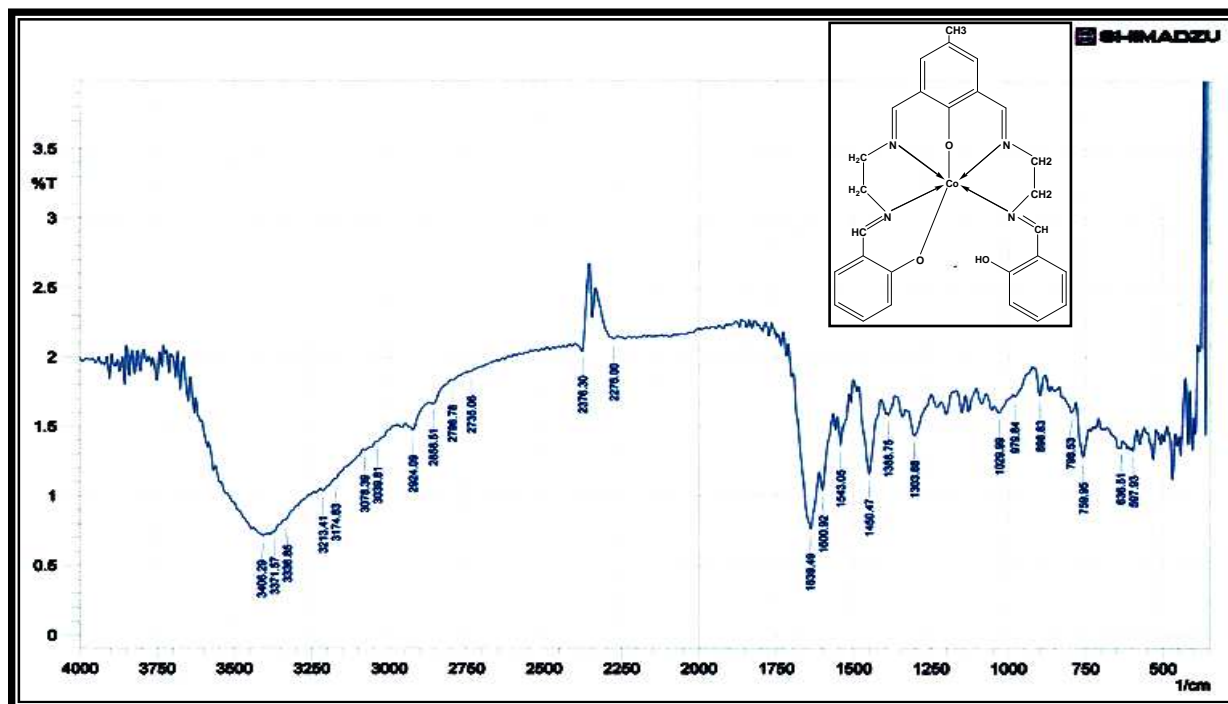


Fig. (3-8) I.R spectrum for [Co(L)] complex

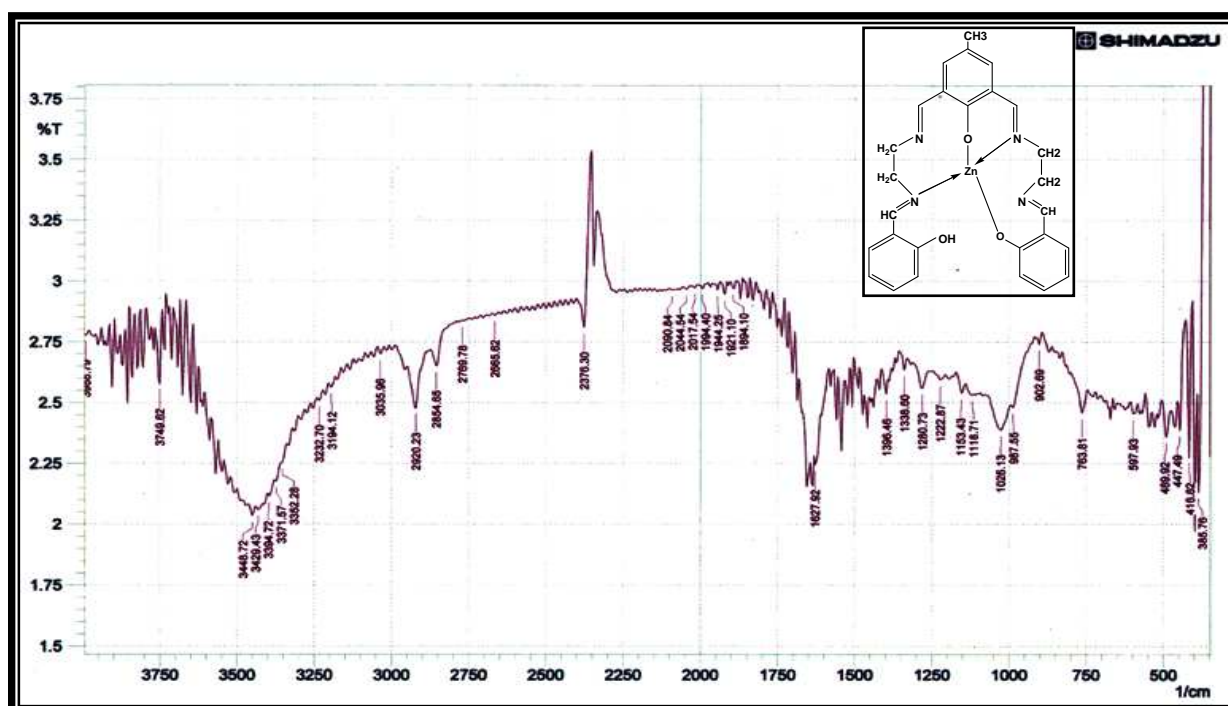


Fig. (3-9) I.R spectrum for [Zn(L)] complex

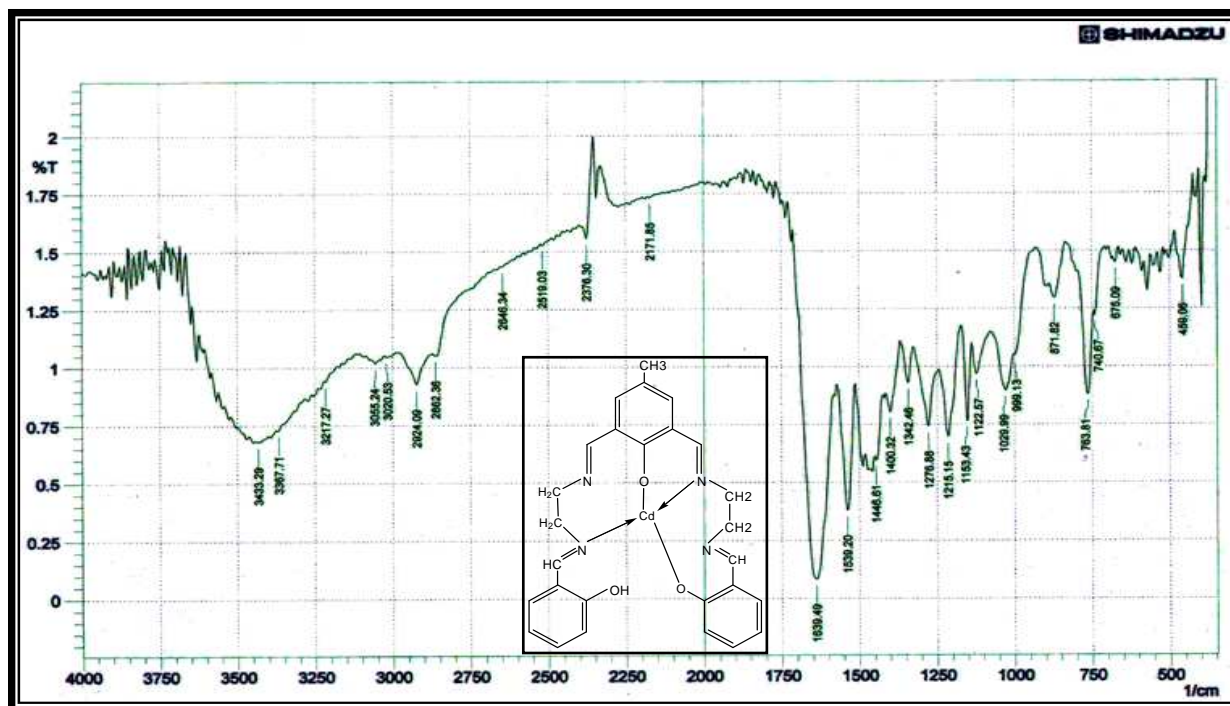


Fig. (3-10) I.R spectrum for [Cd(L)] complex

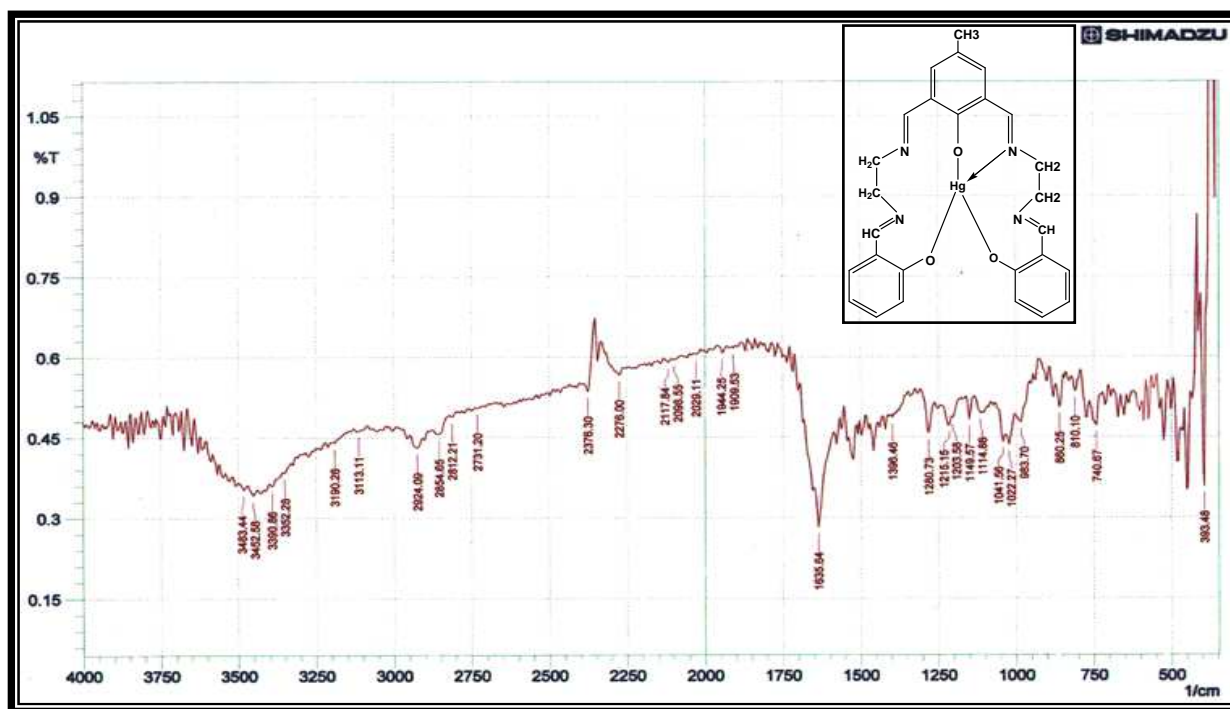


Fig. (3-11) I.R spectrum for K[Hg(L)] complex

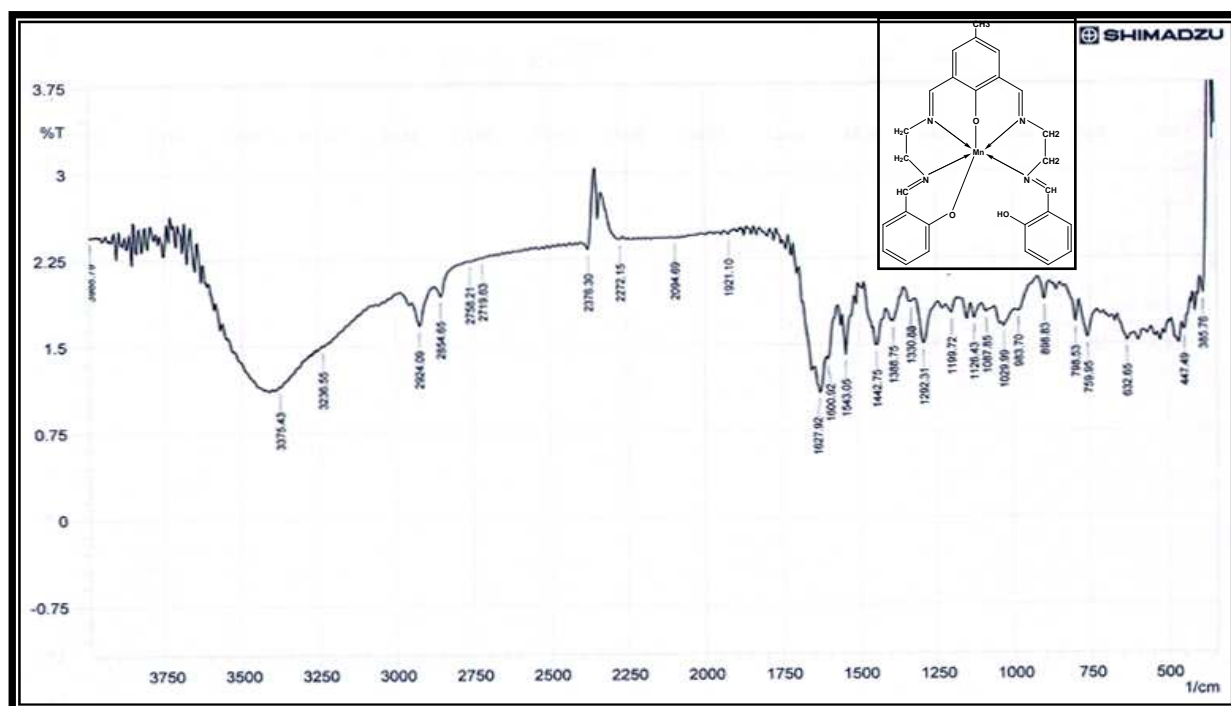


Fig. (3-12) I.R spectrum for [Mn(L)] complex

Table (3-6)

(3.5) UV-Vis Spectra of the ligand and complexes

(3.5.1) UV-Vis spectrum of the ligand (L)

The (UV-Vis) spectrum for (L) Fig. (3-13), exhibits intense absorption peak at (288 nm) (34722 cm^{-1}) ($\Sigma_{\text{max}} = 900 \text{ molar}^{-1} \text{ cm}^{-1}$) and absorption peak at (312 nm) (32051 cm^{-1}) ($\Sigma_{\text{max}} = 2258 \text{ molar}^{-1} \text{ cm}^{-1}$), which are assigned to ($\pi \rightarrow \pi^*$) and ($n \rightarrow \pi^*$) transitions respectively⁽¹⁰⁹⁾, Table (3-7).

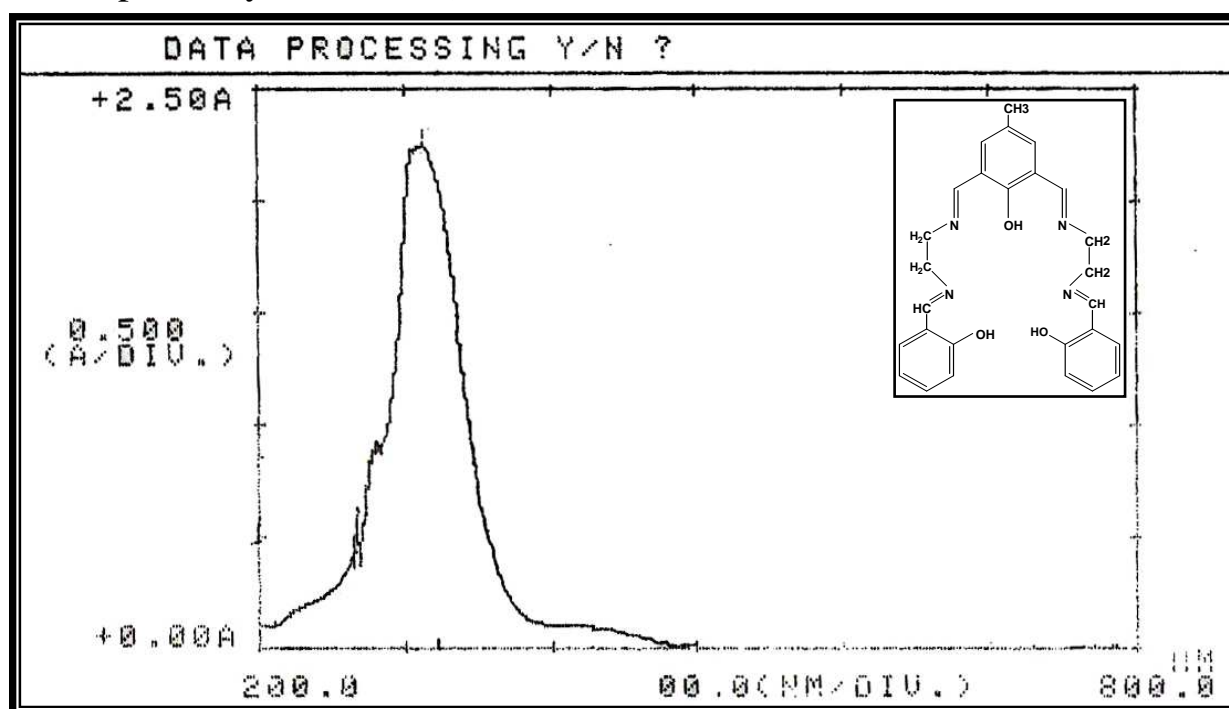


Fig. (3-13) Electronic spectrum of ligand

(3.5.2) UV-Vis Spectra of the complexes

(3.5.2.1) (UV-Vis) spectra for the [Cu(L)]Cl and [Ni(L)]Cl complexes

The (UV-Vis) spectra of these complexes are shown in Figures (3-14) and (3-15) respectively. The absorption dates are given in Table (3-7).

The spectrum of [Cu(L)]Cl complexes displayed three intense peaks in the (UV) region at (288) (24722cm^{-1}) ($\Sigma_{\text{max}}=2018 \text{ molar}^{-1} \cdot \text{cm}^{-1}$), at (340nm) (29411cm^{-1}) ($\Sigma_{\text{max}}= 2250 \text{ molar}^{-1} \cdot \text{cm}^{-1}$) and at (360nm) (27777cm^{-1}) ($\Sigma_{\text{max}} = 2100 \text{ molar}^{-1} \text{ cm}^{-1}$), these peaks were assigned to ligand field of the type ($\pi \rightarrow \pi^*$), ($n \rightarrow \pi^*$) and charge transfer respectively⁽¹¹⁶⁾. The visible region in the complexes, [Cu(L)]Cl showed a weak band at (570nm) (17544cm^{-1}) ($88 \text{ molar}^{-1} \cdot \text{cm}^{-1}$) assigned to (d-d) transition type (${}^2\text{B}_{1g} \rightarrow {}^2\text{B}_{2g}$) and (${}^2\text{B}_{1g} \rightarrow {}^2\text{E}_g$)⁽¹¹⁷⁾ confirming square planner structure around Copper(II) ion.

The spectrum of [Ni(L)]Cl complex displayed two intense in the (U.V) region at (288nm) (34722cm^{-1}) ($\Sigma_{\text{max}} = 1100 \text{ molar}^{-1} \cdot \text{cm}^{-1}$) and at (317nm) (31545cm^{-1}) ($\Sigma_{\text{max}}= 1099 \text{ molar}^{-1} \cdot \text{cm}^{-1}$), these peaks were assigned to ligand field of the type ($\pi \rightarrow \pi^*$), ($n \rightarrow \pi^*$) respectively. The visible region in the complex, [Ni(L)]Cl₂ showed weak bonds at (408nm) (24509 cm^{-1}) ($\Sigma_{\text{max}}=622 \text{ molar}^{-1} \text{ cm}^{-1}$) and to (d-d) transition type (${}^1\text{A}_{1g} \rightarrow {}^1\text{A}_{2g}$) and (${}^1\text{A}_{1g} \rightarrow {}^1\text{B}_{1g}$). Confirming square planner structure around Nickel(II) ion. One of the characteristic features of square planner Nickel complexes^(118,119), the absence of absorption bond at (10000cm^{-1}).

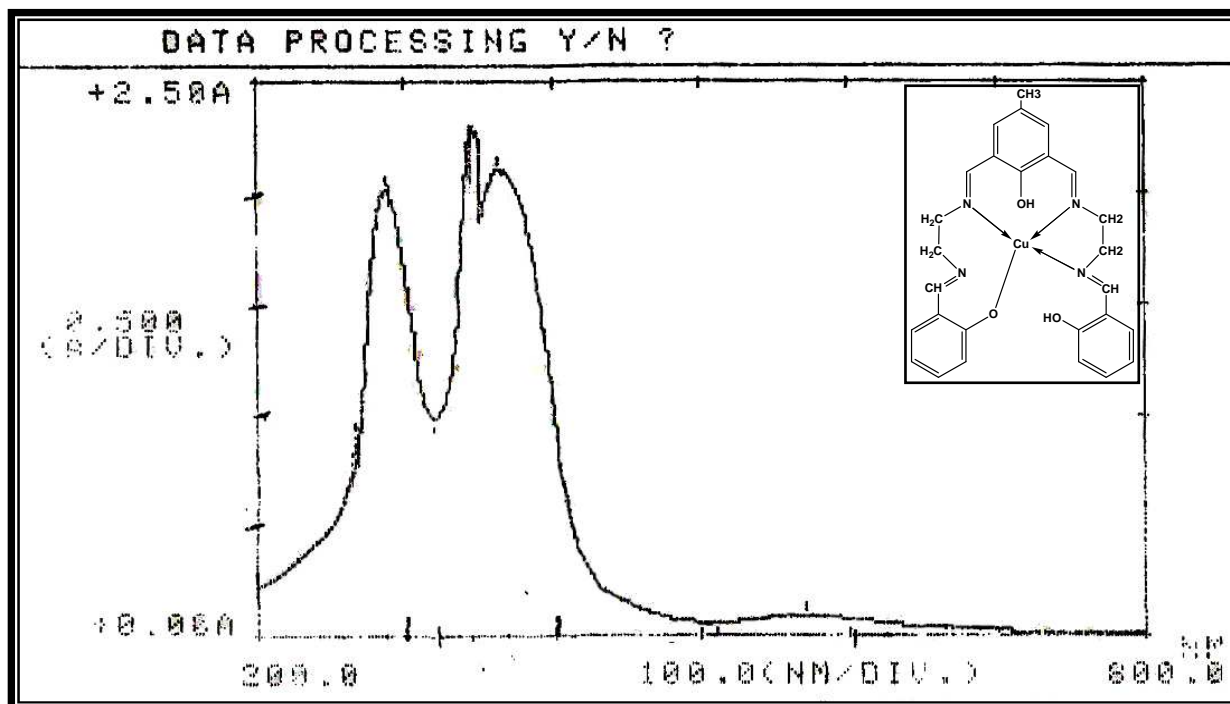


Fig. (3-14) Electronic spectrum of [Cu(L)]Cl complex

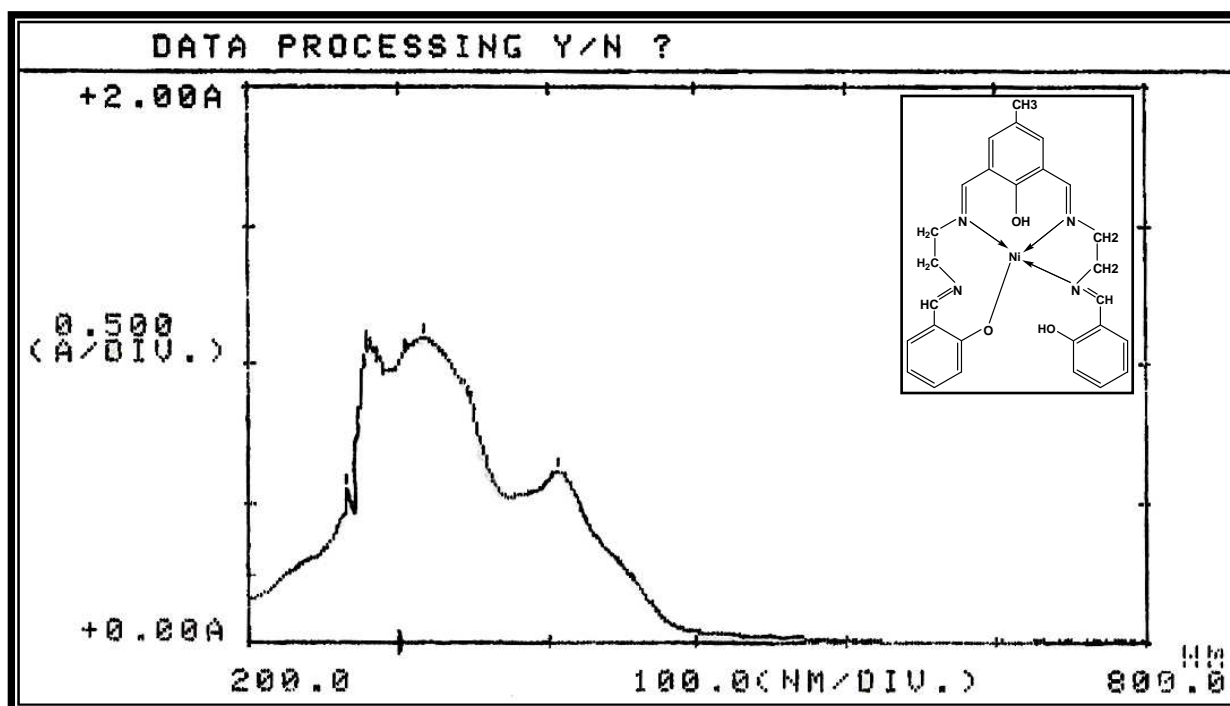


Fig. (3-15) Electronic spectrum of [Ni(L)]Cl complex

(3.5.2.2) (UV-Vis) spectrum of the [Cr(L)Cl]Cl complex

The spectrum of [Cr(L)Cl]Cl complex Fig. (3-16) displayed one band in the (UV) at (288nm) (34722cm^{-1}) ($\Sigma_{\text{max}}=2028\text{ molar}^{-1}\cdot\text{cm}^{-1}$) assigned to (${}^4A_{2g}\rightarrow{}^4T_{1g}(\text{P})$) transition, and two bands at (413nm) (24213cm^{-1}) ($\Sigma_{\text{max}}=1385\text{ molar}^{-1}\cdot\text{cm}^{-1}$) and at (625nm) (1000cm^{-1}) ($\Sigma_{\text{max}}=370\text{ molar}^{-1}\cdot\text{cm}^{-1}$), assigned to (${}^4A_{2g}\rightarrow{}^4T_{1g}(\text{F})$) and (${}^4A_{2g}\rightarrow{}^4T_{2g}(\text{F})$) transition respectively⁽¹²⁰⁾, confirming octahedral structure around chromium (III) ion.

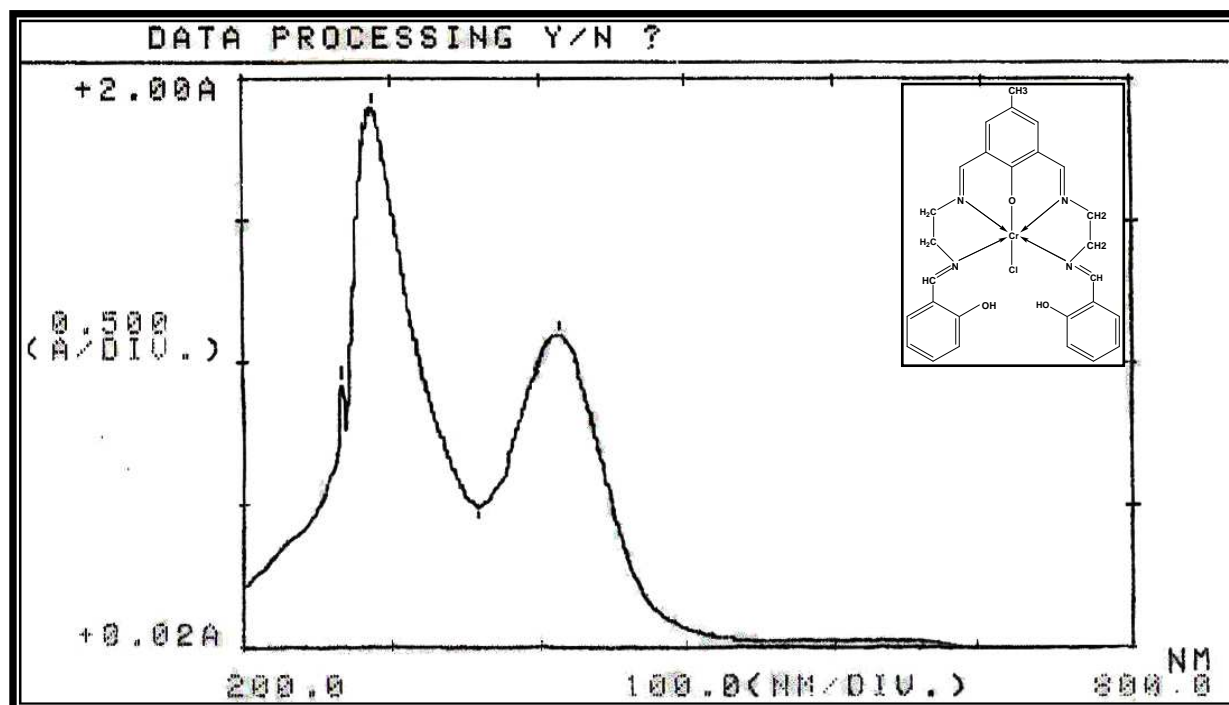


Fig. (3-16) Electronic spectrum of [Cr(L)Cl]Cl complex

(3.5.2.3) (UV-Vis) Spectra of the [Co(L)] and [Mn(L)] complexes

The spectrum of [Co(L)] complex Fig. (3-17) displayed two bands in the (UV) region at (288nm) (34722cm^{-1}) ($\Sigma_{\text{max}}=1993 \text{ molar}^{-1} \cdot \text{cm}^{-1}$), and at (385nm) (29740cm^{-1}) ($\Sigma_{\text{max}}=1219 \text{ molar}^{-1} \cdot \text{cm}^{-1}$) assigned to ligand field of the ($\pi \rightarrow \pi^*$) and ($n \rightarrow \pi^*$) respectively. The visible region in the complexes, [Co(L)] showed weak bands at (607nm) (16501cm^{-1}) ($\Sigma_{\text{max}} = 88 \text{ molar}^{-1} \cdot \text{cm}^{-1}$) and at (674nm) (14836cm^{-1}) ($\Sigma_{\text{max}}=123 \text{ molar}^{-1} \cdot \text{cm}^{-1}$) assigned to (d-d) transitions type (${}^4T_{1g}(\text{F}) \rightarrow {}^4T_{1g}(\text{P})$) and (${}^4T_{1g}(\text{F}) \rightarrow {}^4A_{2g}(\text{F})$). Confirming Octahedral structure around Cobalt (II) ion^(121,122,123).

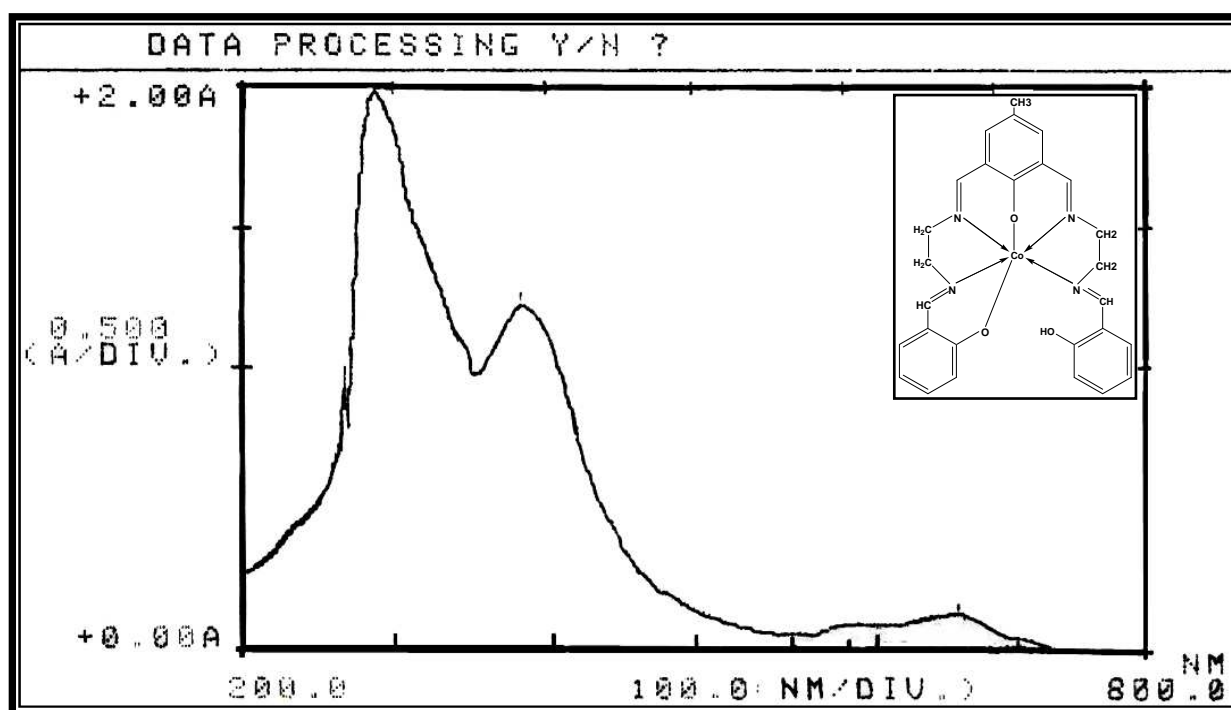


Fig. (3-17) Electronic spectrum of [Co(L)] complex

The spectrum of [Mn(L)] complex Fig. (3-18) displayed two bands in the (UV) region at (315nm) (31746cm^{-1}) ($\Sigma_{\text{max}}=2490 \text{ molar}^{-1}.\text{cm}^{-1}$), and at (357nm) (28011cm^{-1}) ($\Sigma_{\text{max}}=2025 \text{ molar}^{-1}.\text{cm}^{-1}$) assigned to ligand field of type ($\pi \rightarrow \pi^*$) and to charge transfer respectively. The visible region in the complexes, [Mn(L)] showed strong bond at (400nm) (25000cm^{-1}) ($\Sigma_{\text{max}}=1452 \text{ molar}^{-1}.\text{cm}^{-1}$) assigned to (d-d) transition type (${}^6A_{1g} \rightarrow {}^4T_{1g}(G)$). Confirming Octahedral structure around Manganese (II) ion^(124,121).

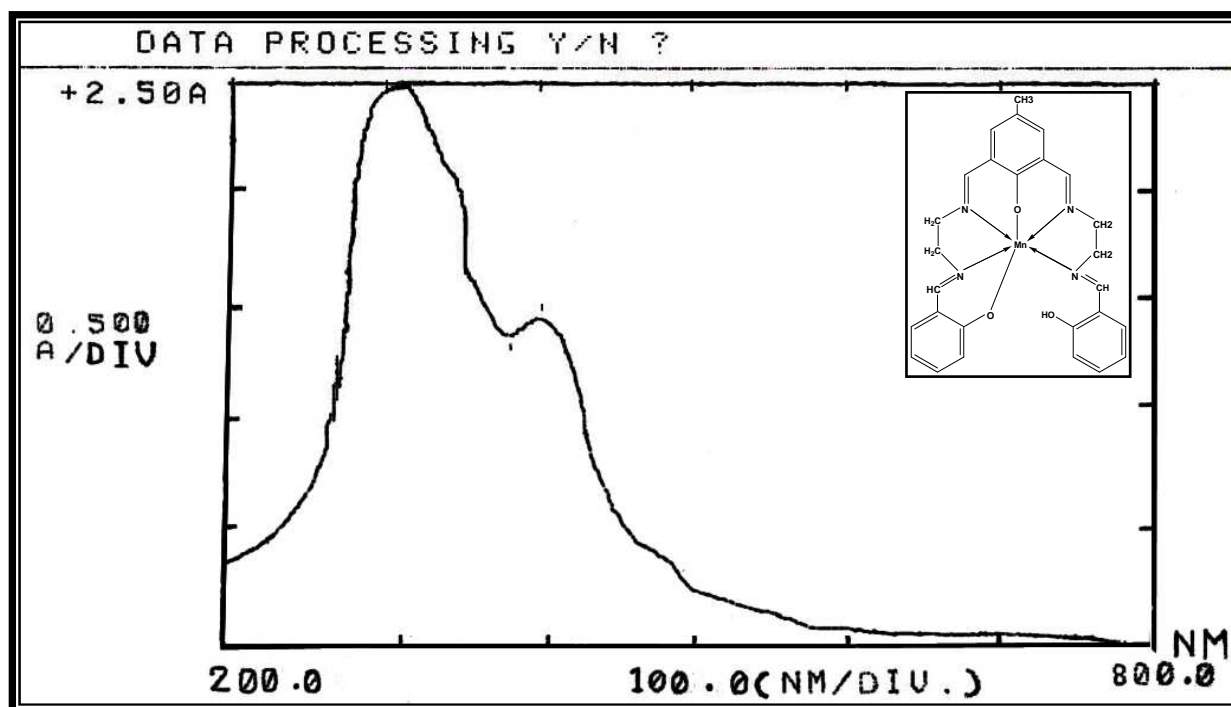


Fig. (3-18) Electronic spectrum of [Mn(L)] complex

(3.5.2.4) (UV-Vis) spectra of [Fe(L)], [Zn(L)], [Cd(L)] and K[Hg(L)]Cl₂ complexes

The (UV-Vis) spectrum of [Fe(L)] compound Fig. (3-19) displayed two bands in the (UV) region at (280nm) (35714cm^{-1}) ($\Sigma_{\text{max}}=800 \text{ molar}^{-1}.\text{cm}^{-1}$) and at (302nm) (33114cm^{-1}) ($\Sigma_{\text{max}}=1812$

molar⁻¹.cm⁻¹), these bands were assigned to ligand field of the type ($\pi \rightarrow \pi^*$) and ($n \rightarrow \pi^*$).

A third band appeared at (477nm) (20964cm⁻¹) ($\Sigma_{\max}=587$ molar⁻¹. cm⁻¹) assigned to (d-d) transition type (${}^5E \rightarrow {}^5T_2$), confirming tetrahedral structure around Iron (II) ion⁽¹²⁵⁾.

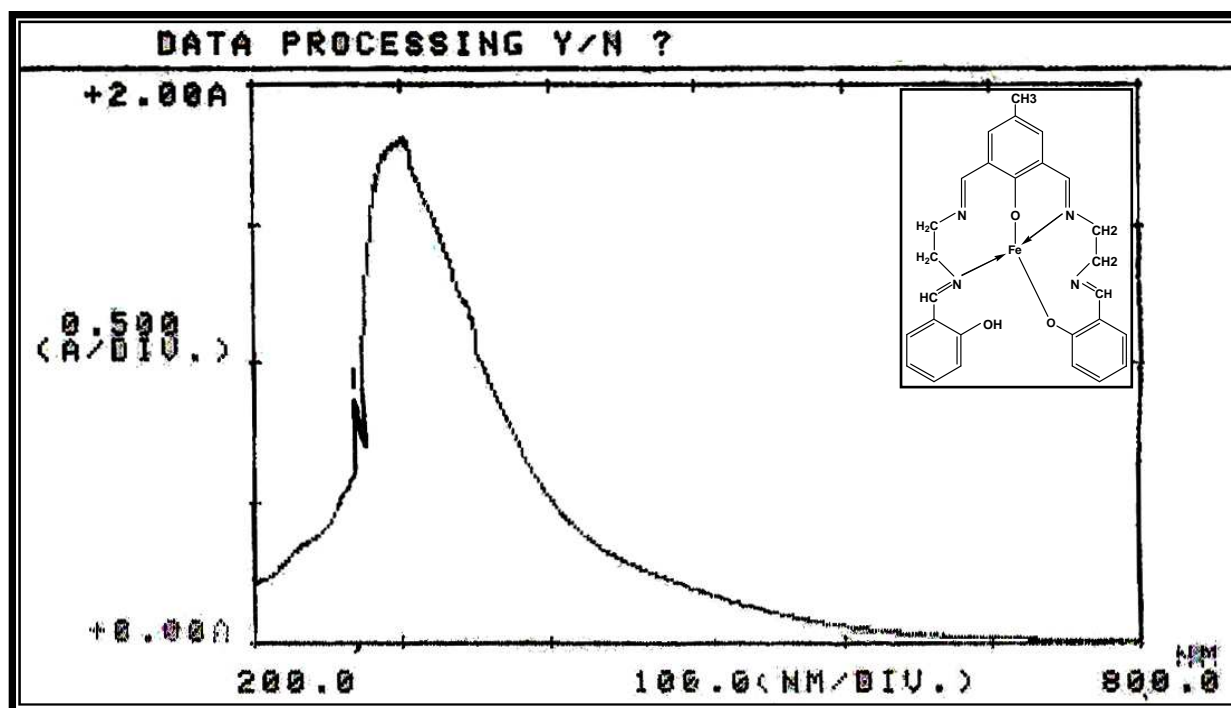


Fig. (3-19) Electronic spectrum of [Fe(L)] complex

The (UV-Vis) spectra of [Zn(L)], [Cd(L)] and K[Hg(L)]Cl₂ Figures (3-20), (3-21) and (3-22) displayed three bands in the (UV) region at (280nm) (25714cm⁻¹) ($\Sigma_{\max}=1252$ molar⁻¹.cm⁻¹) for zinc complex, at (288nm) (34722cm⁻¹) ($\Sigma_{\max}=800$ molar⁻¹.cm⁻¹) for cadmium complex, at (288nm) (34722cm⁻¹) ($\Sigma_{\max}=1080$ molar⁻¹.cm⁻¹) for Mercury complexes, these bands are assigned to ($\pi \rightarrow \pi^*$), ($n \rightarrow \pi^*$) and charge transfer, confirming tetrahedral structure around zinc (II), cadmium (II) and mercury (II) ions respectively^(126,127).

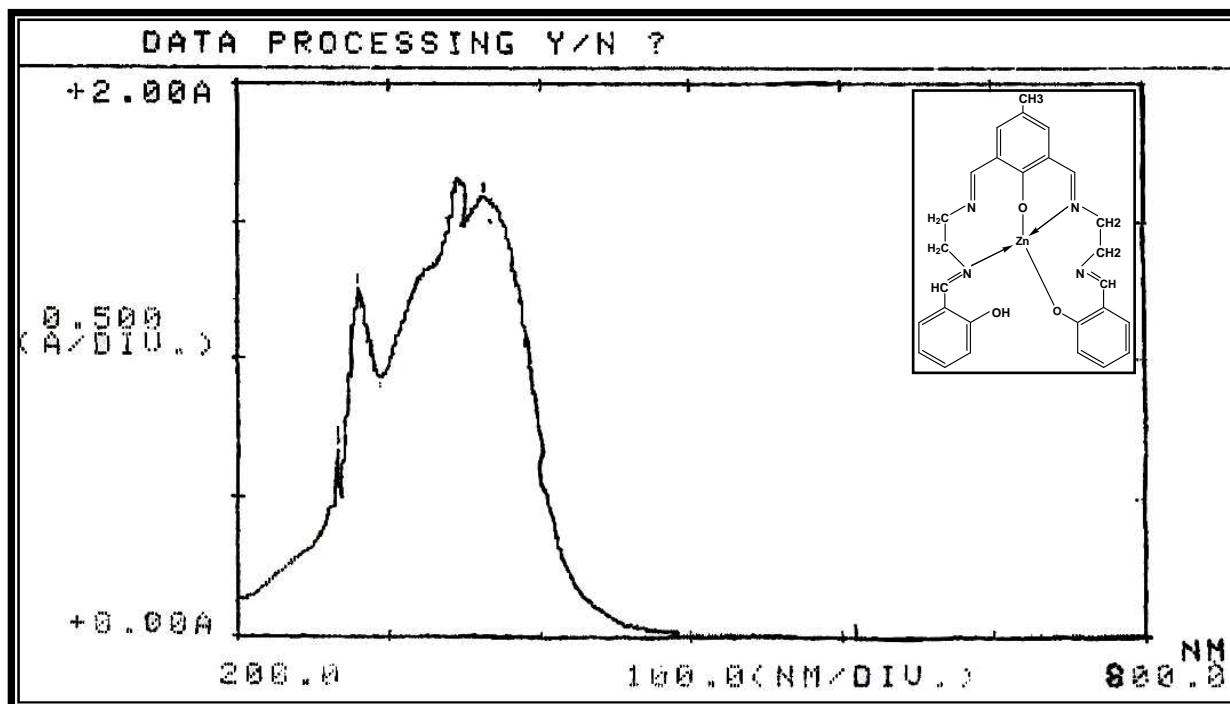


Fig. (3-20) Electronic spectrum of [Zn(L)] complex

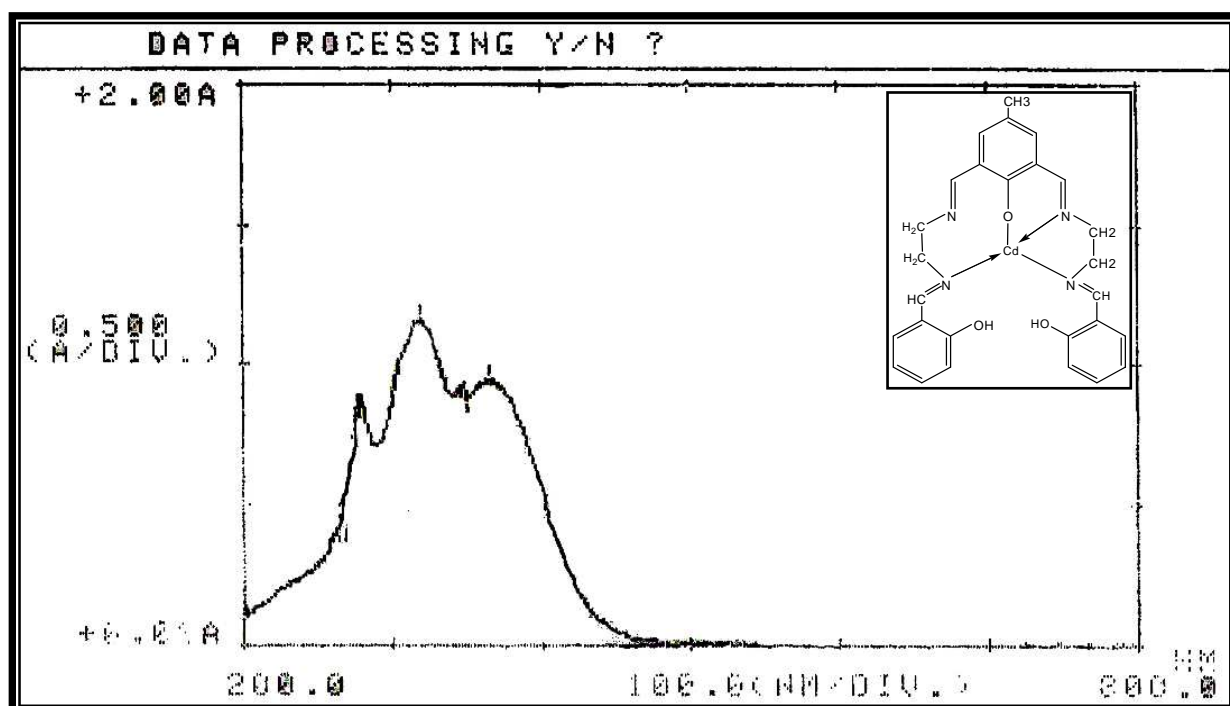


Fig. (3-21) Electronic spectrum of [Cd(L)] complex

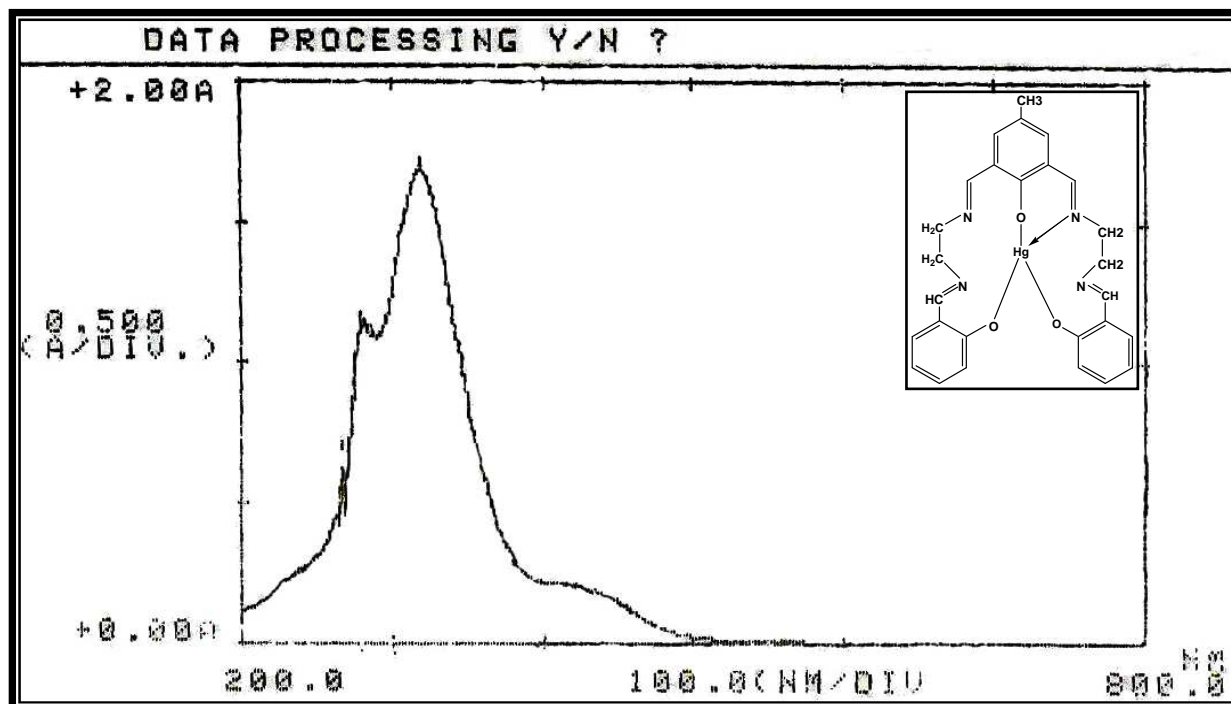


Fig. (3-22) Electronic spectrum of K[Hg(L)] complex

Table (3-7) Electronic Spectral data of [L] complexes in DMF solvent

No.	Compound	λ nm	A	ν cm ⁻¹	Σ_{\max} (molar ⁻¹ . cm ⁻¹)	Assignment	Proposed structure
1	Ligand(L)	288 312	0.900 2.258	34722 32051	900 2258	$\pi \rightarrow \pi^*$ $n \rightarrow \pi^*$	
2	[Cu(L)]Cl	288 340 360 570	2.018 2.25 2.10 0.088	24722 29411 27777 17544	2018 2250 2100 88	$\pi \rightarrow \pi^*$ $n \rightarrow \pi^*$ charge transfer ${}^2B_{1g} \rightarrow {}^2B_{2g}, {}^2B_{1g} \rightarrow {}^2E_g$	Sq. Planner
3	[Fe(L)]	280 302 477	0.8 2.395 0.587	35714 33112 20964	800 1812 587	C.T C.T ${}^5E \rightarrow {}^5T_2$	Tetra hedral
4	[Ni(L)]Cl	288 317 408 460	1.10 1.090 0.622 0.25	34722 31545 24509 21739	1100 1099 622 250	$\pi \rightarrow \pi^*$ $n \rightarrow \pi^*$ ${}^1A_{1g} \rightarrow {}^1A_{2g}$ ${}^1A_{1g} \rightarrow {}^1B_{1g}$	Sq. Planner
5	[Cr(L)Cl]Cl	625 413 288	0.037 1.385 2.028	16000 24213 34722	370 1185 2028	${}^4A_{2g} \rightarrow {}^4T_{2g}(F)\nu_1$ ${}^4A_{2g} \rightarrow {}^4T_{1g}(F)\nu_2$ ${}^4A_{2g} \rightarrow {}^4T_{1g}(P)\nu_3$	Octa hedral
6	[Co(L)]Cl	288 385 607 674	1.993 1.219 0.098 0.123	34722 29740 16501 14836	1993 1219 88 123	$\pi \rightarrow \pi^*$ $n \rightarrow \pi^*$ ${}^4T_{1g}(F) \rightarrow {}^4T_1(p)\nu_3$ ${}^4T_{1g}(F) \rightarrow {}^4A_{2g}(F)\nu_2$	Octa hedral
7	[Zn(L)]	280 350 363	1.252 1.680 1.586	35714 28571 27548	1252 1680 1586	$\pi \rightarrow \pi^*$ $n \rightarrow \pi^*$ charge transfer	Tetra hedral
8	[Cd(L)]	288 319 366	0.800 1.16 0.944	34722 31347 27322	800 1160 844	$\pi \rightarrow \pi^*$ $n \rightarrow \pi^*$ charge transfer	Tetra hedral
9	K[Hg(L)]	288 319 440	1.08 1.678 0.2	34722 31347 22727	1080 1678 200	$\pi \rightarrow \pi^*$ $n \rightarrow \pi^*$ charge transfer	Tetra hedral
10	[Mn(L)]	400 357 315	1.452 2.025 2.490	25000 28011 31746	1452 2025 2490	${}^6A_{1g}(S) \rightarrow {}^4T_{1g}(G)$ charge transfer $\pi \rightarrow \pi^*$	Octa hedral

C.T: Charge transfer

(3.6) Magnetic moment measurement

Magnetic moment has been determined in the solid state by Faraday's method. The magnetic properties of these complexes should provide a testing ground for the oxidation state of the complexes, therefore provides a way of counting the number of unpaired electrons. This should help in predicting the bonding model and electronic structure⁽¹²⁸⁾.

The magnetic susceptibility for complexes was measured at room temperature, Table (3-8), the effective magnetic moment (μ_{eff} /B.M) is given by

$$\mu_{\text{eff}} = 2.828 \sqrt{X_A T}$$

Where; T= Absolute temperature (298) °K

X_A = Atomic susceptibility corrected from diamagnetic presence.

The magnetic susceptibility was calculated according to the example shown below.

The complex $[\text{Cu}(\text{L})]\text{Cl}$ or $[\text{Cu}(\text{C}_{27}\text{H}_{27}\text{N}_4\text{O}_3)]\text{Cl}$

$$X_g \text{ (Gram susceptibility)} = 1.94 \times 10^{-6}$$

$$X_M \text{ (molar susceptibility)} = X_g \times \text{M.wt}$$

$$= 1.94 \times 10^{-6} \times 554.266$$

$$= 1075.2 \times 10^{-6}$$

$$X_A \text{ (Atom susceptibility)} = X_M - D$$

Where D is the diamagnetic correction of the complex which is equal to 136.57×10^{-6}

$$X_A = 1075.2 \times 10^{-6} - (-136.57 \times 10^{-6})$$

$$X_A = 1212.6 \times 10^{-6}$$

$$\begin{aligned}\mu_{\text{eff}} &= 2.828\sqrt{X_A \cdot T} \\ &= 2.828\sqrt{1212.6 \times 10^{-6} \times 298} \\ &= 1.70 \text{ B.M}\end{aligned}$$

Table (3–8) Data of magnetic moment ($\mu_{\text{eff}} = \text{B.M}$) of solid at 298 K° and suggested stereo chemical structure of complexes

No.	complex	$X_g \times 10^{-6}$ gram susceptibility	$X_M \times 10^{-6}$ molar susceptibility	$X_A \times 10^{-6}$ atom susceptibility	μ (B.M) actual	μ (B.M) calculated	Suggested structure
1	[Cu(L)]Cl	1.94	1076.03	1212.6	1.70	1.73	Square planer
2	[Fe(L)]	19.92	10164.4	10280.9	4.95	4.90	Tetrahedral
3	[Cr(L)Cl]Cl	10.27	5942.33	6058.8	3.80	3.88	Octahedral
4	[Co(L)]	11.5	5954.33	6090.8	3.81	3.88	Octahedral
5	[Mn(L)]	30.05	15292.33	15408.8	6.06	5.92	octahedral

Table (3–9) Magnetic moments of metal complexes

No.	compound	Actual mag. moment $\mu(\text{B.M})$	Theo mag. moment $\mu(\text{B.M})$	Expected configurations	Remarks
1	Ligand (L)	—	—	—	
2	[Cu(L)]Cl	1.70	1.73	Square planner	
3	[Fe(L)]	4.95	4.90	Tetra hedral	
4	[Ni(L)]Cl	Zero	Zero	Square planner	
5	[Cr(L)Cl]Cl	3.80	3.88	Octahedral	
6	[Co(L)]	3.81	3.88	Octahedral or tetrahedral	This complexe needs X–ray analysis for structural determintion
7	[Zn(L)]	Zero	Zero	Dia.Mag.	
8	[Cd(L)]	Zero	Zero	Dia Mag.	
9	K[Hg(L)]	Zero	Zero	Dia Mag	
10	[Mn(L)]	6.06	5.92	Octahedral	

* Magnetic moment due to spin of electrons only. $\mu\sqrt{n(n+2)}$

(3.7) Nuclear magnetic resonance (NMR) spectra for precursor (I), ligand and metal complexes

The ^1H , ^{13}C and $^1\text{H}-^{13}\text{C}$ correlated NMR analysis are used to characterize the ligand and complexes. The spectra have been recorded in CDCl_3 solution, interpretations of signals were made according to the information given by Chem. Office Program.

(3.7.1) ^1H NMR spectrum for precursor (I) [2,6-diformyl-4-methyl phenol]

The ^1H NMR spectrum of 2,6-diformyl-4-methyl phenol, Fig. (3–23) in DMSO-d_6 solvent shows a broad signal at ($\delta= 11.40$ ppm) equivalent to one proton assigned to (O–H) group⁽¹²⁹⁾. The signal at resonance ($\delta= 10.25$ ppm, 2H) assigned to aliphatic aldehydic proton ($\text{C}_7, \text{C}_8\text{-H}$). This signal appears as a singlet indicating the equivalent of the two protons in solution. The chemical shift at ($\delta=7.80$ ppm, 2H) which is due to aromatic protons of ($\text{C}_3, \text{C}_5\text{-H}$), appears as expected as a singlet. The signal at chemical shift ($\delta=2.40$ ppm, 3H) is assigned to methyl group protons ($\text{C}_9\text{-H}$). Table (3–10) summarizes the details of the chemical shifts.

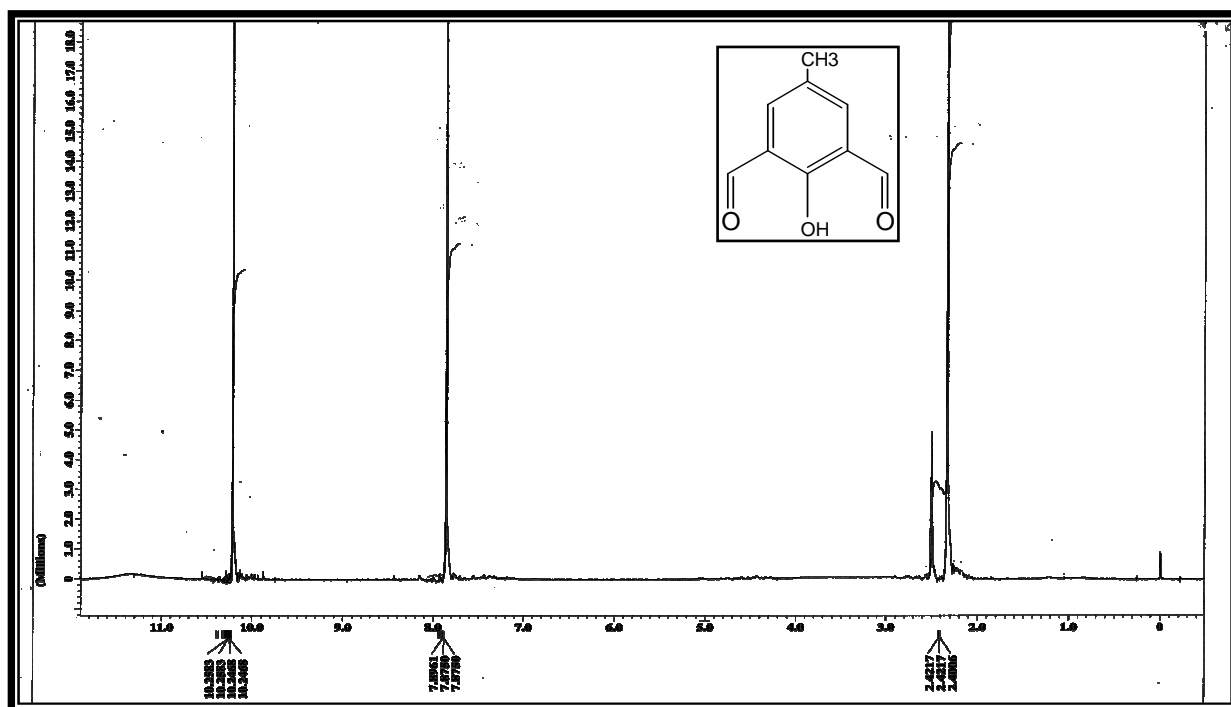


Fig. (3–23) ^1H NMR spectrum of precursor (I)

Table (3-10) ^1H NMR data for precursors (I) measured in DMSO- d_6 and chemical shift (δ) in ppm.

Compound	O-H	H-C=O (C ₈)	Aromatic C-H(C _{3,5})	CH ₃ (C ₇)
2,6-diformyl-4-methyl phenol	11.40 (1H,s)	10.25, (2H,s)	7.8 (2H,s)	2.4, (3H,s)

s: Singlet, br: broad

(3.7.2) ^1H NMR spectrum of the ligand

The ^1H NMR spectrum of the ligand, Fig. (3-24) In CDCl_3 solvent shows a broad signal at ($\delta_{\text{H}}=13.25\text{ppm}$) equivalent to three protons assigned to (O-H) groups.

The signal at ($\delta_{\text{H}}=8.40\text{ppm}$, 4H) assigned to protons of carbon number (8) and (11). The signal at ($\delta_{\text{H}}=7.31\text{ ppm}$, 2H) assigned to protons of carbon number (13). The signal at ($\delta_{\text{H}}=7.21\text{ppm}$, 2H) assigned to protons of carbon number (15) which is in meta position with respect to (OH) group. The signal at ($\delta_{\text{H}}=6.95\text{ ppm}$, 2H) assigned to protons of carbon number (14) which is in para position with respect to (OH) group. The signal at ($\delta_{\text{H}}=6.85\text{ ppm}$. 2H) assigned to protons of number (16) which is on ortho position with respect to (OH) group.

The signal at ($\delta_{\text{H}}=3.91\text{ ppm}$, 8H) assigned to protons of carbon number (9) and (10) of the ethylene group. The signal at ($\delta_{\text{H}}=2.35$, 3H) assigned to protons of carbon number (7) of the methyl group. All ^1H NMR data for the ligand could be seen in Table (3-11).

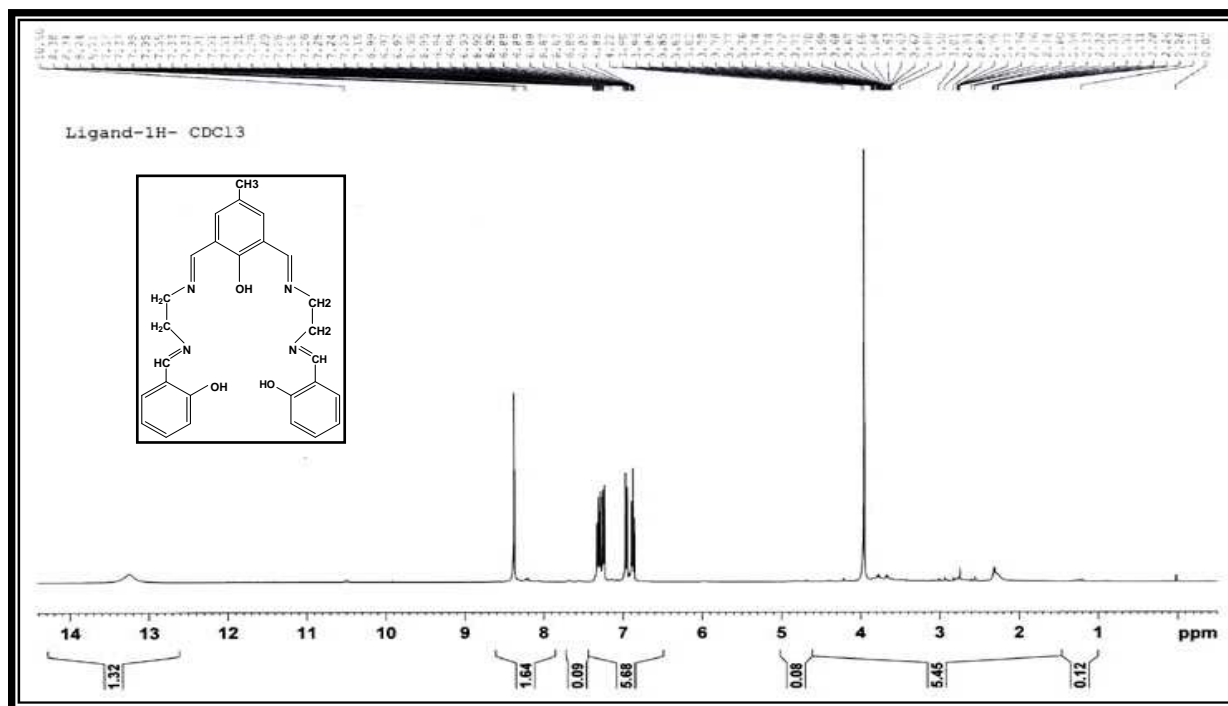


Fig. (3–24) ¹H NMR spectrum of ligand

(3.7.3) ¹H NMR spectra for the complexes

(3.7.3.1) ¹H NMR spectra for copper and Nickel complexes

The ¹H NMR spectrum for the complexes [Cu(L)]Cl and [Ni(L)]Cl Figs. (3–25) & (3–26) showed no signals at 13.25 ppm for protons of (OH) groups of the free ligand, and no signals at 8.4 ppm for protons of azomethine, this indicates that coordination of the ligand with metal ions are through oxygen atoms of the phenol group and also through Nitrogen atom's of the imine groups. Figs. (3–25) and (3–26) indicate that chemical shifts in ¹H NMR to lower values for all protons of complexes happend, this could be rendered to the transfer of charge density from metal ion to the ligand's coordination sites, which consequently resulted in more shielding of ligand's protons.

^1H NMR chemical shifts in these complexes for protons of carbon (8, 11, 17, 15, 14, 16, 9, 10 and 7) to the verified region compared to that in the free ligand is verified by strong back donation in these complexes.

The similarities of ^1H NMR spectra of the copper and Nickel complexes indicate the similarity in chemical structure of the two complexes, as can be seen in Fig. (3–25) and Fig. (3–26) respectively. Table (3–11) summarized ^1H NMR data for all complexes prepared.

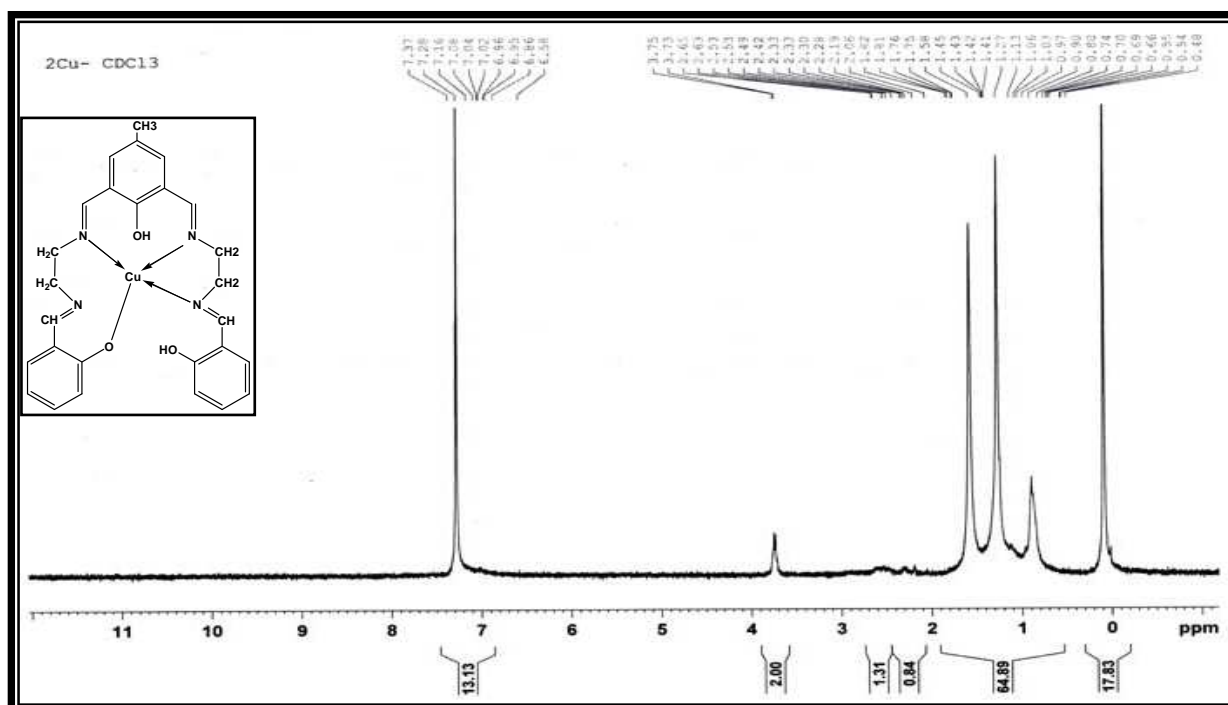


Fig. (3–25) ^1H NMR spectrum of $[\text{Cu}(\text{L})]\text{Cl}$

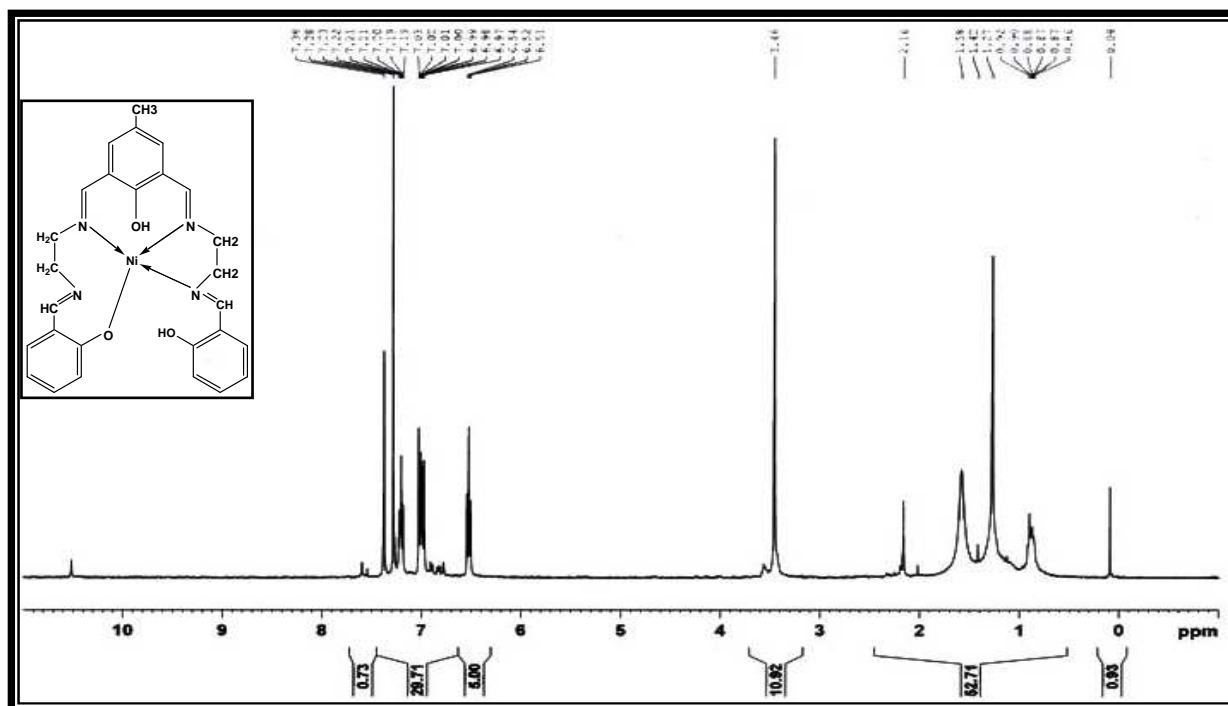


Fig. (3-26) ^1H NMR spectrum of $[\text{Ni}(\text{L})]\text{Cl}$

(3.7.3.2) ^1H NMR spectra for Zinc, Cadmium, Mercury and Iron complexes

^1H NMR spectrum for ligand [L] Fig. (3-24) in CDCl_3 displayed, a broad signal at chemical Shifts ($\delta_{\text{H}}=13.25$ ppm, 3H) attributed to the three protons of (O-H) phenolic group. On complexation with Zinc, Cadmium, Mercury and Iron ions this band almost disappear in the spectra, indicating that coordination ought be through phenolic groups. On the other hand, reduction of the intensity of Azomethine protons occurred in complexes of Zinc, Cadmium and Iron, indicating additional coordination sites through Nitrogen atom of the imine groups, as can be seen in Figures (3-27), (3-28) and (3-29) comparison of ^1H NMR of the ligand Fig. (3-24) and that of Mercury complexes Fig. (3-30) indicates the following; first disappearance of (OH) signal while proton signal of imine

group remains uncharged, this indicates coordination of Mercury ions to the ligand through oxygen atoms of phenolic groups, second ^1H NMR signals of ethylene diamine do not change in chemical shift or in intensity indicating that coordination through Nitrogen atoms of the diamines has not occurred.

^1H NMR signals in all four metal complexes are much less than that of the corresponding protons of the free ligand, as can be seen from Figures (3–27), (3–28), (3–29) and (3–30) summarized in Table (3–11).

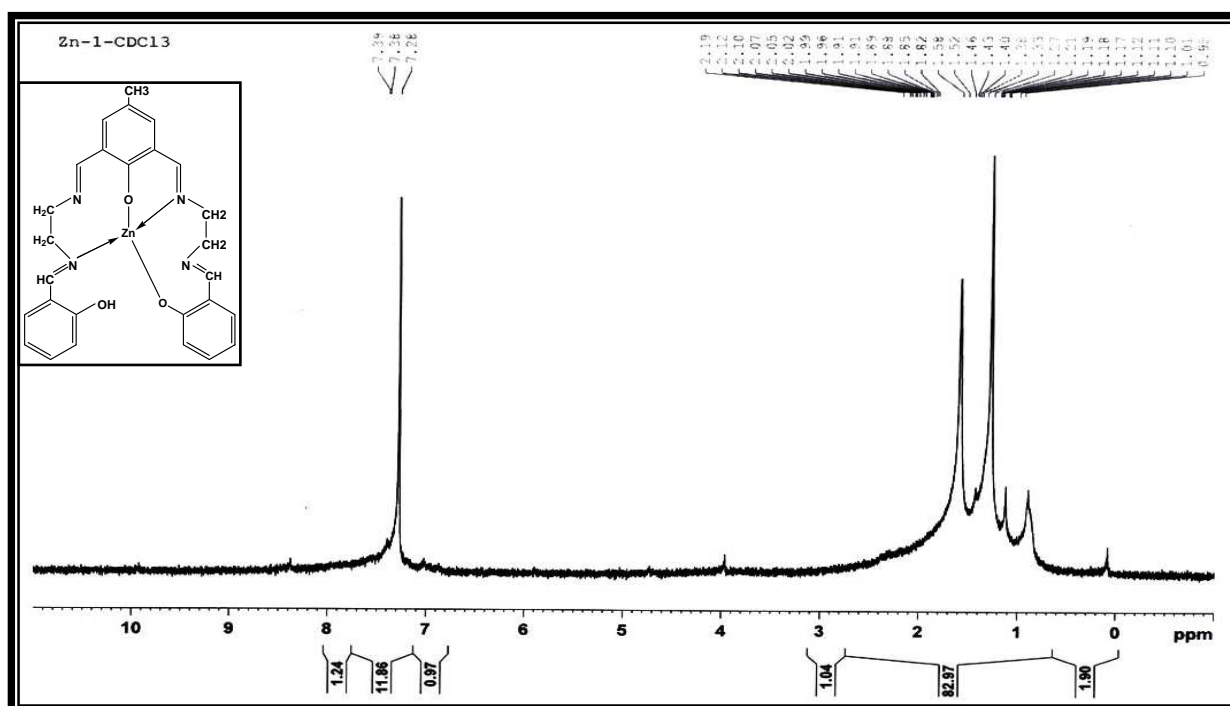
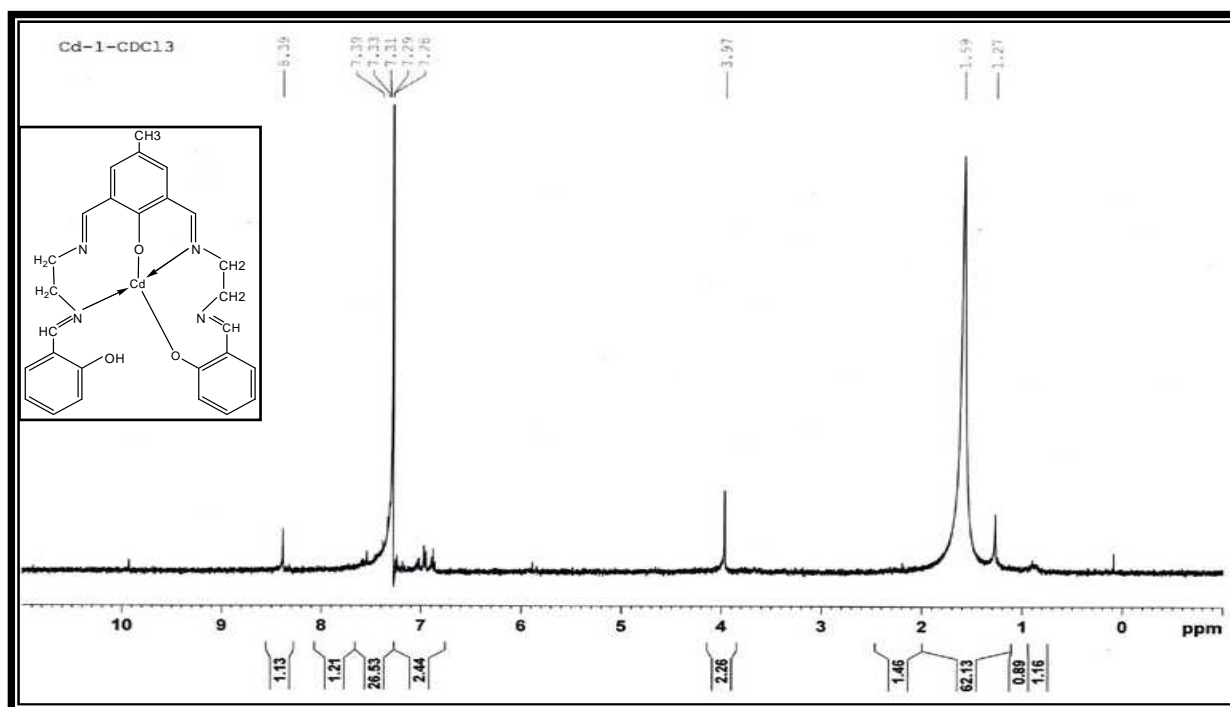
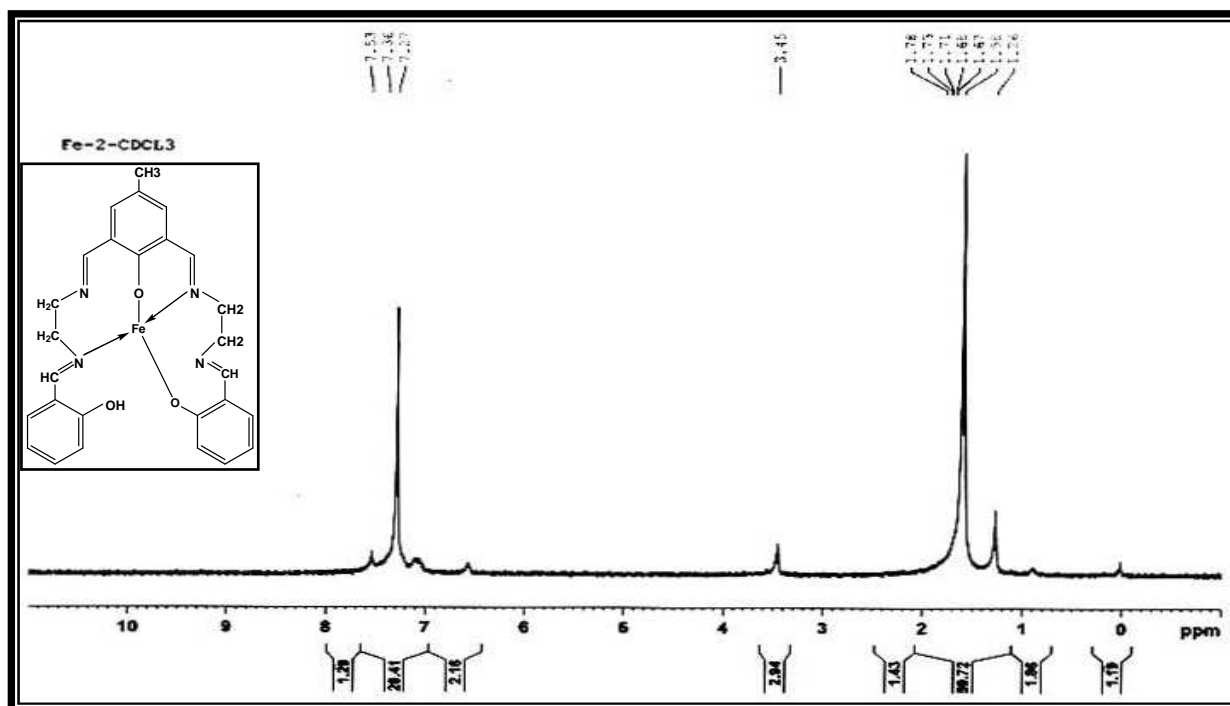


Fig. (3–27) ^1H NMR spectrum of $[\text{Zn}(\text{L})]$

Fig. (3-28) ^1H NMR spectrum of $[\text{Cd}(\text{L})]$ Fig. (3-29) ^1H NMR spectrum of $[\text{Fe}(\text{L})]$

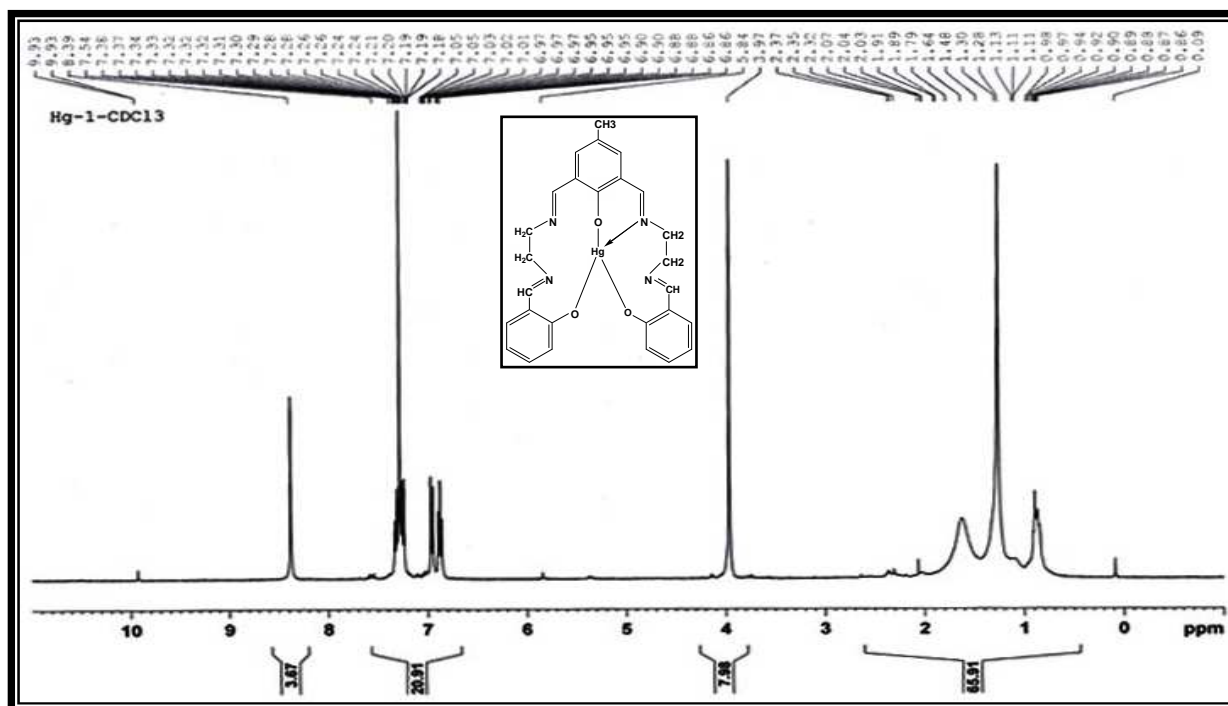
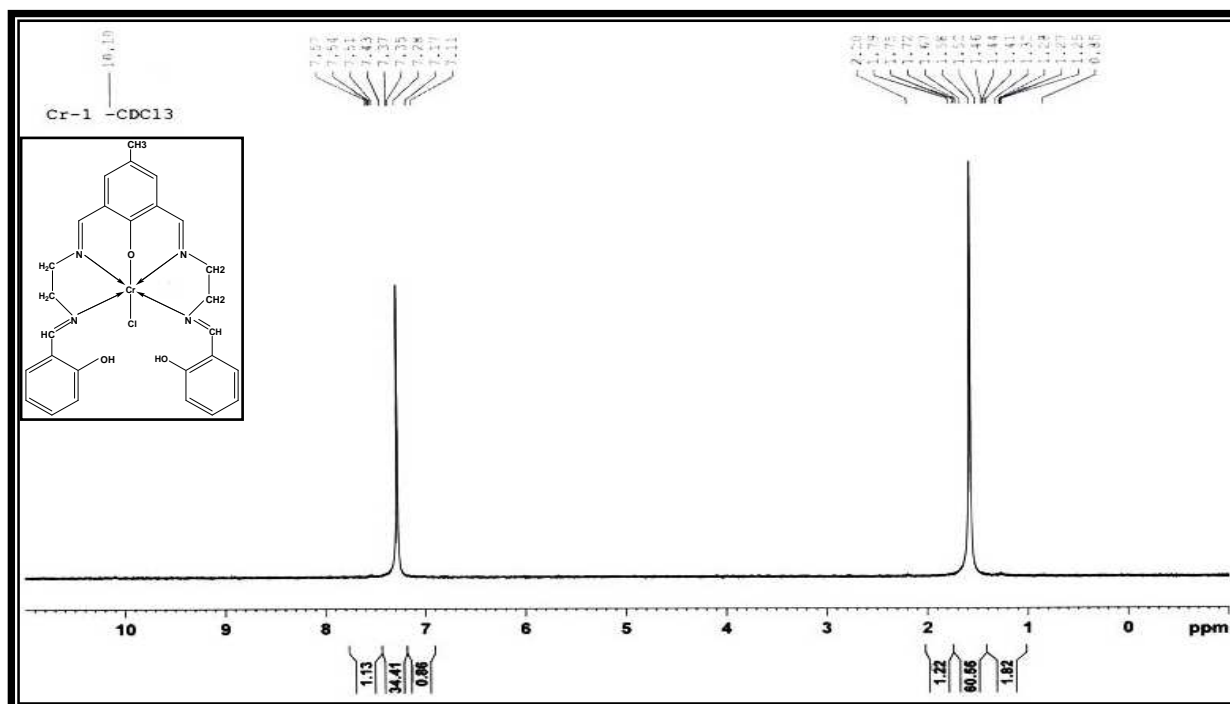
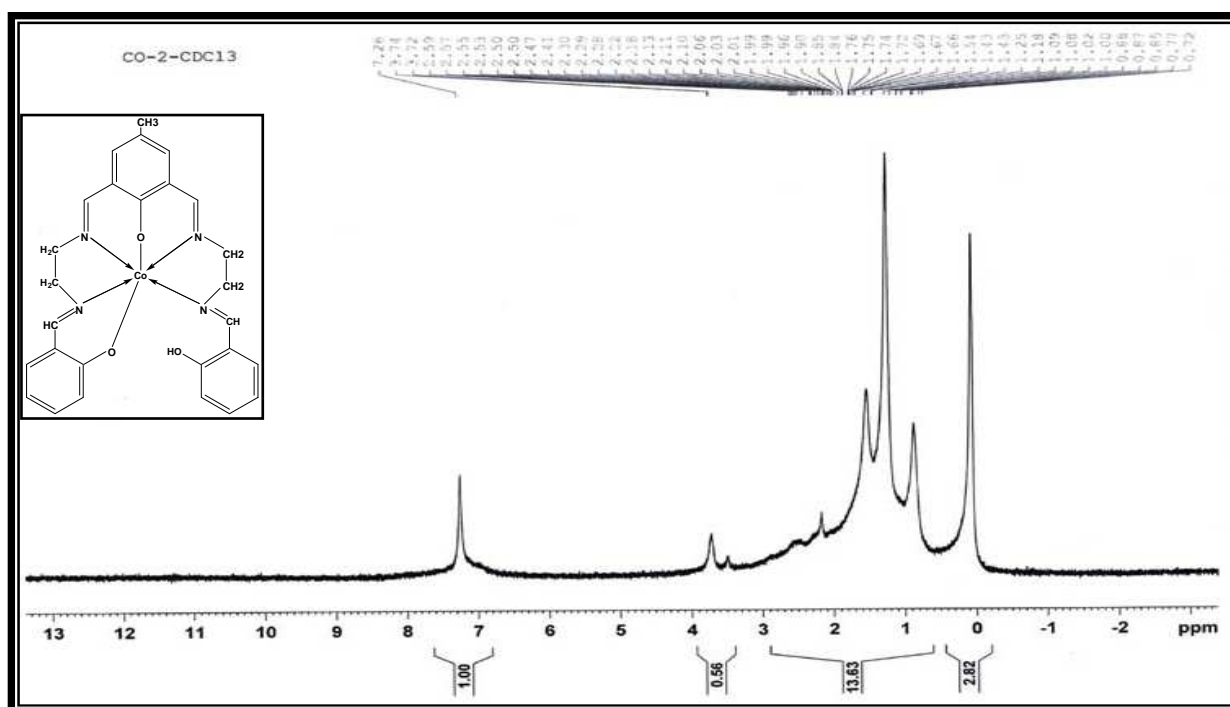


Fig. (3–30) ^1H NMR spectrum of $\text{K}[\text{Hg}(\text{L})]$

(3.7.3.3) ^1H NMR spectra for Chromium, Cobalt and Manganese complexes

Comparing ^1H NMR spectra of Chromium, Cobalt and Manganese complexes of Figures (3–31), (3–32), and (3–33) with the corresponding spectrum of the free ligand Fig. (3–24) indicate the following; first, all proton signals in complexes are shifted toward lower values of chemical shifts, indicating coordination taking place between metal ions and the ligand, second reduction of the three proton signals, namely; phenolic protons, imine protons and ethylene diamine protons, indicating coordination of the metal ions to these sites and suggesting the formation of high symmetry octahedral complexes. Results are summarized in Table (3–11).

Fig. (3-31) ^1H NMR spectrum of $[\text{Cr}(\text{L})\text{Cl}]\text{Cl}$ Fig. (3-32) ^1H NMR spectrum of $[\text{Co}(\text{L})]$

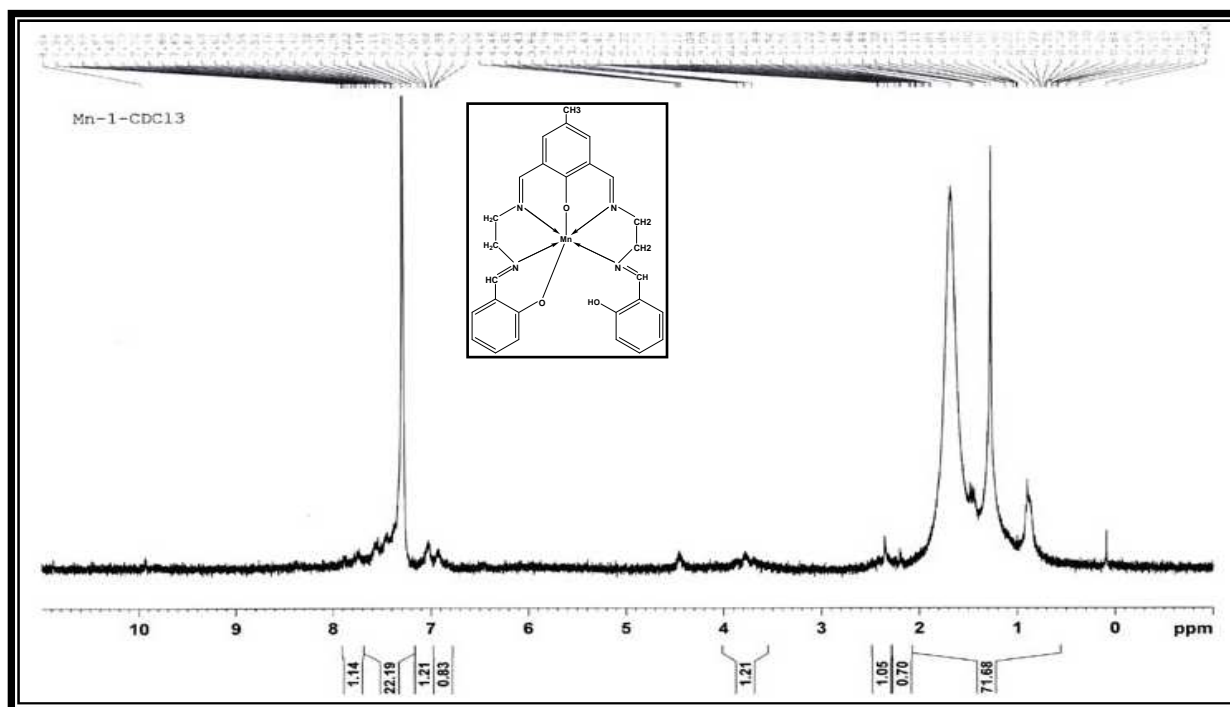
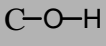
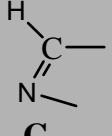
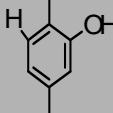
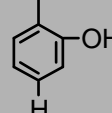
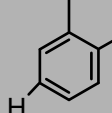
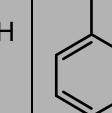
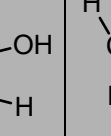
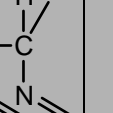


Fig. (3-33) ^1H NMR spectrum of $[\text{Mn}(\text{L})]$

Table (3–11) ^{13}H NMR data for the ligand and metal complexes in DCCl_3 and chemical shift in ppm (δ)

Compound	 $\text{C}_1, \text{C}_{17}$	 $\text{C}_{8, 11}$	 C_{13}	 C_{15}	 C_{14}	 C_{16}	 $\text{C}_{9, 10}$	 C_7
Ligand(L)	13.25 3H,s	8.40 4H,s	7.31 2H,s	7.21 2H,s	6.95 2H,s	6.85 2H,s	3.91 8H,s	2.35 3H,s
[Ni(L)]Cl	—	—	7.29 2H,s	7.21 2H,s	6.95 2H,s	6.52 2H,s	3.46 8H,s	1.27 3H,s
[Cr(L)Cl]Cl	10.1w	—	7.2s	7.0	6.8	6.4		1.58s
K[Hg(L)]	9.9 3H,w	8.39 4H,s	7.28 2H,s	6.96 2H,s	6.94 2H,s	6.90 2H,s	3.97 8H,s	1.3 3H,s
[Zn(L)]	9.9 3H,w	8.39 4H,w	7.29 2H,s	7.02 2H,s	6.85 2H,w	6.6 2H,w	2.2 8H,s	1.5 3H,s
[Cd(L)]	9.95w	8.39w	7.31	6.98	6.9	5.9	3.97	1.59
[Fe(L)]	9.9w	8.4w	7.3	6.95	6.88	5.83	3.95	1.32
[Co(L)]	—	—	7.0	6.9	6.7	5.55	3.75	1.31
[Mn(L)]	—	—	7.28	7.1	6.95	4.45	3.8	1.8
[Cu(L)]Cl	—	—	7.3	7.0	6.90	5.35	3.85	1.3

s: Singlet, w: weak

(3.8) ^{13}C NMR spectrum for precursor (I), ligand and Nickel complexes

(3.8.1) ^{13}C NMR spectrum for [2,6-diformyl-4-methyl phenol]

The ^{13}C NMR spectrum of 2,6-diformyl-4-methyl phenol, Fig. (3–34) in DMSO-d_6 solvent shows chemical shift at ($\delta=192.80$ ppm) assigned to aldehydic carbon atoms (C_7, C_8) (CHO). The resonance of

the chemical shift at ($\delta=162.92$ ppm) attributed to the phenolic carbon atom (C_1) (C–O), while the resonance chemical shift at ($\delta=137.89$, 123.81, 129.81, ppm) are assigned for carbon aromatic ring atoms ($C_{3,5}$, C_4 , $C_{2,6}$) respectively. The signal at ($\delta=20.10$ ppm) assigned to methyl group carbon atom (C_9). The details are listed in Table (3–12).

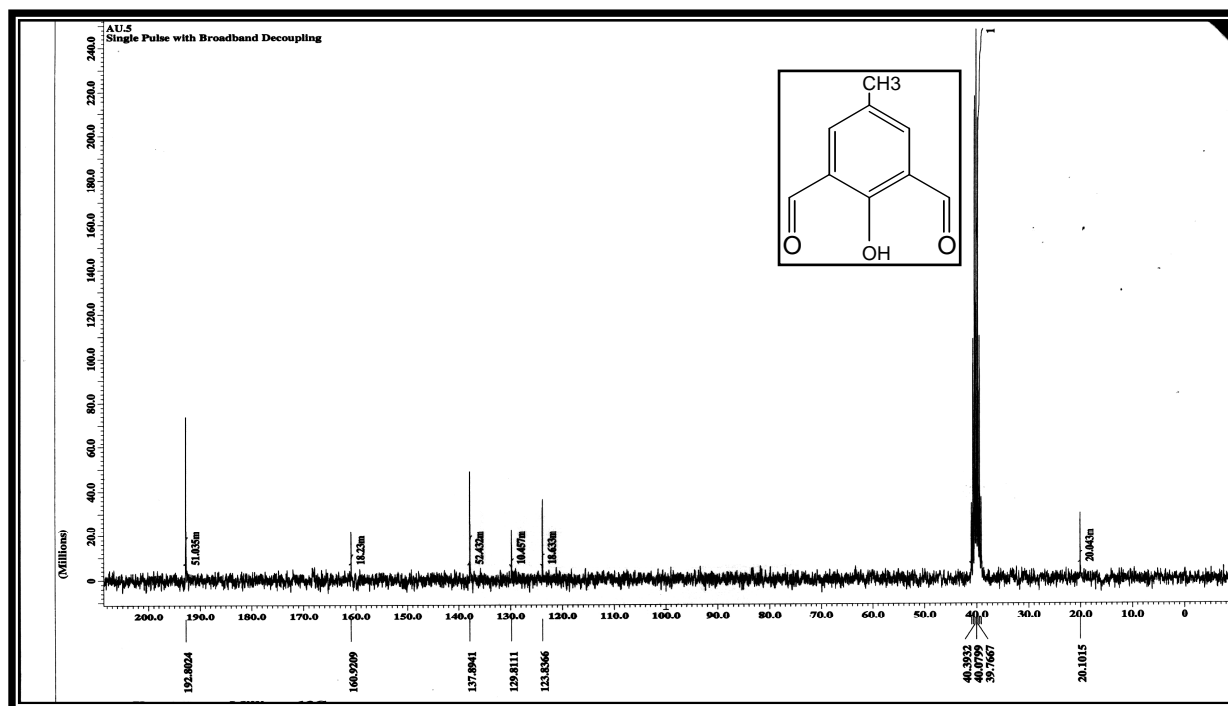


Fig. (3–34) ^{13}C NMR spectrum of precursor (I)

Table (3-12) ^{13}C NMR data for precursor (I) measured in DMSO- d_6 and chemical shift in ppm

compound	H–C=O ($C_{7,8}$)	C–OH (C_1)	Aromatic C–H($C_{3,5}$)	Aromatic C=C($C_{2,6}$)	Aromatic C–C (C_4)	Aliphatic CH ₃ , (C_9)
2,6-diformyl-4-methyl phenol	192.80	162.93	137.89	129.81	123.81	20.10

(3.8.2) ^{13}C NMR spectrum of the ligand

^{13}C NMR spectrum for the ligand shown in Fig. (3–35) displayed, the four Azomethine group ($\text{N}=\text{C}-$) are equivalent ($\text{C}_{8,11}$) and appeared at chemical shift ($\delta_{\text{C}} = 166.53\text{ppm}$). The chemical shift of the aromatic carbon atoms are shown at ($\delta_{\text{C}} = 118.71\text{ ppm}, 118.63$ and 116.96ppm) representing $\text{C}_{15,14,16}$ while chemical shift shown at ($\delta_{\text{C}} = 132\text{ppm}, 131.51\text{ppm}$) represented C_{15} and C_{17} of aromatic ring. The chemical shift at ($\delta_{\text{C}} = 59.77\text{ppm}$) assigned to ethylene carbon atoms ($\text{C}_{9,10}$). The appearance of the chemical shift at ($\delta_{\text{C}} = 161.00\text{ ppm}$) is related to carbon atoms ($\text{C}_{1,17}$) attached to (OH) moiety.

The difference in C_{13} chemical shift with that of carbon number one attached to (OH) group of ($\delta_{\text{C}} = 161.00\text{ppm}$) and that of carbon number four attached to methyl group of ($\delta_{\text{C}} \approx 130\text{ppm}$) is due to the high electronegativity of (OH) group.

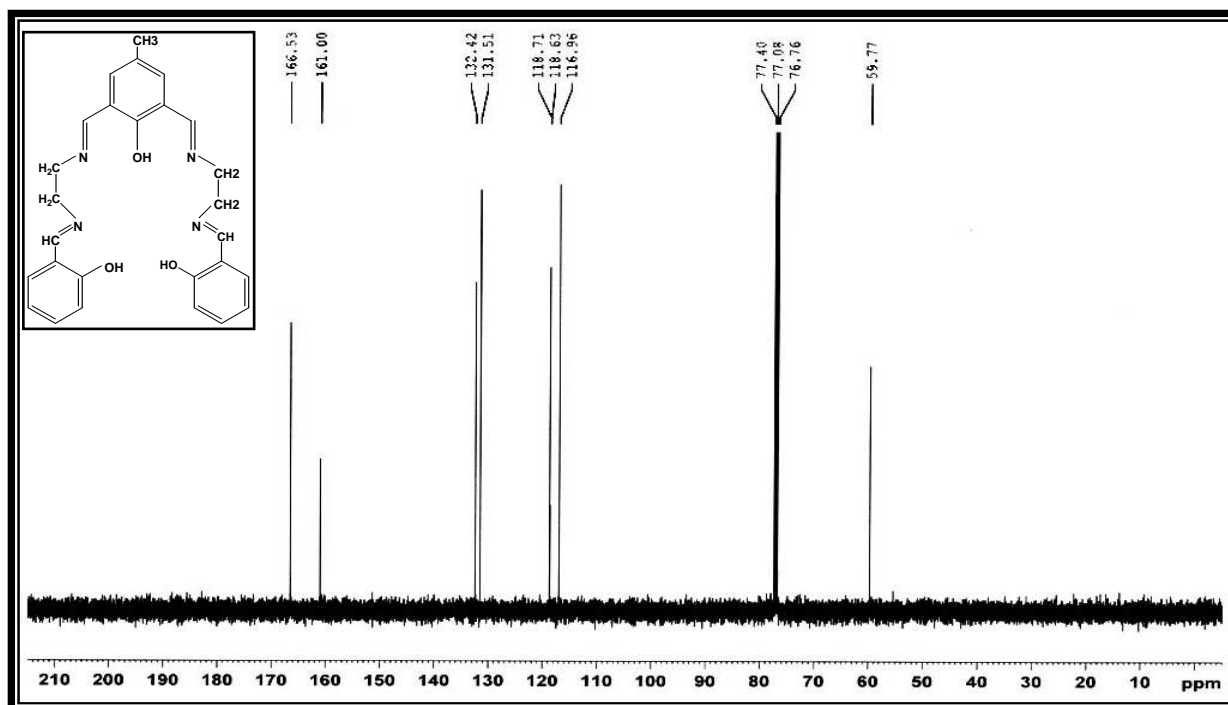
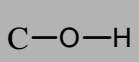
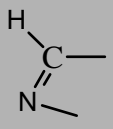
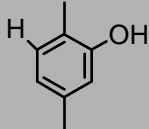
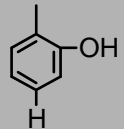
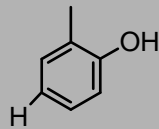
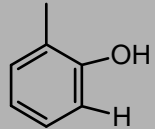
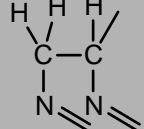



Fig. (3–35) ^{13}C NMR spectrum of ligand

Table (3–13) ^{13}C NMR data for the ligand in DCCl_3 and chemical shift in ppm (δ)

Compound								
	$\text{C}_{1,17}$	$\text{C}_{8,11}$	C_{13}	C_{15}	C_{14}	C_{16}	$\text{C}_{9,10}$	C_7
Ligand	161.00	166.52	131.51	118.71	118.63	116.96	59.77	20.3

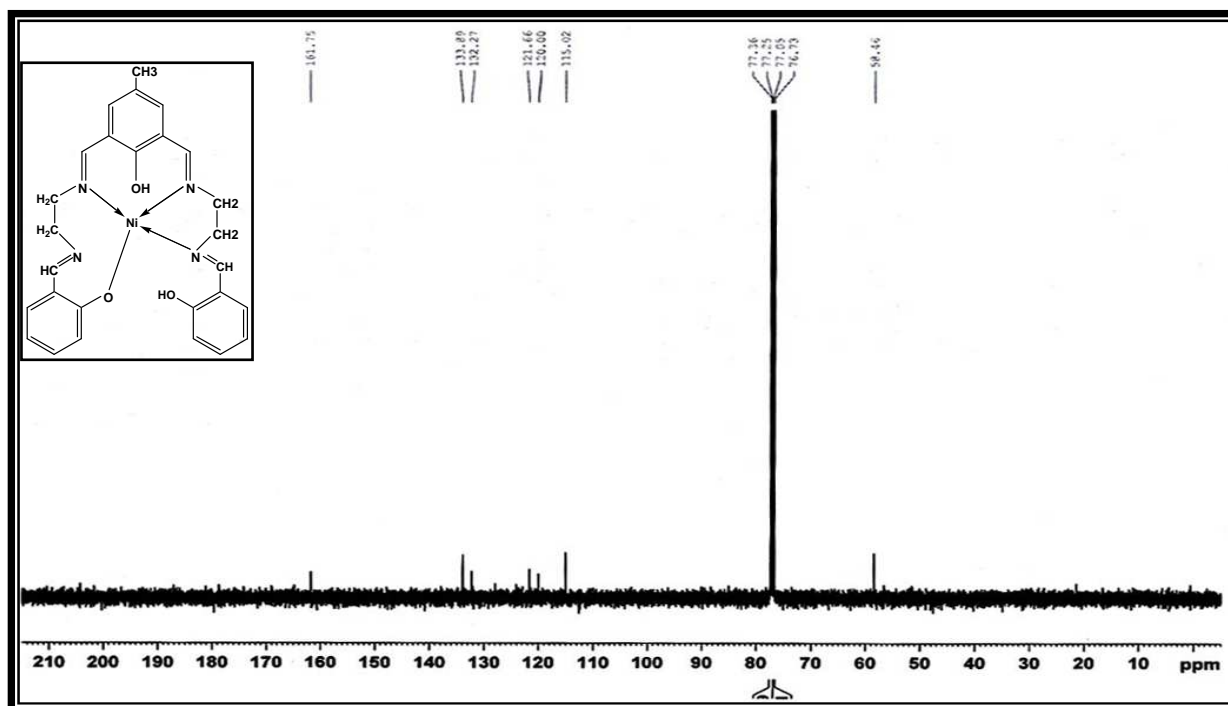
(3.8.2) ^{13}C NMR spectra for Nickel complexes

The ^{13}C NMR spectrum for the ligand, Fig. (3–35) in CDCl_3 solvent shows resonance at chemical shifts ($\delta_{\text{C}}=166.53$ ppm) assigned to carbon atoms of azomethine groups⁽¹³⁰⁾ ($\text{C}_{8,11}$), indicating that, the two azomethine groups are non equivalents due to intra hydrogen bonding. This result supported that obtained in ^1H NMR. The aromatic carbon atoms are shown in the chemical shift at ($\delta_{\text{C}}=132.26$ ppm, Ar- C_{15}), ($\delta_{\text{C}}=131.51$ ppm, Ar- C_{13}), ($\delta_{\text{C}}=118.7$ ppm, Ar- C_{12}), ($\delta_{\text{C}}=116.96$ ppm, Ar- C_{16}). The methylene carbon atoms appeared at chemical shift ($\delta_{\text{C}}=59.77$ ppm, $\text{C}_{9,10}$). The carbon atom attached to (OH) group resonate at chemical shift ($\delta_{\text{C}}=161.0$ ppm).

The carbon atom of the methyl group (C_7) have been detected at ($\delta_{\text{C}}=20.3$ ppm). The above chemical shift assignment are summarized in Table (3–13).

The ^{13}C NMR spectrum of Nickel complex, as can be seen in Fig. (3–36) in CDCl_3 solvent shows reduction in all chemical shifts values for all carbon atoms of the complex, this situation indicates clearly the formation of metal complex where electron charge

density being transferred from the metal to the ligand through synergic mechanism (back donation).



(3-36) ^{13}C NMR spectrum of $[\text{Ni}(\text{L})]\text{Cl}$

Table (3-14) ^{13}C NMR data for the Nickel complex in DCl_3 and chemical shift in ppm (δ)

Compound	C-O-H C _{1,17}	H-C-N C _{8,11}	H-C-OH C ₁₁	H-C-OH C ₁₅	H-C-OH C ₁₄	H-C-OH C ₁₆	H-C-C C _{9,10}	H-C-H C ₇
$[\text{Ni}(\text{L})]\text{Cl}$	—	161.75	133.89	132.26	115.02	77.36	58.46	20.3

(3.9) Molar Conductivity

The molar conductance of the ligand and complexes in (DMF) are summarized in Table (3–15).

The conductance of the ligand, Fe^(II), Co^(II), Cd^(II), Mn^(II) and Zn^(II) complexes are in the range (10.00–17.44) S.cm².mole⁻¹ indicating the non electrolytic nature.

While for the complexes Cu^(II), Ni^(II), Cr^(II) and Hg^(II) are in the range of (65–76) S.cm².mole⁻¹ indicating the (1:1) the electrolyte nature⁽¹²⁸⁾.

Table (3-15) The molar conductivity of the ligand and the complexes

No.	compound	Solvent	Conductivity (S.cm ² .mole ⁻¹)	Ratio
1	Ligand (L)	DMF	10.0	Non electrolyte
2	[Fe(L)]	DMF	16.04	Non electrolyte
3	[Co(L)]	DMF	14.2	Non electrolyte
4	[Cd(L)]	DMF	11.70	Non electrolyte
5	[Mn(L)]	DMF	17.44	Non electrolyte
6	[Zn(L)]	DMF	10.42	Non electrolyte
7	[Cu(L)]Cl	DMF	65	1:1
8	[Ni(L)]Cl	DMF	70	1:1
9	[Cr(L)Cl]Cl	DMF	75	1:1
10	K[Hg(L)]	DMF	76	1:1
11	DMF		8	

(3.10) Conclusions and the proposed molecular structures for the complexes **[Mn(L)], [Fe(L)], [Zn(L)], [Ni(L)]Cl, [Co(L)], [Cr(L)Cl]Cl, [Cd(L)], K[Hg(L)] and [Cu(L)]Cl .**

The molecular structures for these complexes were proposed according to the results shown below:

A. (I.R) spectra

The (I.R) spectra of the complexes, Table (3–6) and Figures (3-4 to 3-12) (Mn), (Fe), (Zn), (Ni), (Co), (Cr), (Cd), (Hg) and (Cu) respectively, display bands in the range (1650–1635) cm^{-1} assigned to the $\nu(\text{C}=\text{N})$ group stretching. These bands are shifted to lower frequencies in comparison with that of the free ligand which appeared at (1660) cm^{-1} , indicating the weak bonding nature between the metal ions and the iminic group (C=N), This can be attributed to the decrease of bond order, as a results of delocalization of metal ion electron density to the ligand, indicating coordination through the Nitrogen atom. The new band appeared in the range (675–570) cm^{-1} and (447-309) cm^{-1} in the complexes (I.R) spectra are assigned to $\nu(\text{M}-\text{N})$ and $\nu(\text{M}-\text{O})$ respectively, these bands support the coordination through nitrogen and oxygen atoms of the ligand to metal.

B. (UV-Vis) spectra

The (UV–Vis) spectral data for complexes are shown in Table (3–7) and the absorption spectra for the complexes are shown in Figures (3–14) to (3–22). These could be classified into three categories namely:

Octahedral complexes

Chromium complex $[\text{Cr}(\text{L})\text{Cl}]\text{Cl}$ exhibited bands at λ_{max} (288, 413 and 625)nm assigned to (${}^4\text{A}_{2\text{g}} \rightarrow {}^4\text{T}_{1\text{g}}(\text{P})$), (${}^4\text{A}_{2\text{g}} \rightarrow {}^4\text{T}_{1\text{g}}(\text{F})$) and (${}^4\text{A}_{2\text{g}} \rightarrow {}^4\text{T}_{2\text{g}}(\text{F})$) transitions respectively.

Cobalt complex $[\text{Co}(\text{L})]$ exhibited band at λ_{max} (607 and 674)nm assigned to (${}^4\text{T}_{1\text{g}}(\text{F}) \rightarrow {}^4\text{T}_{1\text{g}}(\text{P})$) and (${}^4\text{T}_{1\text{g}}(\text{F}) \rightarrow {}^4\text{A}_{2\text{g}}(\text{F})$) transitions respectively. Manganese complex $[\text{Mn}(\text{L})]$ exhibited band at λ_{max} (400nm) assigned to (${}^6\text{A}_{1\text{g}}(\text{S}) \rightarrow {}^4\text{T}_{1\text{g}}(\text{G})$). These transition suggests an octahedral geometry around the metal ions.

Square planner complexes

The (UV–Vis) spectrum for $[\text{Cu}(\text{L})]\text{Cl}$, Fig. (3–14) shows a peak at (570nm), which is assigned to (d–d) transition type (${}^2\text{B}_{1\text{g}} \rightarrow {}^2\text{B}_{2\text{g}}$) indicating square planar structure around Copper ion.

The (UV–Vis) spectrum for $[\text{Ni}(\text{L})]\text{Cl}$ of Fig. (3–15) shows peak at (408 and 460)nm, which is assigned to transitions type (${}^1\text{A}_{1\text{g}} \rightarrow {}^1\text{A}_{2\text{g}}$) and (${}^1\text{A}_{1\text{g}} \rightarrow {}^1\text{B}_{1\text{g}}$) respectively; also the absence of 10000 cm^{-1} band is a clear indication to the square planner Nickel complexes⁽¹²⁸⁾.

Tetrahedral complexes

The (UV–Vis) spectrum for $[\text{Fe}(\text{L})]$, Fig. (3–19) shows a peak at (477nm), which is assigned to (d–d) transition type (${}^5\text{E} \rightarrow {}^5\text{T}_2$) indicating tetrahedral structure around Iron ion.

The (UV–Vis) spectrum of the $[\text{Zn}(\text{L})]$, $[\text{Cd}(\text{L})]$ and $\text{K}[\text{Hg}(\text{L})]$ complexes of Figures (3–20), (3–21) and (3–22) show absorption peaks at (280, 350 and 363)nm, (288, 319 and 366)nm and (288, 319 and 440)nm for Zinc, Cadmium and Mercury complexes respectively

These absorptions are assigned to ($\pi \rightarrow \pi^*$), ($n \rightarrow \pi^*$) and charge transfer transitions, indicating tetrahedral structures around Zinc, Cadmium and Mercury ions.

C. Conductivity measurements

The molar conductance in DMF solvent of the ligand and Fe^(II), Co^(II), Cd^(II), Mn^(II) and Zn^(II) complexes are in the range (10.00–17.44) S.cm².mole⁻¹, indicating non electrolyte nature. While for the complexes Cu^(II), Ni^(II), Cr^(III) and Hg^(II) were in the range (65–76) S.cm².mole⁻¹ indicating the (1:1) electrolyte nature.

D. Micro analysis

The micro analysis of Nitrogen (by modified Kjeldahl method) along with chloride and metal content by Atomic Absorption technique for complexes are in good agreement with the calculated values, these results supported the formation of complexes.

E. ¹H NMR and ¹³C NMR Spectra

On comparison of ¹H NMR and ¹³C NMR of free ligand and metal complexes, many conclusions could be drawn on the type of the bonding and complexes formation between the ligand and metal ions; these results supported the formation of the complexes.

According to the results of ¹HNMR & ¹³CNMR, it is concluded that, the geometries of Cu⁺² and Ni⁺² complexes are square planar, the geometries of Cr⁺³, Co⁺² and Mn⁺² complexes are octahedral, while the geometries of Fe⁺², Zn⁺², Cd⁺² and Hg⁺² complexes are tetrahedral.

The proposed molecular structure for (Cr⁺³, Co⁺², Ni⁺², Zn⁺², Hg⁺² and Cu⁺²) complexes were drawn according to a computed program Chem. Office 2003. Figures (3–37), (3–38), (3–39), (3–40), (3–41) and (3–42) depicts the proposed structure for [M(L)]Cl, [where:

M= Ni and Cu] complexes, [M(L)] [where: M= Co and Zn] complexes, [M(L)Cl]Cl [where M= Cr] and K[M(L)] [where M= Hg].

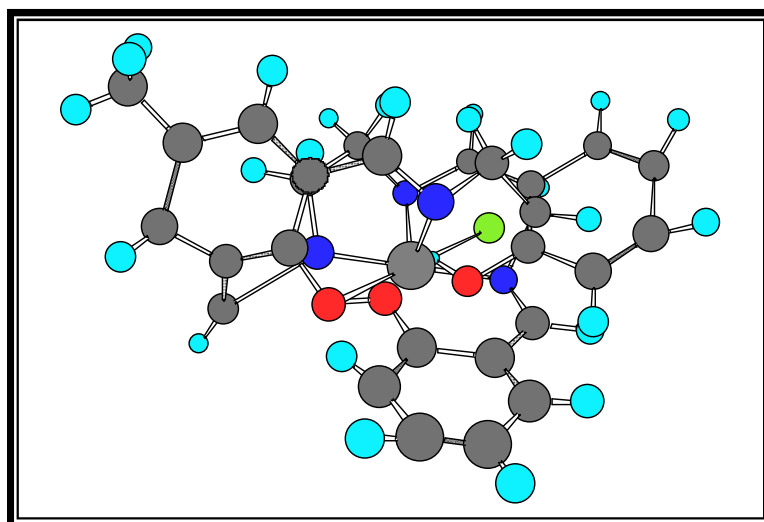


Fig. (3-37) The proposed molecular structure of $[\text{Cr}^{\text{III}}(\text{L})\text{Cl}]^+$ complex

Table (3-16) The calculated bond lengths and bond Angles of $[\text{Cr}^{\text{III}}(\text{L})\text{Cl}]^+$ complex

Type of bond	Bond length (Å)	Type of bond	Bond angle (°)
N ₁₀ - Cr ₃₇	1.438	O ₇ -Cr ₃₇ -N ₁₀	39.539
N ₁₁ - Cr ₃₇	1.856	O ₇ -Cr ₃₇ -N ₁₁	87.790
O ₇ - Cr ₃₇	2.232	O ₇ -Cr ₃₇ -N ₁₇	129.454
N ₁₇ - Cr ₃₇	1.856	O ₇ -Cr ₃₇ -N ₁₈	139.888
N ₁₈ - Cr ₃₇	1.856	O ₇ -Cr ₃₇ -Cl ₃₈	180.000
Cr ₃₇ - Cl ₃₈	2.170	N ₁₀ -Cr ₃₇ -N ₁₁	90.000
		N ₁₀ -Cr ₃₇ -N ₁₇	90.000
		N ₁₀ -Cr ₃₇ -N ₁₈	179.451
		N ₁₀ -Cr ₃₇ -Cl ₃₈	140.461
		N ₁₁ -Cr ₃₇ -N ₁₇	90.000
		N ₁₁ -Cr ₃₇ -N ₁₈	90.002
		N ₁₁ -Cr ₃₇ -Cl ₃₈	92.210
		N ₁₇ -Cr ₃₇ -N ₁₈	90.576
		N ₁₇ -Cr ₃₇ -Cl ₃₈	50.548
		N ₁₈ -Cr ₃₇ -Cl ₃₈	40.113

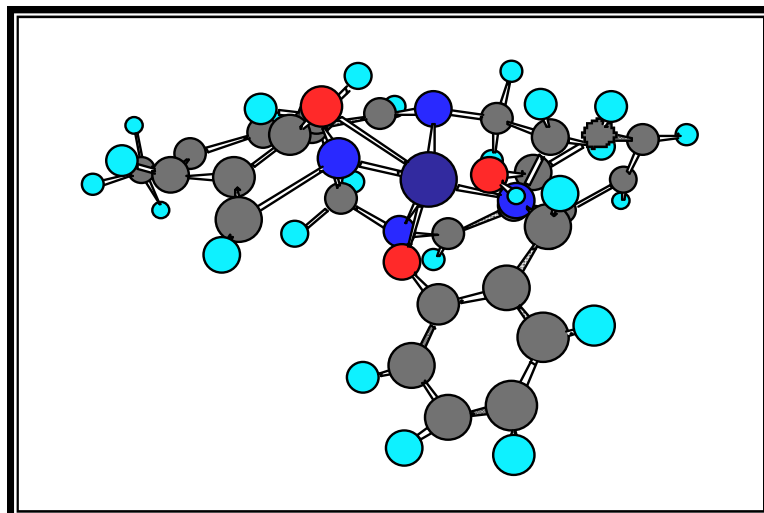


Fig. (3-38) The proposed molecular structure of $[\text{Co}^{\text{II}}(\text{L})]$ complex

Table (3-17) The calculated bond lengths and bond Angles of $[\text{Co}^{\text{II}}(\text{L})]$ complex

Type of bond	Bond length (Å)	Type of bond	Bond angle (°)
$\text{O}_7-\text{Co}_{36}$	2.640	$\text{O}_7-\text{Co}_{36}-\text{N}_{10}$	21.134
$\text{N}_{10}-\text{Co}_{36}$	1.836	$\text{O}_7-\text{Co}_{36}-\text{N}_{11}$	77.236
$\text{N}_{11}-\text{Co}_{36}$	1.836	$\text{O}_7-\text{Co}_{36}-\text{N}_{17}$	106.554
$\text{N}_{17}-\text{Co}_{36}$	1.836	$\text{O}_7-\text{Co}_{36}-\text{N}_{18}$	158.410
$\text{N}_{18}-\text{Co}_{36}$	1.836	$\text{O}_7-\text{Co}_{36}-\text{O}_{31}$	111.589
$\text{O}_{31}-\text{Co}_{36}$	1.800	$\text{N}_{10}-\text{Co}_{36}-\text{N}_{11}$	90.000
		$\text{N}_{10}-\text{Co}_{36}-\text{N}_{17}$	90.000
		$\text{N}_{10}-\text{Co}_{36}-\text{N}_{18}$	179.451
		$\text{N}_{10}-\text{Co}_{36}-\text{O}_{31}$	90.457
		$\text{N}_{11}-\text{Co}_{36}-\text{N}_{17}$	90.000
		$\text{N}_{11}-\text{Co}_{36}-\text{N}_{18}$	90.000
		$\text{N}_{11}-\text{Co}_{36}-\text{O}_{31}$	127.111
		$\text{N}_{17}-\text{Co}_{36}-\text{N}_{18}$	90.574
		$\text{N}_{17}-\text{Co}_{36}-\text{O}_{31}$	37.116
		$\text{N}_{18}-\text{Co}_{36}-\text{O}_{31}$	90.000

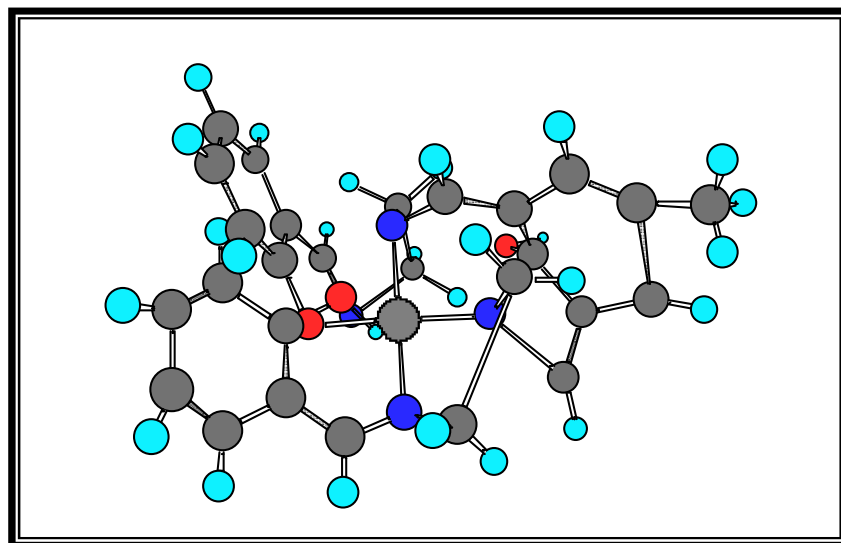


Fig. (3–39) The proposed molecular structure of $[\text{Ni}^{\text{II}}(\text{L})]^+$ complex

Table (3–18) The calculated bond lengths and bond Angles of $[\text{Ni}^{\text{II}}(\text{L})]^+$ complex

Type of bond	Bond length(A ^o)	Type of bond	Bond angle (°)
N ₁₁ –Ni ₃₇	1.826	N ₁₁ –Ni ₃₇ –N ₁₂	90.000
N ₁₂ –Ni ₃₇	1.826	N ₁₁ –Ni ₃₇ –N ₁₈	89.000
N ₁₈ –Ni ₃₇	1.826	N ₁₁ –Ni ₃₇ –O ₃₂	180.000
O ₃₂ –Ni ₃₇	1.790	N ₁₂ –Ni ₃₇ –N ₁₈	179.451
		N ₁₂ –Ni ₃₇ –O ₃₂	89.999
		N ₁₈ –Ni ₃₇ –O ₃₂	90.002

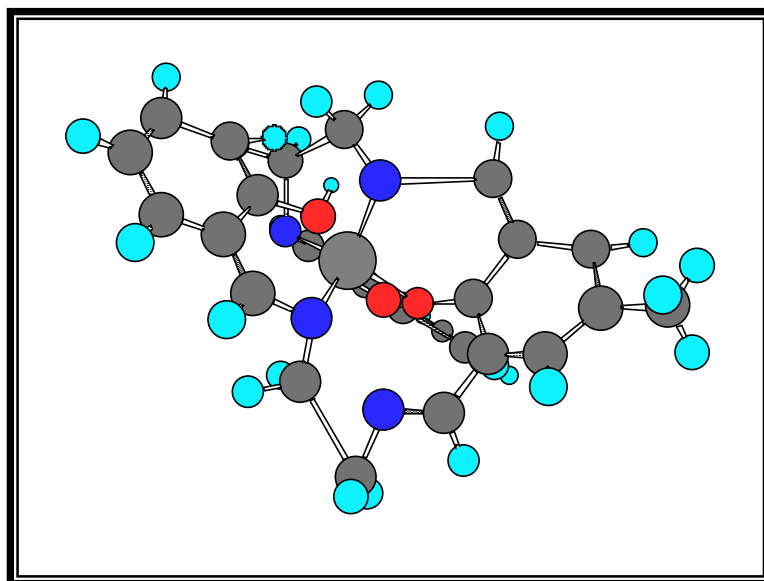


Fig. (3-40) The proposed molecular structure of $[\text{Zn}^{\text{II}}(\text{L})]$ complex

Table (3-19) The calculated bond lengths and bond Angles of $[\text{Zn}^{\text{II}}(\text{L})]$ complex

Type of bond	Bond length (Å)	Type of bond	Bond angle (°)
$\text{O}_7\text{-Zn}_{37}$	1.890	$\text{O}_7\text{-Zn}_{37}\text{-N}_{10}$	109.467
$\text{N}_{10}\text{-Zn}_{37}$	1.926	$\text{O}_7\text{-Zn}_{37}\text{-N}_{17}$	109.475
$\text{N}_{17}\text{-Zn}_{37}$	1.926	$\text{O}_7\text{-Zn}_{37}\text{-N}_{18}$	109.461
$\text{N}_{718}\text{-Zn}_{37}$	1.926	$\text{N}_{10}\text{-Zn}_{37}\text{-N}_{17}$	104.508
		$\text{O}_{10}\text{-Zn}_{37}\text{-N}_{18}$	109.470
		$\text{N}_{17}\text{-Zn}_{37}\text{-N}_{18}$	114.298

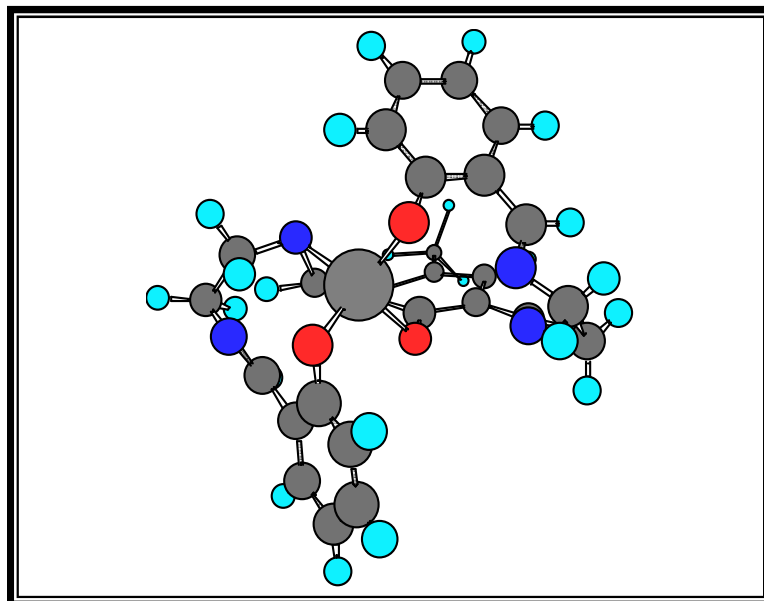


Fig. (3-41) The proposed molecular structure of $[\text{Hg}^{\text{II}}(\text{L})]^{-}$ complex

Table (3-20) The calculated bond lengths and bond Angles of $[\text{Hg}^{\text{II}}(\text{L})]^{-}$ complex

Type of bond	Bond length (\AA°)	Type of bond	Bond angle ($^{\circ}$)
$\text{O}_7\text{-Hg}_{35}$	2.130	$\text{O}_7\text{-Hg}_{35}\text{-N}_{10}$	109.472
$\text{N}_{10}\text{-Hg}_{35}$	2.166	$\text{O}_7\text{-Hg}_{35}\text{-O}_{31}$	109.467
$\text{O}_{31}\text{-Hg}_{35}$	2.130	$\text{O}_7\text{-Hg}_{35}\text{-O}_{34}$	109.470
$\text{O}_{34}\text{-Hg}_{35}$	2.130	$\text{N}_7\text{-Hg}_{35}\text{-O}_{31}$	109.470
		$\text{N}_7\text{-Hg}_{35}\text{-O}_{34}$	109.472
		$\text{O}_7\text{-Hg}_{35}\text{-O}_{34}$	109.474

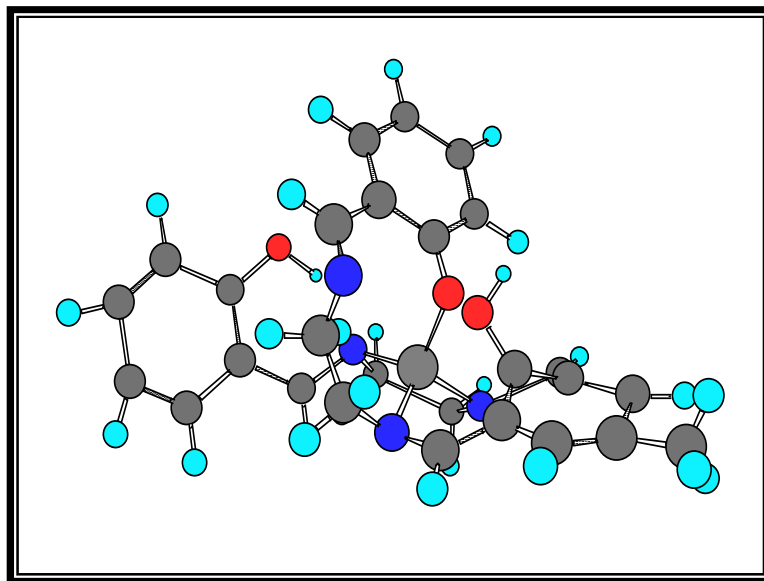


Fig. (3-42) The proposed molecular structure of $[\text{Cu}^{\text{II}}(\text{L})]^+$ complex

Table (3-21) The calculated bond lengths and bond Angles of $[\text{Cu}^{\text{II}}(\text{L})]^+$ complex

Type of bond	Bond length (Å)	Type of bond	Bond angle (°)
$\text{N}_{11}-\text{Cu}_{37}$	1.846	$\text{N}_{11}-\text{Cu}_{37}-\text{N}_{12}$	109.472
$\text{N}_{12}-\text{Cu}_{37}$	1.846	$\text{N}_{11}-\text{Cu}_{37}-\text{N}_{18}$	104.501
$\text{N}_{18}-\text{Cu}_{37}$	1.846	$\text{N}_{11}-\text{Cu}_{37}-\text{O}_{32}$	109.470
$\text{O}_{32}-\text{Cu}_{37}$	1.810	$\text{N}_{12}-\text{Cu}_{37}-\text{N}_{18}$	109.472
		$\text{N}_{12}-\text{Cu}_{37}-\text{O}_{32}$	109.472
		$\text{N}_{18}-\text{Cu}_{37}-\text{O}_{32}$	114.293

Prospective studies

1. Preparation of new poly dentate macrocyclic ligand with different substituents.
2. Synthesis of ^{60}Cu and ^{99}Tc complexes with this ligand to be used as radio pharmaceuticals in nuclear medicine.
3. Thermodynamic and kinetic studies for the ligand and its complexes.
4. Stability constant measurements of metal complexes of the prepared ligand.

(4.1) Biological activity

Microorganisms cause different kinds of diseases to humans and animals. Discovery of chemotherapeutic agents play a very important role in controlling and preventing such diseases.

The roles of the inorganic species in medicines are promising for logical design of inorganic therapeutic agents that are relatively innocuous to the host, while being toxic to unwanted types of cell components⁽¹³¹⁾. Chemotherapeutic agents were isolated either from living organisms are known as antibiotics, like penicillin and tetracycline ...etc., or they are chemical compounds prepared by chemists such as sulfa drugs. Certain metal complexes are active at low concentrations against types of bacteria, fungi and viruses.

Issues of concern regarding Gram– negative bacteria and gram-positive bacteria include the extended drug resistance spectrum of pseudomonas mallei and staphylococcus aureus became common causes of infection in the acute and long term care units in hospitals.

The emergence of these resistance bacteria have created a major concern and an urgent need to synthesize agents of structural classes which resemble the known chemotherapeutic agents. It is clear that the metal chelates can act in a number of ways. Thus they may inactivate the virus by occupying sites on its surface which would normally be utilized in the initiation of the infection of the host cell. The first step in the infection would be the adsorption reaction involving electrostatic interactions. Alternatively, the complex cations may penetrate through the cell wall and prevent virus reproduction. The most essential feature of good chemotherapeutic agent is that, it must show a high degree of selective toxicity towards a microorganism, so that, it can be given in

sufficient doses to inhibit or kill microorganisms through out the blood without harming the body cell. Complexes are considered an important class of compounds having a wide spectrum of biological activity⁽¹³²⁾.

(4.2) Chemicals.

- 1- Dimethyl forma amide
- 2- Methanol (%96)
- 3- Nutrient Agar medium from maknus lab.

(4.3) Apparatus

- 1- Autoclave from Hiramama company
- 2- Biological hood
- 3- Petri dishes
- 4- Cotton swab
- 5- Micro pipette

(4.4) Type of bacteria.

- 1- Staphylococcus aureus (gram positive).
- 2- Pseudomonas mallei (gram negative).

(4.5) Preparation of nutrient agar medium

Dry nutrient agar 20 grams were added to one liter of distilled water in a conical flask and stirred with heating until it was completely dissolved.

The flask was closed by cotton and the medium was sterilized by placing it in an autoclave for 20 minutes at 121°C under pressure of 15pounds/sq. inch. After that the medium was cooled to (45-55°C) and placed in a Petri dish about (15-20mL) for each one, left to cool and solidify.

The medium was ready for bacterial growth, the studied bacteria were placed on the nutrient agar surface using the loop and by streaking processor⁽¹³³⁾. After that the disc saturated with the tested compound solution was placed in the dishes which were then incubated for 18 hours at (37°C).

(4.6) Result and discussion.

In this antibacterial study of all metal complexes and the ligand, the results are shown in Table (4-1).

Bacteria which were studied are gram negative *Pseudomonas mallei* and gram positive *Staphylococcus Aureus*. DMF was used as a solvent. These plates were incubated at (37°C) for 18 hours for bacteria⁽¹²⁷⁾. The inhibition zone caused by various compounds was examined. The result of the preliminary screening tests listed in Table (4-1) and Figures (4-1), (4-2), (4-3), (4-4), (4-5), (4-6), (4-7), (4-8), (4-9) and (4-10).

Table (4-1) Antibacterial activities of the ligand and the metal complexes

Compound	Staphylococcus Aureus	Inhibition Diameter (mm)	Pseudomonas mallei	Inhibition Diameter(mm)
L	+	9	+	5
[Mn ^{II} (L)]	+	4.5	-	3
[Zn ^{II} (L)]	+	9.5	+	1
K[Hg ^{II} (L)]	+	12	+	7
[Ni ^{II} (L)]Cl	+	0.5	+	3
[Co ^{II} (L)]	+	2	+	1.5
[Fe ^{II} (L)]	+	0	-	-1.5
[Cr ^{III} (L)Cl]Cl	+	6.5	+	6
[Cd ^{II} (L)]	+	14	+	7.5
[Cu ^{II} (L)]Cl	+	2.5	-	1

Results are summarized as follows;

First: Inhibition effect of all compounds studied with *Pseudomonas mallei* was lower than that with *Staphylococcus aureus*.

Second: Results of table (4-1) showed that, except Zinc, Cadmium and Mercury complexes, Inhibition of all complex ions studied were less than the inhibition of the ligand can offer by itself.

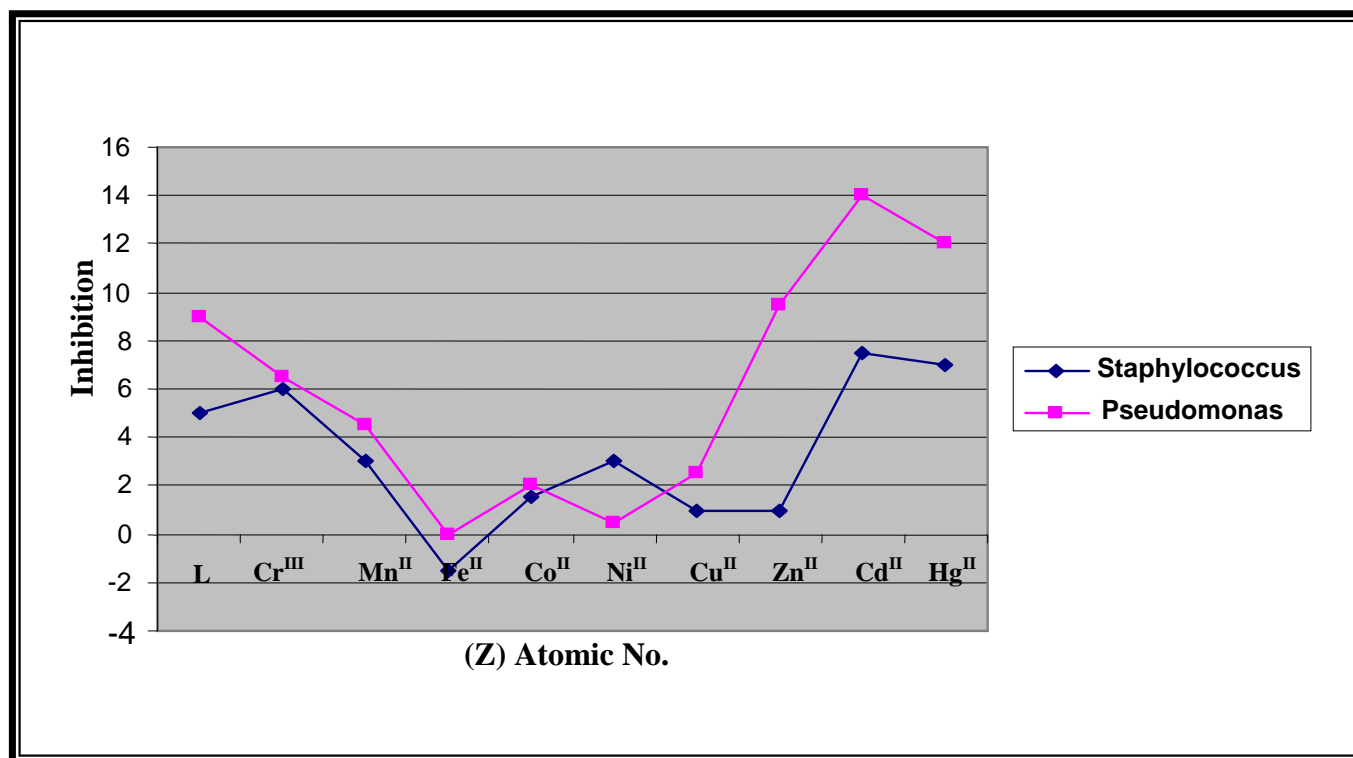


Fig (4-1) The inhibition according to atomic number



Fig. (4-2) Effect of $[Zn(L)]$ and $K[Hg(L)]$ on *staphylococcus aureus*



Fig. (4-3) Effect of ligand (L) and $[Mn(L)]$ on *staphylococcus aureus*



Fig.(4-4) Effect of [Cd(L)] and [Cu(L)]Cl on staphylococcus aureus

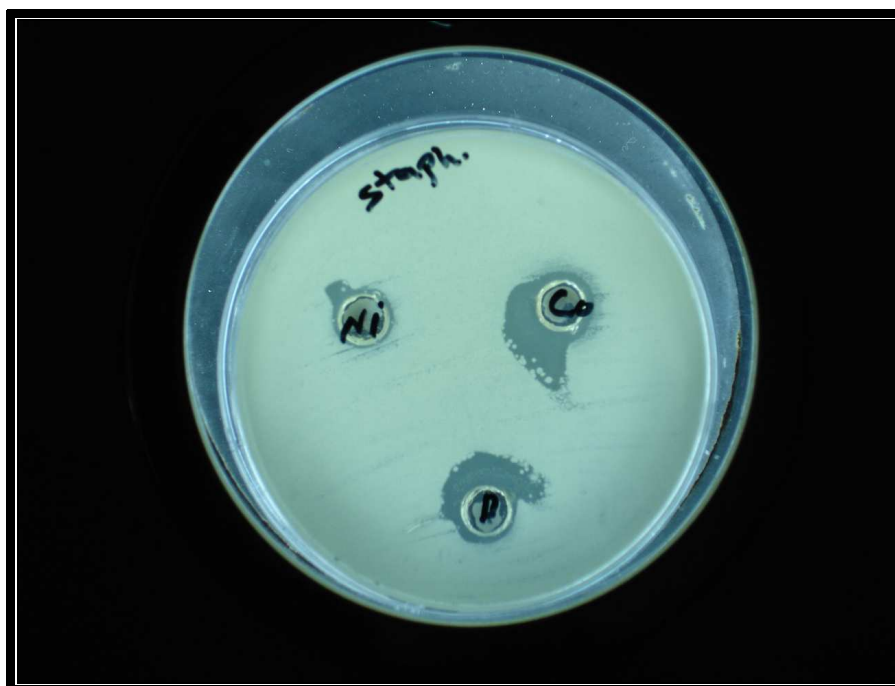


Fig. (4-5) Effect of [Ni(L)]Cl and [Co(L)] on staphylococcus aureus



Fig. (4-6) Effect of $[\text{Fe}(\text{L})]$ and $[\text{Cr}(\text{L})\text{Cl}]\text{Cl}$ on *staphylococcus aureus*



Fig. (4-7) Effect of $[\text{Zn}(\text{L})]$ and $\text{K}[\text{Hg}(\text{L})]$ on *pseudomonas mallei*



Fig. (4-8) Effect of Ligand (L) and [Mn(L)] on *pseudomonas mallei*



Fig. (4-9) Effect of [Cd(L)] and [Cu(L)]Cl on *pseudomonas mallei*

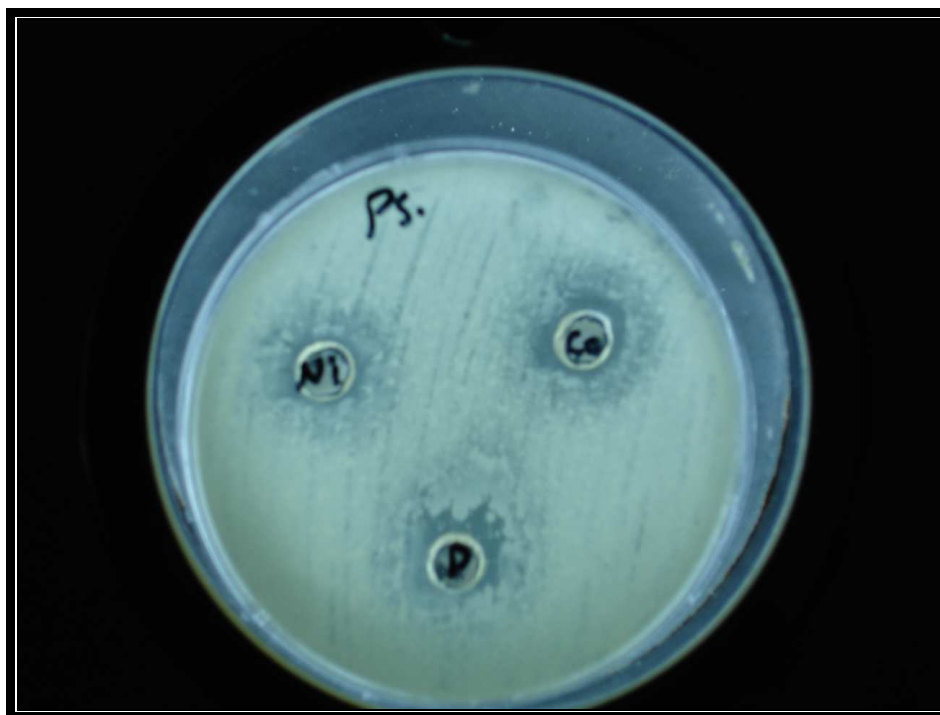


Fig. (4-10) Effect of $[\text{Ni}(\text{L})]\text{Cl}$ and $[\text{Co}(\text{L})]$ on *Pseudomonas mallei*

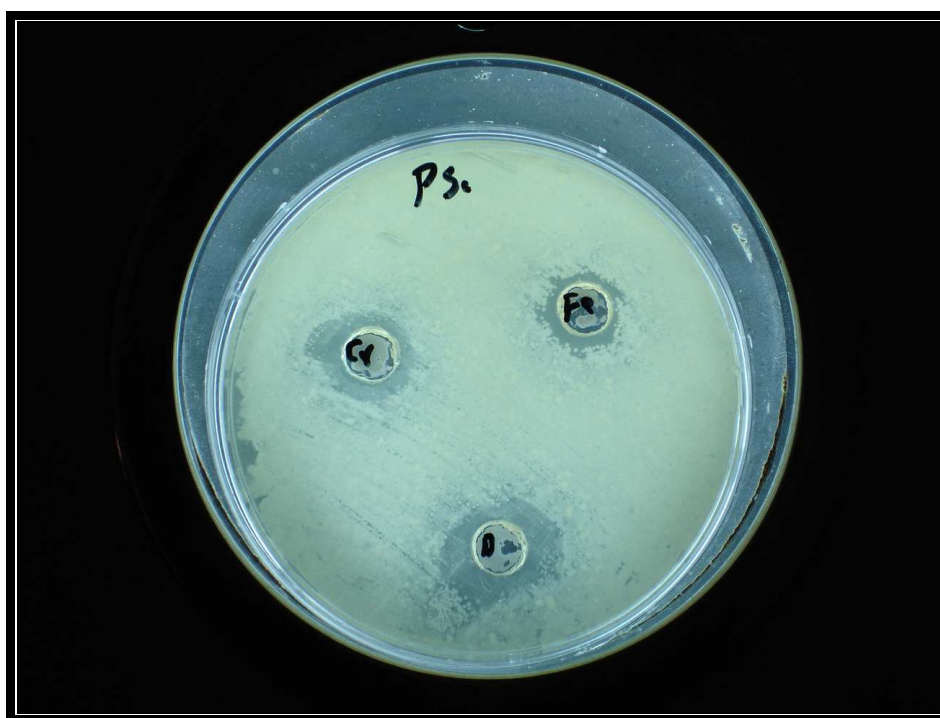


Fig. (4-11) Effect of $[\text{Fe}(\text{L})]$ and $[\text{Cr}(\text{L})\text{Cl}]\text{Cl}$ on *Pseudomonas mallei*

Dedication

To my great country, Iraq, the cradle of civilizations.

To my dear parents, sisters, brothers and uncles.

To my teachers from whom I have learned so much.

*To all my friends, with my endless love, gratitude
and fidelity.*

To all whom I love.

Munaf

Acknowledgment

Thanks to Allah the one and single for all his blessing during the pursuit of my academic and career goals.

*I would like to express my sincere thanks and my appreciation to my supervisors Prof. Dr. **Yahya Abdul Majid** and Assist. Prof. Dr. **Mohamad J. Al –Jeboori** for their kind interest, encouragement, and guidance throughout the course of this work. Also my grateful thanks are due to the staff members of the departments of chemistry at the College of Science for Women and Ibn Al-Hiatham Education College. My deep grateful thanks are due to Dr. Ahlam Mohammed Farhan, Dr. Hassan Salehy, and my deep gratitude to my friends Rayadh, Baid'a, Bahaa, Worood, Muthana, Sallah and all others who gave me help and sincere cooperation.*

I am deeply indebted to my family for their support and patience during the years of my study.

Munaf

Examination Committee Certificate

We chairman and members of the examination committee, certify that we have studied this thesis entitled (Synthesis and characterization of mononuclear metal complexes with a ligand derived from 2,6-diformyl para cresol) and as examining committee, examined the student **Munaf Ammar Mustafa Al-khazraji** in its contents and what are connected with it and that in our opinion, it meets the standard of a thesis for the degree of Master of Science in Chemistry with **(excellent rate)**.

Signature:

Name: **Dr. Basima M. Sarhan**

Title: **Professor**

Date: 21/ 12/ 2008

(Chairman)

Signature:

Name: **Dr. Jalil R. Ugal**

Title: Assistant Professor

Date: 21/ 12/ 2008

(Member)

Signature:

Name: **Dr. Hussein I. Abdullah**

Title: Assistant Professor

Date: 21/ 12/ 2008

(Member)

Signature:

Name: **Dr. Yahya Abdul Majid**

Title: Professor

Date: 21/ 12/ 2008

Member (Supervisor)

Signature:

Name: **Dr. Mohamad J. Al-jeboori**

Title: Assistant Professor

Date: 21/ 12/ 2008

Member (Supervisor)

Approved by the deanship of College of Science for Women/University of Baghdad

Signature:

Name: **Dr. Nada Abed Al-majeed Al-Ansari**

Title: Assistant Professor

Address: Dean of the College of Science for Women/ University of Baghdad

Date: / /2008

List of Contents

<i>Subject</i>	<i>Page</i>
Summary	I–III
List of contents	IV–XVII
List of Tables	IX–X
List of Figures	XI–XIV
List of Schemes	XV
Abbreviations	XVI–XVII
<i>Chapter One Introduction</i>	
	1–40
(1.1) Schiff Bases	1
(1.2) Macrocycles	2
(1.2.1) Curtis Macrocycles	2
(1.2.2) Robson Macrocycles	6
(1.3) Compartmental Ligands	7
(1.3.1) Head units	8
(1.3.1.1) DHTMBA	9
(1.3.2) Pendant Arms	9
(1.3.2.1) BBIM	10
(1.4) Macrocyclic compounds containing nitrogen as donor atoms.	12
(1.5) Reactivity of 2,6-diformylimino compounds toward metal ions	12
(1.6) uses and application of 2,6- Diformylimino and their complexes	28
(1.6.1) Applications in Industry	28
(1.6.2) Applications In Biochemistry	29

<i>Subject</i>		<i>Page</i>
(1.6.3)	Applications in Chemistry	29
(1.6.4)	Applications in Medicine	30
(1.6.5)	Applications in Analytical Chemistry	30
(1.7)	Reactivity of tetraaz derivatives Toward metal ions	31
(1.8)	Applications of tetraaza ligands and their complexes	35
(1.8.1)	the Medical uses of macrocyclic tetraaza compounds	35
(1.8.2)	Macrocyclic and pharmacology	36
(1.8.3)	Extraction and separation of metals using macrocyclic tetraaza molecules	37
(1.9)	The Aim of the Work	40
<i>Chapter Two: Experimental part</i>		41–52
(2.1)	Chemicals	41
(2.2)	Instruments	42
(2.2.1)	Melting point measurements	42
(2.2.2)	Infrared spectra	42
(2.2.3)	Electronic spectra	42
(2.2.4)	Metal analysis	43
(2.2.5)	Chloride contents	43
(2.2.6)	Conductivity measurements	43
(2.2.7)	Proton Nuclear magnetic resonance spectra (^1H -NMR) and Carbon Nuclear magnetic resonance spectra (^{13}C -NMR)	43
(2.2.8)	Magnetic Measurements	43
(2.2.9)	Determination of Nitrogen by modified Kjeldahl method	44
(2.2.10)	The proposed molecular structure	44

<i>Subject</i>		<i>Page</i>
(2.3)	Abbreviation of the precursors and ligand	44
(2.4)	Synthesis of precursor(I) 2,6-diformyl-4-methylphenol	46
(2.4.1)	Synthesis of [2,6-diformyl-4-methyl phenol] the first method	46
(2.4.2)	Synthesis [2,6 diformyl-4-methylphenol] the Second method	46
(2.5)	Synthesis of the precursors(II) 2,6-bis(Azomethine-ethylamine)-4-methylphenol	47
(2.6)	Synthesis of ligand [2,6-bis(Azomethine ethyl Azomethine ortho phenol) 4-methyl phenol]	48
(2.7)	Synthesis of the [L] complexes	48
(2.7.1)	Synthesis of the $[\text{Cr}^{\text{III}}(\text{L})\text{Cl}]\text{Cl}$	48
(2.7.2)	Synthesis of $[\text{Mn}^{\text{II}}(\text{L})]$, $[\text{Fe}^{\text{II}}(\text{L})]$, $[\text{Co}^{\text{II}}(\text{L})]$, $[\text{Ni}^{\text{II}}(\text{L})]\text{Cl}$, $[\text{Cu}^{\text{II}}(\text{L})]\text{Cl}$, $[\text{Zn}^{\text{II}}(\text{L})]$, $[\text{Cd}^{\text{II}}(\text{L})]$ and $\text{K}[\text{Hg}^{\text{II}}(\text{L})]$	49
(2.8)	Determination of Nitrogen by modified Kjeldahl method	50
<i>Chapter Three: Results and Discussion</i>		53–110
(3.1)	Synthesis and characterization of the precursors and ligand	53
(3.1.1)	Synthesis and characterization of [2,6-diformyl-4-methyl phenol]	53
(3.1.2)	Synthesis and characterization of [2,6-bis-(Azo methine-ethylamine)-4-methyl phenol]	54
(3.1.3)	Synthesis and characterization of ligand [2,6-bis-(Azomethine ethyl-Azomethine ortho phenol) 4-methyl phenol]	55

<i>Subject</i>		<i>Page</i>
(3.2)	Synthesis and characterization of the complexes	56
(3.3)	(I.R) Spectra for compounds	59
(3.3.1)	(I.R) Spectrum for the precursor (I)	59
(3.3.2)	(I.R) Spectrum for the precursor(II) 2,6-bis-(Azomethine- ethyl amine)-4-methyl phenol	60
(3.3.3)	(I.R) Spectrum for the Ligand 2,6-bis-(Azomethine ethyl Azomethine ortho phenol) 4-methyl phenol	61
(3.4)	(I.R) Spectral Data for the [L] complexes	64
(3.5)	UV–Vis Spectra of the ligand and complexes	71
(3.5.1)	UV–Vis spectrum of the ligand (L)	71
(3.5.2)	UV–Vis Spectra of the complexes	71
(3.5.2.1)	(UV–Vis) spectra for the [Cu(L)]Cl and [Ni(L)]Cl complexes	71
(3.5.2.2)	(UV-Vis) spectrum of the [Cr(L)]Cl complex	74
(3.5.2.3)	(UV–Vis) spectra of the [Co(L)] and [Mn(L)] complexes	75
(3.5.2.4)	(UV–Vis) spectra of [Fe(L)], [Zn(L)], [Cd(L)] and K[Hg(L)] complexes	76
(3.6)	Magnetic moment measurement	81
(3.7)	Nuclear Magnetic Resonance (NMR) spectra for precursor(I), ligand and metal complexes	83
(3.7.1)	¹ H NMR spectrum for precursor(I) [2,6-diformyl-4-methyl phenol]	84
(3.7.2)	¹ H NMR spectrum of the ligand	85
(3.7.3)	¹ H NMR spectra for the complexes	86

<i>Subject</i>	<i>Page</i>
(3.7.3.1) ^1H NMR spectra for copper and Nickel complexes	86
(3.7.3.2) ^1H NMR spectra for Zinc, Cadmium, Mercury and Iron complexes	88
(3.7.3.3) ^1H NMR spectra for Chromium, Cobalt and Manganese complexes	91
(3.8) ^{13}C NMR spectrum for precursor (I), ligand and Nickel complex	94
(3.8.1) ^{13}C NMR spectrum for [2,6-diformyl-4-methylphenol]	94
(3.8.2) ^{13}C NMR spectrum of the ligand	96
(3.8.3) ^{13}C NMR spectra for Nickel complexes	97
(3.9) Molar Conductivity	99
(3.10) Conclusions and the proposed molecular structure for the complexes	100
(4.1) Biological activity	110
(4.2) Chemicals.	111
(4.3) Apparatus	111
(4.4) Type of bacteria	111
(4.5) Preparation of nutrient agar medium	111
(4.6) Result and discussion.	112
Results are summarized as follows	113
References	119
Abstract (In Arabic Language)	أ-ج

List of Tables

<i>Table</i>		<i>Page</i>
(1-1)	Reactivity of tetraaza derivatives toward metal ions	31
(1-2)	Emission and half-life period of Technetium and Rhenium	35
(2-1)	Chemicals used in this work and their suppliers	41
(2-2)	Abbreviation of structure and nomenclature of the ligand and precursor	45
(2-3)	some physical properties of the prepared [L] complexes and their reactant quantity & yield	49
(2-4)	Determination of Nitrogen content by modified Kjeldahl method	52
(3-1)	The elemental analysis and some physical properties of precursors and ligand	56
(3-2)	The solubility of the prepared precursors and Ligand in different solvents	56
(3-3)	The solubility of [L] complexes in different solvents	58
(3-4)	Results of Analysis of metal ions, chloride ions and Nitrogen percentage of metal complexes	59
(3-5)	Infrared spectral data for the starting material, precursors and ligand	63
(3-6)	Infrared spectral data (wave) cm^{-1} of the complexes	70
(3-7)	Electronic Spectral data of [L] complexes in DMF solvent	80
(3-8)	Data of magnetic moment ($\mu_{\text{eff}}=\text{B.M}$) of solid at 298k and suggested stereo chemical structure of complexes	82
(3-9)	Magnetic moments of metal complexes	83

<i>Table</i>	<i>Page</i>
(3–10) ¹ H, NMR data for precursors1 measured in DMSO-d ₆ and chemical shift (δ) in ppm.	85
(3–11) ¹³ H NMR data for the ligand and metal complexes in DCCl ₃ and chemical shift in ppm (δ)	94
(3–12) ¹³ C NMR data for precursor(I) measured in DMSO-d ₆ and chemical shift in ppm	95
(3–13) ¹³ C NMR data for the ligand in DCCl ₃ and chemical shift in ppm (δ)	97
(3–14) ¹³ C NMR data for the Nickel complex in DCCl ₃ and chemical shift in ppm (δ)	98
(3–15) The molar conductivity of the ligand and the complexes	99
(3–16) The calculated bond lengths and bond Angles of [Cr ^{III} (L)Cl] ⁺ complex	103
(3–17) The calculated bond lengths and bond Angles of [Co ^{II} (L)] complex	104
(3–18) The calculated bond lengths and bond Angles of [Ni ^{II} (L)] ⁺ complex	105
(3–19) The calculated bond lengths and bond Angles of [Zn ^{II} (L)] complex	106
(3–20) The calculated bond lengths and bond Angles of [Hg ^{II} (L)] ⁻ complex	107
(3–21) The calculated bond lengths and bond Angles of [Cu ^{II} (L)] ⁺ complex	108
(4–1) Antibacterial activities of the ligand and the metal complexes	112

List of Figures

<i>Figures</i>	<i>Page</i>
(1-1) structure of the first macrocyclic ligand; 5,7,7,12,14,14-hexamethyl-1,4,8,11-tetraazacyclotetradeca-4,11-diene	3
(1-2) Proposed structures of macrocycles; (I) and (II) respectively	4
(1-3) Mesityl oxide	5
(1-4) Formation of a Curtis Macrocyclic	5
(1-5) example of a simple Robson macrocycle	6
(1-6) Model for the active site of Urease, which illustrates an enzyme with more than metal present in the active site	7
(1-7) Basic examples of different types of compartmental ligands	8
(1-8) DFMP and DHTMBA head units	9
(1-9) Examples of pendant arms. The bottom structure is Bis(benzimidazole-2-ylmethyl)amine	10
(1-10) 2,2-(N,N'-bis(benzimidazole-2-ylmethyl)methyl-amine-5,5'-ditertiobutyl-3,3'methanediyl-dibenzyl alcohol	11
(1-11) part of the histidin side chain	12
(1-12) The chemical structure of Zn ^{II} and Cu ^{II} complexes with macrocyclic ligands	13
(1-13) The chemical structure of the Binuclear complexes of Pd(II)	14
(1-14) The chemical structure of macrocyclic ligands	15
(1-15) X-ray Structure of [Cu ₂ L ¹] [BF ₄] ₂ .H ₂ O	15

<i>Figures</i>		<i>Page</i>
(1-16)	The chemical structure of schiff base ligand	18
(1-17)	X-ray Structure of Trinuclear Complex [(tmtacn) Co ^{III} (μ-OH) ₂ Cu ^{II} (LOX) Ni ^{II} (OH ₂) ₂] ⁺²	20
(1-18)	The chemical structure of macrocyclic ligand	20
(1-19)	The chemical structure of [BTBP] ligand	21
(1-20)	Cell packing diagram of homodinuclear [Fe ₂ BTBP(CO ₃) ₂].(H ₂ O) ₁₂ complex	22
(1-21)	Monochelate system of [Cu(BTBP)] ⁺³ complex	23.
(1-22)	ORTEP structure of homodinuclear [Ni ₂ (BTBP)].ClO ₄ complex	23
(1-23)	The chemical structure of four macrocyclic ligands	24
(1-24)	Molecular Structure of [Cd ₄ (L) ₂ (OAc) ₄] ₂	25
(1-25)	The Chemical Structure of <i>bis</i> (2-hydroxy-3-formyloxime-5 methyl benzaidimine) N-ethylene] Ligand	26
(1-26)	General Structure of The Schiff Base Ligands	27
(1-27)	The Chemical Structure of [Cu ₂ (L ⁿ)Cl ₃] and [Cu ₂ (L ⁿ)(dp) ₂]Cl ₃ Complexes	28
(1-28)	Porphyrin Structure	37
(1-29)	Structure of saturated macrocyclic	38
(1-30)	The chemical structure for unsaturated macrocyclic Amide	38
(1-31)	The structure of the unsaturated compounds	39
(1-32)	Phethalosynin Structure	39
(3-1)	I.R spectrum for precursor (I)	60
(3-2)	I.R spectrum for precursor (II)	61
(3-3)	I.R spectrum for ligand	62

<i>Figures</i>		<i>Page</i>
(3-4)	I.R spectrum for [Cu(L)]Cl complex	65
(3-5)	I.R spectrum for [Fe(L)] complex	65
(3-6)	I.R spectrum for [Ni(L)]Cl complex	66
(3-7)	I.R spectrum for [Cr(L)Cl]Cl complex	66
(3-8)	I.R spectrum for [Co(L)] complex	67
(3-9)	I.R spectrum for [Zn(L)] complex	67
(3-10)	I.R spectrum for [Cd(L)] complex	68
(3-11)	I.R spectrum for K[Hg(L)] complex	68
(3-12)	I.R spectrum for [Mn(L)] complex	69
(3-13)	Electronic spectrum of ligand	71
(3-14)	Electronic spectrum of [Cu(L)]Cl complex	73
(3-15)	Electronic spectrum of [Ni(L)]Cl complex	73
(3-16)	Electronic spectrum of [Cr(L)Cl]Cl complex	74
(3-17)	Electronic spectrum of [Co(L)] complex	75
(3-18)	Electronic spectrum of [Mn(L)] complex	76
(3-19)	Electronic spectrum of [Fe(L)] complex	77
(3-20)	Electronic spectrum of [Zn(L)] complex	78
(3-21)	Electronic spectrum of [Cd(L)] complex	78
(3-22)	Electronic spectrum of K[Hg(L)] complex	79
(3-23)	¹ HNMR spectrum of precursor (I)	84
(3-24)	¹ HNMR spectrum of ligand	86
(3-25)	¹ HNMR spectrum of [Cu(L)]Cl	87
(3-26)	¹ HNMR spectrum of [Ni(L)]Cl	88
(3-27)	¹ HNMR spectrum of [Zn(L)]	89

<i>Figures</i>	<i>Page</i>
(3-28) ^1H NMR spectrum of $[\text{Cd}(\text{L})]$	90
(3-29) ^1H NMR spectrum of $[\text{Fe}(\text{L})]$	90
(3-30) ^1H NMR spectrum of $\text{K}[\text{Hg}(\text{L})]$	91
(3-31) ^1H NMR spectrum of $[\text{Cr}(\text{L})\text{Cl}]\text{Cl}$	92
(3-32) ^1H NMR spectrum of $[\text{Co}(\text{L})]$	92
(3-33) ^1H NMR spectrum of $[\text{Mn}(\text{L})]$	93
(3-34) ^{13}C NMR spectrum of precursor (I)	95
(3-35) ^{13}C NMR spectrum of ligand	96
(3-36) ^{13}C NMR spectrum of $[\text{Ni}(\text{L})]\text{Cl}$	98
(3-37) The proposed molecular structure of $[\text{Cr}^{\text{III}}(\text{L})\text{Cl}]^+$ complex	103
(3-38) The proposed molecular structure of $[\text{Co}^{\text{II}}(\text{L})]$ complex	104
(3-39) The proposed molecular structure of $[\text{Ni}^{\text{II}}(\text{L})]^+$ complex	105
(3-40) The proposed molecular structure of $[\text{Zn}^{\text{II}}(\text{L})]$ complex	106
(3-41) The proposed molecular structure of $[\text{Hg}^{\text{II}}(\text{L})]^-$ complex	107
(3-42) The proposed molecular structure of $[\text{Cu}^{\text{II}}(\text{L})]^+$ complex	108
(4-1) The inhibition according to atomic number	113
(4-2) Effect of $[\text{Zn}(\text{L})]$ and $\text{K}[\text{Hg}(\text{L})]$ on staphylococcus aureus	114
(4-3) Effect of ligand (L) and $[\text{Mn}(\text{L})]$ on staphylococcus aureus	114
(4-4) Effect of $[\text{Cd}(\text{L})]$ and $[\text{Cu}(\text{L})]\text{Cl}$ on staphylococcus aureus	115
(4-5) Effect of $[\text{Ni}(\text{L})]\text{Cl}$ and $[\text{Co}(\text{L})]$ on staphylococcus aureus	115
(4-6) Effect of $[\text{Fe}(\text{L})]$ and $[\text{Cr}(\text{L})\text{Cl}]\text{Cl}$ on staphylococcus aureus	116
(4-7) Effect of $[\text{Zn}(\text{L})]$ and $\text{K}[\text{Hg}(\text{L})]$ on pseudomonas mallei	116
(4-8) Effect of Ligand (L) and $[\text{Mn}(\text{L})]$ on pseudomonas mallei	117
(4-9) Effect of $[\text{Cd}(\text{L})]$ and $[\text{Cu}(\text{L})]\text{Cl}$ on pseudomonas mallei	117
(4-10) Effect of $[\text{Ni}(\text{L})]\text{Cl}$ and $[\text{Co}(\text{L})]$ on Pseudomonas mallei	118
(4-11) Effect of $[\text{Fe}(\text{L})]$ and $[\text{Cr}(\text{L})\text{Cl}]\text{Cl}$ on Pseudomonas mallei	118

List of Scheme

<i>Scheme</i>	<i>Page</i>
(1-1) The general equation of Schiff	1
(1-2) The synthesis route of the template condensation of 6,6'-bis(aminomethyl)-2,2'-bipyridyl With 2,6-diformyl- <i>p</i> -cresol	16
(1-3) The synthesis route of the non template condensation of 2,6-bis(aminomethyl)- <i>p</i> -cresol with 2,6-diformylpyridyl	17
(1-4) The preparation route of heteronuclear complexes	19
(1-5) The synthesis route of $[Cd_4(L^n)_2(OAc)_4]_2$ complexes	25
(3-1) One pot synthesis route of 2,6-diformyl-4-methylphenol	54
(3-2) Synthesis route of precursorII	54
(3-3) Synthesis route of ligand	55
(3-4) Synthesis route of complexes	57

List of Abbreviations

AA	Atomic absorption
¹ HNMR	Hydrogen nuclear magnetic resonance
¹³ CNMR	Carbon-13-nuclear magnetic resonance
Tsc	Thiosemcarbazone
DMF	Dimethylformamide
DMSO	Dimethyl Sulfoxide
DCM	Dichloromethane
m.p	Melting point
IR	Infrared
U.V-Vis	Ultraviolet and visible
λ	Wavelength
ϵ_{\max}	Molar absorptivity
Abs	Absorbance
nm	Nanometer
$\bar{\nu}$	Wave number
Ev	Electron volt
$^{\circ}\text{A}$	Angstrom
MHz	Megahertz
ORTEP	Oak Ridge Thermal Ellipsoid Program
EI	Electron Impact
α	Alpha ray
β	Beta ray
γ	Gamma ray
FAB	Fast Atomic Bombardment

ESR	electron spin resonance
BBIM	Bis(benzimidazole-2-ylmethyl)amine
BTBP	2,6-Bis(hydroxymethyl)-4-tert-butylphenol
DHTMBA	5,5'-Di-tert-butyl-2,2'-dihydroxy-3,3'-methanediyl-dibenzene methanol
DFMP	2,6-Diformyl methyl phenol
Precursor (I)	2,6-dimethylol 4-methyl phenol
Precursor (II)	2,6-bis-(Azomethine-ethylamine)-4-methyl phenol

References

1. H. Schiff, *Ann. Chem. Pharm.*, **150**, 193 (1869).
2. M. A. Bayomi, M. El-Asser, M. Msser, and F. A. Abid- Halim, *J. Am. Chem. Soc.*, **39**, 586 (1971).
3. M. Chatterjee and Saktiprosad Ghosh, *Trans. Met. Chem.*, **23**, 355 (1998)
4. J. March, "Advanced Organic Chemistry" Third edition, John Wiley and Sons. Inc., New York (1979).
5. G. Reddelien, and H. Danil of, *Ber*, **5** (48), 3132(1927).
6. S. Patati, "The chemistry of Carbon-nitrogen double bond", John Wiley and sons, Inc., New York (1979).
7. A. A. H. Saeed, M. N AL- Zagoumand, and M. H. Walton, *Canadian J. Spectroscopy*, **25**, 137 (1980).
8. H. A. Staab, *Ber.*, **98**(8), 2681 (1965).
9. D. P. Fryberg, and G. M. Mockler, *J. Chem. Soc. Dalton Trans*, **5**, 445 (1976).
10. J. A. Godiawn and L. J. Wilson, *Inorg. Chem*, **28**, 42 (1989).
11. M. W. Hosseni, J. M. Lehn, S. R. Duff, K. Gu and M. P. J. Mertes, *Org. Chem.* **52**, 1662 (1987).
12. R. M. Izan, J. S. Brandshaw, S. A. Neilsen, J. D. Lamb, J. J. Christensen and D. Sen, *Chem. Rev.* **85**, 271 (1985).
13. M. Shakir, S. P. Varkey and O. S. M. Namsmon, *Polyhedron*, **14**, 1283 (1995)
14. N. F. Curtis, *Macrocyclic Ligands*, (2003).
15. J. Wikaira, Ph.D. Thesis, University of Canterbury, (1996).

16. Abe. K. Matsufuji, K. M. Ohba. and H. Okawa, *Inorganic Chemistry*, **41**, 4461-4467 (2002).
17. S. Karthikeyan, T. M. Rajendiran, R. Kannappan, R. Mahalakshmy, R. Venkatesan and P. S. Rao, Proc. *Indian Acad. Sci. (Chem. Sci.)*, **113**, 245-256 (2001).
18. V. McKee, J. B. Fontecha and S. Goetz, Angew. *Chem. Int. Ed.*, **41**, 4553-4556 (2002).
19. V. McKee, J. B. Fontecha and S. Goetz, *Dalton Transactions*, **5**, 923-929 (2005).
20. Pilkington, R. R. N. H. *Australian Journal of Chemistry* 1970, **23**, 2225-2236.
21. E. C. Constable, *Coordination Chemistry of Macrocyclic Compounds*; Oxford University Press: New York, Vol. 72 (1999).
22. *Wikipedia Foundation*, I., p.
http://en.wikipedia.org/wiki/Methane_monooxygenase (2006)
23. W. Kaim and B. Schwederski, *Bioinorganic Chemistry: Inorganic Elements in the Chemistry of Life*; John Wiley & Sons Ltd: England, (1996).
24. M. G. Patch, H. K. Choi, D. R. Chapman, R. Bau. V. McKee and C. A. Reed, *Inorganic Chemistry*, **29**, 110-119 (1990).
25. D. O. Hall and K. K. Rao, *Photosynthesis* Sixth Edition; Cambridge University Press: Cambridge, (1999).
26. J. Wikaira and S. M. Gorun, In *Bioinorganic Catalysis*; J. Reedijk and E. Eds. Bouwman. Marcel Dekker, Inc: New York, pp. 395-408 (1999).
27. D. E. Fenton and S. E. Gayda, *Journal of the Chemical Society, Dalton Transactions*, 2095-2101 (1977).

28. O. C. W. Linert, *Metal Mediated Template Synthesis of Ligands*; World Scientific Publishing Co. Pte. Ltd, (2004).
29. H. Adams, S. Clunas, L. R. Cummings, D. E. Fenton and P. E. McHugh, *Inorganic Chemistry Communications*, **6**, 837-840 (2003).
30. H. Adams, S. Clunas and D. E. Fenton, *Acta Crystallographica Section E*, **60**, 338-339 (2004).
31. H. Adams, S. Clunas, D. E. Fenton, T. J. Gregson, P. E. McHugh and S. E. Spey, *Inorganica Chimica Acta*, **346**, 239-247 (2003).
32. W. A. Flomer, S. C. O'Neal, J. W. Kolis, D. Jeter and A. W. Cordes, *Inorganic Chemistry*, **27**, 971-973 (1988).
33. J. B. Fontecha and V. McKee, *Personal Communication*, (2005).
34. S. Abuskhuna, J. Briody, M. McCann, M. Devereux, K. Kavanagh, J. B. Fontecha and V. McKee, *Polyhedron*, **23**, 1249-1255 (2004).
35. A. Eshwika, B. Coyle, M. Devereux, M. McCann and K. Kavanagh, *Biometals*, **17**, 415-422 (2004).
36. N. F. Curtis and D. A. House, *Chem. and Ind.*— London, 9 – 1708 (1961).
37. N. F. Curtis, *Coordination Chemistry Reviews*, **3**, 3-47 (1968).
38. N. F. Curtis, *Coordination Chemistry Reviews*, **3**, 4 (1968).
39. S. Z. Lever and J. Nucl, Med, **26**, 1287, (1985).
40. K. E. Baidovo and S. Z. Lever, *Bio conjugate chem.*, **1**, 132, (1990).
41. K. E. Baidovo and S. Z. Lever, *Cancer Res. (suppl.)*, **50**, 7995, (1990).

42. B.S. Synder, C. P. Rao and R. H. Holm, *Aust. J. chem.*, **39**, 963, (1986).
43. L. G. Kazmina, and Y. T. Struchkov, *Cryst. Struct. Commun*, **8**, 715 (1979).
44. R. M. Izatt, K. Pawlak and J. S. Bradshaw, *Chem. Rev.*, **95**, 2529 (1995).
45. H. Okawa, J. N. Bridson, *Inorg. Chem.*, **32**, 2949 (1993).
46. A. J. Atkins, A. J. Blake and M. Schroder, *J. Chem. Soc. Chem. Commun*, 353-355 (1993).
47. S. T. Santokh, L. K. Thompson and J. N. Bridson, *Inorg. Chem.*, **32**, 32-39 (1993).
48. Z. Wang, J. Reibenspies and E. M. Arthur, *Inorg. Chem.* **36**, 629-636 (1997).
49. A. Erxleben and J. Hermann, *J. Chem. Soc., Dalton Trans*, 569-575 (2000).
50. V. N. Ghaudhuri, P. Claudio and E. R. Thoma, *J. Chem. Soc., Dalton Trans*, 569-575 (2000).
51. M. J. Al-Jeboori, A. A. K. Mukhlus, and K. J. Al-Abedy, *Iraqi J. Chemistry*, **28**, *1*, 91-95 (2002).
52. D. Kong, J. Reiben Spies and J. Mao, *Inorganica Chimica Acta*, **340**, 170-180 (2002).
53. D. Kong, J. Mao and A. Clearfield, *Inorganica Chimica Acta*, **338**, 78-88 (2002).
54. A. J. Atkins, D. B. Rachel and M. Schroder, *Dalton Trans.*, 1730-1737 (2003).
55. L. Wing-Kit, W. Wai-Kwok and W. Wai-Yeung, *Inorg. Chem.*, 3950-3954 (2005).

56. J. S. Sultan. Aldulaimi. M.Sc. Thesis, University of Baghdad, College of Education– Ibn– AL– Haytham, (2005).
57. M. Tumer, N. Deligonul and M. Dolaz, *Transition Metal Chemistry*, **31**, 1-12 (2006) .
58. G. R. Hedwig, J. L. Love and H. K. L. Powell, *Aus. J. Chem.*, **23**, 981-987 (1970).
59. H. Sakiyama, N. Matsumoto and H. Okawa, *Bull. Chem. Soc., Jpn.*, **68**, 1105 (1995).
60. N. H. Pilkington and R. Robson, *J. Chem.*, **23**, 2225 (1970).
61. H. Yoon, T.R. Wagner and K. J. Oconner, *J. Am. Chem. Soc.*, **112**, (1990).
62. J. F. Kinneary, T. R. Wagner and C. J. Burrows, *Tetrahedron Lett.*, **29**, 77-880 (1988).
63. R. I. Kureshy, N. H. Khan and S. H. R. Abdi, *J. Mol. Catal. A. Chem.* **130**, 41-50 (1998).
64. E. Hough, L. K. Hanson and B. Birknes, *Nature*, **338**, 357 (1989).
65. R. G. Konsler, J. Karl and E.N. Jacobsen, *J. Chem. Soc. Dalton Trans*, **3897** (1995).
66. E. Asato, H. Furutach and T. kawahasbi, *J. Chem. Soc., Dalton Trans*, **3897** (1995).
67. J. M. Perez, V. Cerrillo and A. I. Matesanz, *Chem. Bio Chem.*, **2** (2001).
68. V.W.W. Yam and K. K. W. Lo, *Chem. Soc. Rev.* **28**, 323-334 (1999).
69. W.Y. Wong, *J. Inorg. Organomet. Polym. Matar*, **15**, 197-219 (2005).

70. L. D. Cola, D. L. Smaite and L. M. Vallarino, *Inorg. Chem.*, **25**, 1729 (1986).
71. M. R. Malachowski and M.G. Davidson, *Inorg. Chim. Acta*, **162**, 199 (1989).
72. Yu A. Zolotov, *Macrocyclic Compounds in Analytical Chemistry*, New York, (1979).
73. B. Bosnich, C. H. Poon and M. L. Tobe, *Inorg. Chem.* **4**, 1102, (1965).
74. D. Parker and P. S. Roy, *Inorg. Chimi. Acta*, **148** (1988).
75. C. Floriani, A. Klose, E. Solari, N. RE, A. C. Villa and C. Rizzoli, *Chem. Commun.*, 2279 (1979).
76. M. D. Rausch and Y. F. Chang, and H. B. Cordon, *Inorg. Chem.*, **8**, 1355 (1969).
77. K.M. Long and D. H. Busch, *Inorg. Chem*, Vol. 9, **3** (1970).
78. D. H. Busch, G. Christoph. Gary, L. Lawrence Zimmer, C. Jackels Susan and P. Schammel Wayne, *J. Am. Chem. Soc.* **103**, 5108 (1981).
79. P. A. Gugger, C. R. Hockless David, F. Swiegers Gerhard and S. Bruce Wild, *Inorg. Chem.* **33**, 6571 (1989).
80. J. S. Skurutowicz, L. L. Madden, and D.H. Busch, *Inorg. Chem.* **18**, 1721 (1977).
81. R. Hettich and H. Schneider, *J. Am. Chem. Soc.*, **119**, 5639 (1996).
82. J. Mulzer, Benjamin List, and W. Bats Jan, *J. Am. Chem. Soc.*, **119**, 5514 (1997).
83. I. Morishima, H. Fujii, and Y. Shiro, *Inorg. Chem.* **34**, 1528 (1995).

84. D. David, E. Fenton, *Chem. Soc.* **28**, 159 (1999).
85. A. K. Burrell, B. Hall Simon, *Inorg. Chimi Acta*, **298**, 112 (2000).
86. D.S. Marlin, K. Mascharak Pradip, *Chem. Soc.* **29**, 69 (2000).
87. P. Comba, M. Luther Strphan, O. mass, H. Pritzkow, and A. Vielfort, *Inorg Chem.*, **40**, 2335 (2001).
88. E. Deulsch, M. Nicolini, H. N. JR Wagner, *Technetium in Chemistry and Nuclear Medicine*, Eds: Cortina International, Verona, Italy, **1** (1983).
89. G. Wilkinson, *Comprehensive Coordination Chemistry.*, Vol.4 Pergamon Press, Oxford, England, (1987).
90. R. L. Reeves, *J. Am. Chem. Soc.*, **84**, 3332 (1962).
91. J. Franz, W. A. Volkert, E. K. Barefield, R. A. Holmes, *Nucl. Med. Biol.* **14**, 569 (1987).
92. D. Brenner, A. Davison and A. G. Jones, *Inorg. Chem.*, **23**, 3793 (1984).
93. J.R. Dilworth and S. J Parrott, *Chem. Soc. Rev.*, **27**, 43 (1998).
94. P.B. Choch, and E. O. Titus Prog, *Inorg. Chem.* **18**, 287 (1973).
95. D. G. Brown and E. O. Prog, *Inorg. Chem.*, **13**, 177 (1973).
96. M. J. Warren and H. N. Shah, *Biolog. Chem.*, **275**, 316 (2000).
97. R. Tenhunen, H. S. Marver and R. Schmid, *Proc. Natl. Acad. Sci. U.S.A.*, **61**, 748 (1968).
98. I. L. Handel, E. R. Muller, and R. Guglielmeti, *Inorg. Chimi Acta* **66**, 514 (1983).
99. A. Yu. Nazarenko, and I. N. Loskucheryovayz izr, Vyssh. Uchebn. Zaved, *Khim Tekhmol.* **27**, 639-643 (1984).

100. Yu. A. Zolotov, V. P. Inov, N. V. Nizcva, and A. A. Formanovskii, *Doki. Akad. Nauk SSSR*, **277**, 1145 (1984).
101. N. V. Fsakova, Yu. A. Zolotov, and V. P. Lonov, *Zh. Anal. Khim*, **44**, 859 (1989).
102. H. Ishii, K. Satoh, and H. Koh, *Bunsekikagaku*, **29**, 276 (1980).
103. C. N. Verani, L. Rentschier, W. Thomas, E. Bill and P. Chaudhuri, *J. Chem., Dalton trans*, **251-258** (2000).
104. C. Clark, A. R. Cowley, J. R. Dilworth and P. S. Donnelly, *Dalton. Trans.*, **2402-2403** (2004).
105. W. C. Pierce, E. L. Haenisch and D. T. Sawyer, *Quantitative Analysis*, John Wiley & sons, New York, 4th ed. P. **257** (1976).
106. Y. U. Zoloty, “*Macrocyclic Compounds in Analytical Chemistry*”, John Wiley and Sons Inc, New York, (1997).
107. A. H. D. Al-Qhadeer, Ph.D. Thesis., University of Baghdad, Education college, (2006).
108. F. H. Al-Jeboori, Ph.D. Thesis., University of Baghdad, Education college, (2006).
109. A. R. Cowley, J. R. Dilworth, P. S. Donnelly and J. M. Whilte, *Inorg. Chem.*, **45**, 496 (2006).
110. K. Nakamoto, “*Infrared and Raman spectra of Inorganic and coordination compounds*”, John Wiley, New York, 3rd ed.P. **232** (1978).
111. P. H. Smith, J. R. Morris and G. D. Ryan, *J. Am. Chem.Soc.*, **111**, 7437 (1989).
112. A. M. Brodie, H. D. Hdden and M. J. Taylor, *J. Chem. Soc. Dalton Trans.*, **1 (3)**, 633 (1986).

113. M. Tumer, C. Celik, H. Koksall and S. Serin, *Trans. Met. Chem.*, **24**, 525 (1999).
114. Z. Wang, J. Ribenspies and E. M. Arthur, *Inorg. Chem.* **36**, 629-636 (1997).
115. C. Preti and G. Tosi, *Can. J. Chem.*, **55**, 1409 (1977)
116. K. J. Oberhausen, J. F. Richandon and R. M. Buchanan, *Inorg. Chem.*, **30**, 1357 (1991).
117. A. B. P. Lever, *J. Chem. Edu.*, **45**, 711 (1958).
118. S. Jha and R. P. Verma, *Asian J. Chem.*, **15** (3) and 1719 (2003).
119. M. Joseph, M. P. Kurup, E. Suresh and S. G. Bhat, *Polyhedron*, **25**, 61 (2006).
120. M. A. Mendiola, E. L. Torress and D. G. Galatogu, *Eur. J. Inorg. Chem.* **5**, 657 (2005).
121. U. El-Ayaan, G. Abu El-Reash and I. M Kenawy, *Inorg. And Metal-Org. Chem.*, **33** (2), 327 (2003).
122. S. Chandra and U. Kumar, *J. Indian, Chem. Soc.*, **78**, 273 (2003).
123. S. Chandra, G. Singh and V. P. Tyagi, *Inorg. Met. Org. Chem.*, **31** (10), 1759 (2001).
124. S. Chandra and U. Kumar, *Spectrochemica Acta., Part (A)*, **61**, 219 (2005).
125. A. Kaito, M. Hafano and A. Tajiri, *J. Amer. Chem. Soc.*, **99**, 5241 (1977).
126. R. Kannappan, S. Tanase, L. Mutikainen, U. Turpeinen and J. Reedijk, *Polyhedron*, **25**, 1646-1654 (2006).
127. H. Beraldo and L. Tosi, *Inorg. Chemi. Acta.*, **125**, 127 (1986).

-
128. W. J. Geary. *Coordination Rev.*, **7**, 81 (1971).
129. N. S. Youssef, K. H. Hegab and A. E. Eid, *Synthesis and Reactivity in Inorganic and Metal-Organic Chemistry*, **33**, **9**, 1647-1666 (2003).
130. H. Koksall, M. Tumer and S. Serin, *Synth. Inorg. Met. Org. Chem.*, **26**, 1577 (1996).
131. H. T. Al-Rafaqany, M.Sc. Thesis, Al-Nahrrain University, College of Science (2008).
132. E. O. Lima, E. F. Queroz and V. C. Filho, *Bio. Soc. Chil.*, **44**, 210 (1999).
133. W. F. Harrigan and M. E. Mccacer, Laboraty "*Methods in food and Dairy Microbiology*". Academic press Inc. London. P. **451** (1976).

Scientific Evaluation Report

This is to certify that I have read the thesis entitled, (Synthesis and characterization of mononuclear metal complexes with a ligand derived from 2,6-diformyl para cresol) and corrected the scientific mistakes I found. The thesis is, therefore qualified for debate.

Signature:

Name: Asst. Prof. Dr. Waleed A. Mahmood

Date:

Table (3–5) Infrared spectral data for the starting materials, precursors and ligand

compound	$\nu(\text{C}-\text{N})$	$\nu(\text{C}=\text{N})$	$\nu(\text{C}=\text{C})$	$\nu(\text{CH})$ aliph.	$\nu(\text{CH})$ Aro.	$\nu(\text{C}-\text{O})$	$\nu(\text{CH}_2)$	$\delta(\text{OH})$	$\nu(\text{HO})$	$\nu(\text{NH}_2)$	$\delta(\text{NH})$	$\nu\text{C}=\text{O}$
Precursor (I)			1603 _(s) 1458 _(s)	2922 _(m)	2871 _(m)	1216 _(s)		1404 _(m))	3400 _(w)			1682 _(s)) 1667 _(s))
Precursor (II)	1114	1675 1620	1500 1475	2950	2850	1223	1360 _(s)		3406 _(br)	3240	1696 _(s) in plane 962 out plane	
Ligand	856 _(s)	1640 _(s)	1496 _(s)	2940 _(s)	2870 _(m)	1200 _(s)	1373 _(m)		3394 _(br)			

s: strong,

m: medium,

w: weak,

br: broad

Aliph: aliphatic,

Aro: Aromatic

ν : stretching

δ : bending

Table (3-6) Infrared spectral data (wave) cm^{-1} of the complexes

compounds	$\nu(\text{C-H})$	$\nu(\text{C=N})$	$\nu(\text{C=C})$	$\nu(\text{CH})_{\text{Ali ph.}}$	$\nu(\text{CH})_{\text{Aro.}}$	$\nu(\text{C-O})$	$\nu(\text{CH}_2)$	$\nu(\text{OH})$	$\delta(\text{NH})$	$\nu(\text{M-O})$	$\nu(\text{M-N})$	$\nu_{\text{M-Cl}}$
Ligand	856 _(s)	1660 _(s) 1650 _(s)	1496 _(s)	2940 _(s)	2870 _(s)	1200 _(s)	1373 _(m)	3394 _(br)	1577 _(s)			
[Mn(L)]	898 _(s)	1627 _(s) 1600 _(s)	1442 _(s)	2924 _(s)	2854 _(m)	1292 _(s) 1199 _(m)	1388 _(m)	3375 _(br)		447 _(s)	632 _(m)	
[Fe(L)]	1022 _(br)	1650 _(s) 1608 _(s)	1480 _(s)	2924 _(br)	2854 _(s)	1265 _(br) 1095 _(br)	1377 _(br)	3390 _(br)		439 _(s)	625 _(s)	
[Zn(L)]	1026 _(br)	1650 _(s) 1628 _(s)	1480 _(s)	2920 _(s)	2854 _(s)	1222 _(br)	1396 _(s)	3449 _(s)		447 _(s)	640 _(s)	
[Ni(L)]Cl	1026 _(br)	1650 _(s) 1624 _(s)	1458 _(s)	2924 _(s)	2854 _(m)	1200 _(m)	1390 _(s)	3394 _(br)		443 _(s)	624 _(s)	
[Co(L)]	898 _(s)	1639 _(s) 1600 _(s)	1450 _(s)	2924 _(m)	2858 _(m)	1200 _(s)	1388 _(m)	3406 _(br)		440 _(s)	636 _(br)	
[Cr(L)Cl]Cl	902 _(s)	1640 _(s) 1616 _(s)	1470 _(s)	2924 _(s)	2854 _(m)	1199 _(m)	1400 _(s)	3425 _(br)		440 _(s)	570 _(m)	430 _(s)
[Cd(L)]	872 _(s)	1639 _(s)	1446 _(s)	2924 _(s)	2862 _(m)	1215 _(s)	1400 _(s)	3433 _(br)		400 _(s)	675 _(m)	
K[Hg(L)]	860 _(s)	1650 _(s) 1635 _(s)	1450 _(s)	2924 _(m)	2854 _(m)	1280 _(s)	1396 _(br)	3390 _(br)		447 _(s)	610 _(s)	
[Cu(L)]Cl	875 _(s)	1635 _(s) 1600 _(s)	1458 _(s)	2920 _(m)	2854 _(m)	1280 _(s)	1396 _(s)	3429 _(br)		409	580 _(m)	

s: strong,

m: medium,

w: week,

br: broad

Aliph: aliphatic,

Aro: Aromatic

ν : stretching

δ : bending

θωωωωωωωωωωωωωωωωωε

αΣΣΣΣΣΣΣΣΣΣΣΣΣΣΣΣΣΣΣΣΣΣΣδ

αΣ Σδ

αΣ Σδ

αΣ Σδ

αΣ Σδ

αΣ Σδ

αΣ Σδ بسم الله الرحمن الرحيم

αΣ Σδ

αΣ } نَرْفَعُ دَرَجَاتٍ مِّنْ قِسْءٍ
αΣ Σδ

αΣ Σδ
αΣ Σδ وَفَوْقَ كُلِّ ذِي عِلْمٍ عَلِيمٌ

αΣ Σδ
αΣ Σδ (صدق الله العظيم)

αΣ Σδ (سورة يوسف / جزء من الآية ٧٦)

αΣ Σδ

αΣ Σδ

αΣ Σδ

αΣ Σδ

αΣ Σδ

αΣ Σδ

αΣ Σδ

αΣ Σδ

αΣ Σδ

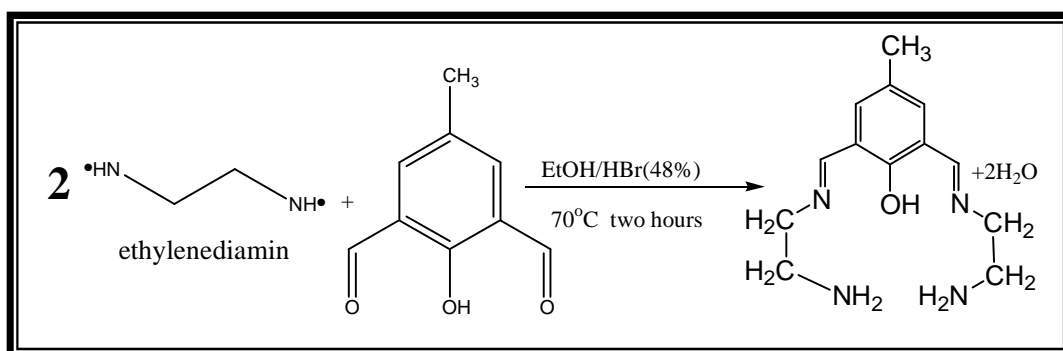
αΣ Σδ

αΣ Σδ

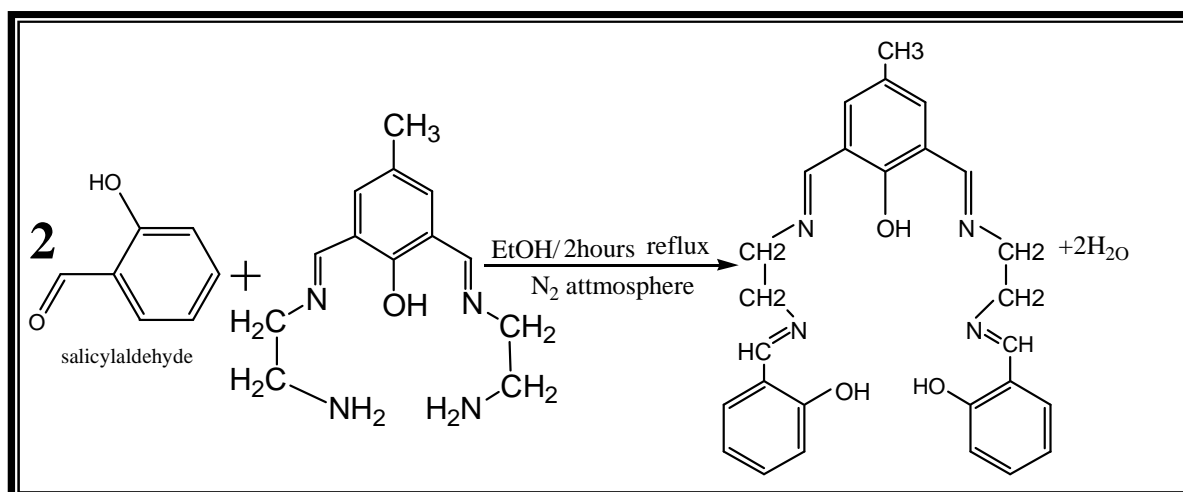
αΣ Σδ

الخلاصة

حضر ليكاند جديد (قاعدة شيف) متعدد السن رباعي ذرات النتروجين (تترازا) ٦، ٢-بس (ازوميثين اثيل ازوميثين اورثو فينول) ٤-مثيل فينول (L)، بخطوتين: أولاً: من تكاثف ٦، ٢-داي فورمايل ٤-ميثيل فينول مع اثيلين داي امين بنسبة وزنية (٢:١) وتحت جو من النيتروجين.



ثانياً: من تفاعل ناتج الخطوة الاولى مع السالسالديهايد بنسبة وزنية (٢:١) وتحت جو من النيتروجين.



شخص الليكاند وتم التوصل الى تركيبه الكيميائي باعتماد التحاليل الطيفية (طيف الاشعة تحت الحمراء، طيف الاشعة فوق البنفسجية والمرئية، طيف الرنين النووي المغناطيسي ¹H، ¹³C).

حضرت سلسلة المعقدات الفلزية لليكاند مع الايونات الفلزية Ni(II) ، Hg(II) ، Co(II) ، Fe(II) ، Cu(II) ، Cd(II) ، Zn(II) و Cr(III) و Mn(II) ، باضافة ١ ملي مول من الليكاند الى ١ ملي مول من ملح ايون الفلز مع هيدروكسيد البوتاسيوم كقاعدة للاحتفاظ بقيمة الحامضية عند (٩) تقريبا وباستخدام الايثانول كمذيب.

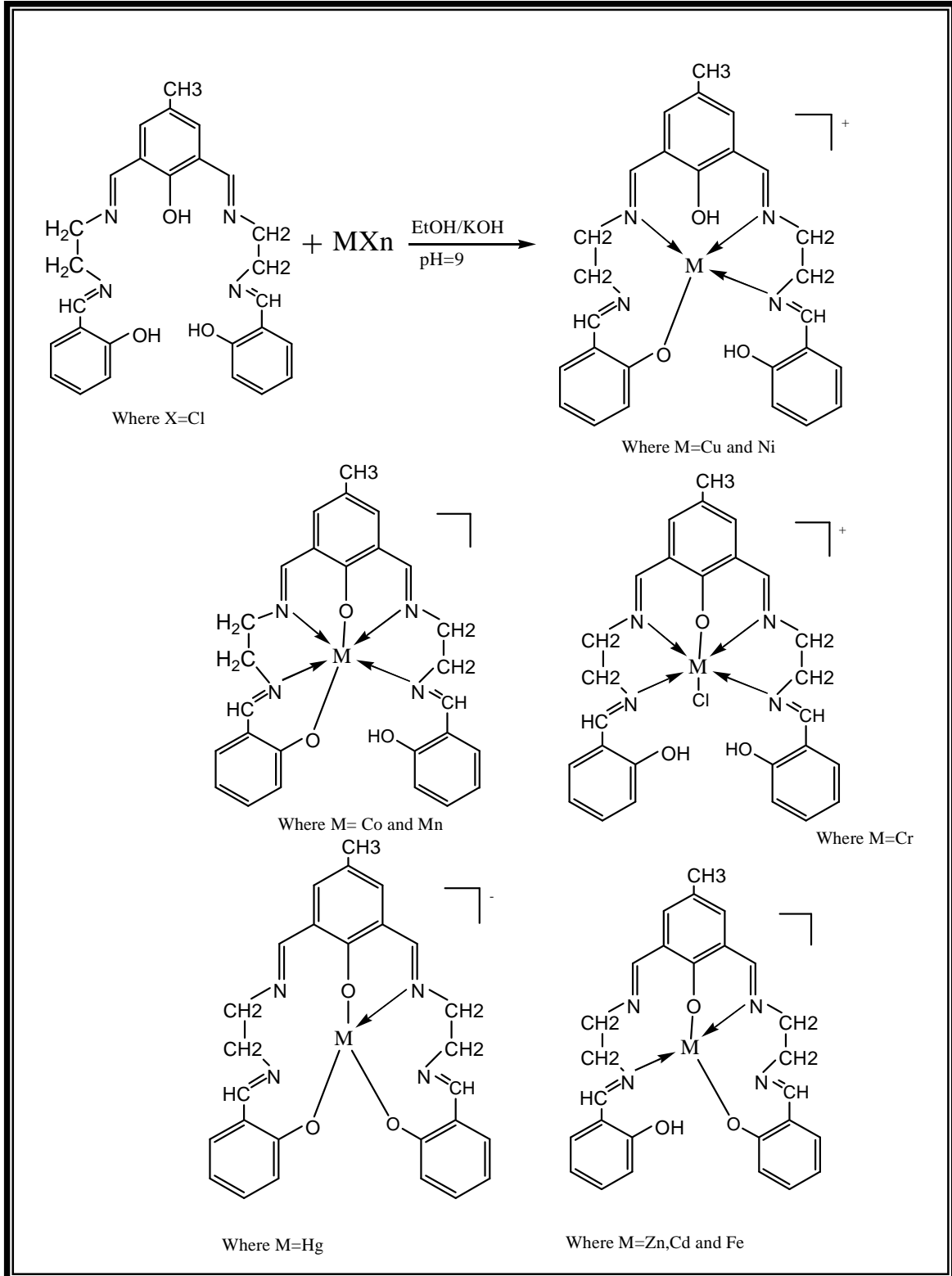
شخصت هذه المعقدات وتم التوصل الى تراكيبها الكيميائية و اشكالها الهندسية بتحليل عنصر النيتروجين بطريقة كدال، الدراسات الطيفية (اطياف الاشعة فوق البنفسجية والمرئية، طيف الأشعة تحت الحمراء، طيف الرنين النووي المغناطيسي (^1H ، $^{13}\text{CNMR}$). فضلا عن قياسات العزم المغناطيسي والتوصيلية الكهربائية، محتوى الكلور ودرجة الانصهار.

تم اقتراح الاشكال الفراغية لهذه المعقدات استنادا الى نتائج هذه التحاليل: فكانت الصيغة $[\text{M(L)}]$ حيث M هي Fe(II) ، Co(II) ، Zn(II) ، Cd(II) ، Mn(II) وعند الصيغة $[\text{M(L)}]\text{Cl}$ حيث M هي Ni(II) ، Cu(II) و الصيغة $[\text{M(L)Cl}]\text{Cl}$ حيث M هي Cr(III) و الصيغة $\text{K}[\text{M(L)}]$ حيث M هي Hg(II) .

أظهرت تحاليل أطياف الأشعة فوق البنفسجية والمرئية مدعمة بقيم الحساسية المغناطيسية، الأشكال الهندسية ثمانية السطوح بالنسبة لمعقدات Co(II) ، Mn(II) ، Cr(III) ، والشكل الهندسي رباعي السطوح بالنسبة لمعقدات Cd(II) ، Zn(II) ، Fe(II) ، Hg(II) ، والشكل الهندسي مربع مستوي بالنسبة لمعقدات Ni(II) ، Cu(II) .

بينت نتائج قياسات التوصيلية للمعقدات المحضرة الجديدة في مذيب (DMF)، بأن معقدات النيكل والكروم والنحاس والزنبق ذات طبيعة (الكتروليتية) موصلة للكهربائية مع محتوى الكلور او البوتاسيوم وان هذه المعقدات ايونية بنسبة (1:١)، بينما أظهرت معقدات الكاديوم، الزنك، الكوبلت، الحديد و المنغنيز طبيعة غير موصلة للكهربائية. درست الفعاليات الحيوية بأستعمال نوعين من البكتريا لليكاند وكذلك المعقدات الفلزية المحضرة وبينت النتائج ان معقدات الزنك، الكاديوم والزنبق لها خواص تثبيط نمو

البكتريا أعلى من الليكاند لوحده، بينما وجدت الفعاليات التثبيطية لباقي المعقدات أقل من الليكاند لوحده.





جمهورية العراق
وزارة التعليم العالي والبحث العلمي
جامعة بغداد / كلية العلوم للبنات
قسم الكيمياء

تحضير وتشخيص معقدات فلزية أحادية النواة مع ليكاند مشتق من

2,6-Diformyl para cresol

رسالة مقدمة

إلى قسم الكيمياء / كلية العلوم للبنات

وهي جزء من متطلبات نيل درجة الماجستير في الكيمياء

من قبل

مناف عمار مصطفى

بكالوريوس ٢٠٠٣ (الجامعة المستنصرية)

بإشراف

أ.د. يحيى عبد المجيد العبيدي أ.م.د. محمد جابر الجبوري

١٤٢٩ هـ

٢٠٠٨ م

Republic of Iraq
Ministry of Higher Education
& Scientific Research
University of Baghdad College of
Science for Women
Chemistry Department



Synthesis and characterization of
mononuclear metal complexes
with a ligand derived from
2,6-diformyl para cresol

A Thesis Submitted

To the Chemistry Department /College of Science for
Women in Partial Fulfillment of the Requirements for the
Degree of Master of Science in Chemistry

By

Munaf Ammar Mustafa

B.Sc. in Chemistry 2003 Al-Mustansiriyah
Supervisor

Prof.Dr.

Yahya Abdul Majid

Asst.Prof.Dr.

Mohamad Jaber Al-
Jeboori

2008 A.C.

1429 A.H.

Chapter One

Introduction

Chapter Two
Experimental Part

Chapter Three
Results & Discussion

Chapter Four
Biological Activity

References